Enrichment of Hg, Sn, As, Al, Mn and Fe in Surface Sediments and Surface Water of Winam Gulf, Lake Victoria

Article · July 2017

CITATIONS
0

READS
555

5 authors, including:

David Ongeri
16 PUBLICATIONS **105** CITATIONS
SEE PROFILE


Solomon Omwoma
Jaramogi Oginga Odinga University of Science and Technology
45 PUBLICATIONS **325** CITATIONS
SEE PROFILE

Joseph Lalah
Kenya Polytechnic University College
72 PUBLICATIONS **992** CITATIONS
SEE PROFILE


Bernhard Michalke
Helmholtz Zentrum München
285 PUBLICATIONS **6,012** CITATIONS
SEE PROFILE

Available online at www.kenchemsoc.org

Journal of the Kenya Chemical Society 10-1 (2017), 3-9

JOURNAL OF THE KENYA CHEMICAL SOCIETY

Antioxidant activities of Triacontanyl-E-cinnamoatesmetabolites from *Caesalpinia volkensii* Root Bark extracts

Charles O. Ochieng[1]*, Atul Shrivastava[2], Upma Chaturvedi[2], Ashok K. Khanna[2], P. Okinda Owuor[1], Lawrence A. O. Manguro[1], Rakesh K. Asthana[3]

[1]Department of Chemistry, Maseno University, PrivateBag, 40105, Maseno, Kenya

[2]Biochemistry Division, Central Drug Research Institute, Lucknow, 226001, Uttar Pradesh, India

[3]Medicinal & Process Chemistry Division, Central Drug Research Institute, Lucknow, 226001, Uttar Pradesh, India

*Correspondence author:*E-Mail: otieno.charles9@gmail.com, Tel.: +254726915429.*

Abstract

Natural antioxidants have been reported to prevent oxidative damage caused by free radicals generated during biochemical processes and thus useful in prevention of several degenerative diseases. The present study evaluated the antioxidant value of Caesalpinia volkensii Harms (Leguminosae) root bark that is reported to have several ethno-medicinal applications. In-vitrofree radical scavenging and inhibition bioassays guided chromatographic separation carriedout on the root bark extracts resulted into isolation of three cinnamic acid esters, namely triacontanyl-E-ferulate (**1**), tricontanyl-(E)-caffaete (**2**) and 30´-hydroxytriacontanyl-(E)-ferulate (**3**) were isolated, along with caesaldekarin C (**4**) and 5-hydroxyvinhaticoic acid (**5**) from the potent antioxidant ethyl acetate extract. The compounds were identified using spectroscopic techniques. Compounds **1**, **2**and **3**exhibited significant ($p \leq 0.05$) inhibition of free radical generation in xanthine oxidase systems, scavenging of superoxide anion ($O_2^{\bullet-}$), inhibition of hydroxyl radical ($^{\bullet}OH$) and inhibition of microsomal lipid peroxidation with comparable LC_{50} to those of respective reference standards. This is the first report on antioxidant principles from C. volkensii and the result thus support in part the folklore use of the plant root bark to manage human ailments.

Keywords: Caesalpiniodeae; *Caesalpinia volkensii*; Antioxidants; triacontanyl-E-ferrulate; 30´-hydroxytricontanyl-(E)-ferrulate.

1. Introduction

Caesalpinia volkensii Harms (Caesalpiniaceae) is bush or liana armed with scattered deflexed prickles found within indigenous forests in Kenya, Uganda, Tanzania and Ethiopia[1]. Herbalists prescribe a decoction of the leaves or root bark to cure malaria, sometimes alone, but more often mixed with other plants[2]. The leaf, root bark or stem bark and powered fruits decoction are consumed to fight pain during pregnancy while powdered pods dissolved in water are used to relieve stomachache[3]. Root barks are also used to manage venereal disease, bilharzias, stomach ulcers and retinoblastoma[3]. In *vitro* tests of leaf extracts of *C. volkensii* showed anti-plasmodial activity against chloroquine-resistant strains of *Plasmodium falciparum*[2]similarly pure isolates including furnaditerpenes from the plants stem and roots bark showed antiplasmodial and antinociptive activities[4,5]. In general, members of the sub-family Caesalpiniaceae contain cassane furanoditerpenes[6], biflavonoids[7], homoisoflavones[8], triterpenes and phenylpropanoids[9]and some of which display antiviral, antimalarial, antibacterial, anti-inflammatory and antioxidant activities[9,10]. However, scarce phytochemical studies have been carried out on the root bark of *C. volkensii*. Some of the ethno medical and reported biological activities of the plant[2,3], prompted an investigation on its antioxidant activity as part of an ongoing investigation for bioactive constituents of the less common East African indigenous plant species, considered to be threatened by extinction. This communication reports a bioassay guided isolation of antioxidant constituents from the root bark of *C. volkensii* against in*vitro* enzymatic and non enzymatic antioxidant activity assays.

2. Experimental Section

2.1. Chemicals and instruments

All the fine chemicals were analytical grade obtained from Sigma Chemical Co. St. Louis MO, USA. Optical density of antioxidant reaction mixtures were recorded on UV-2450 spectrophotometer (Shimadzu, Japan). Centrifugation

performed using Biofuge Centrifuge (Sigma, U.S.A). ^{1}H-NMR (300 MHz) and ^{13}C-NMR (75 MHz) were recorded on $CDCl_3$ (Aldrich) using Bruker Avance ARX 300 MHz (Bruker, Germany) with TMS as internal standard. HREIMS: direct inlet, 70 eV recorded using Micromass Quattro II. IR was performed using Perkin Elmer RXI-IR spectrometer. Kiesalgel 60 F_{254} (Merck) TLC plates were used and *p*-anisaldehyde as visualizing agent. Silica gel (Merck 60-120 mesh ASTM) and Sephadex LH-20 (Amersham Pharmacia Biotech) were used in column chromatographic separation.

2.2. Plant materials

The root barks of *C. volkensii* were collected from Gatamaiyo forest edge (O˚ 55′18.34″S; 36˚42′45.66″E) in Kiambu county, Kenya. A voucher specimen (COO-CV-2010-01) was deposited at the University of Nairobi Herbarium, Department of Botany. Identification of the plant material was done by Mr. Patrick C. Mutiso of the Department of Botany, School of Biological Science of University of Nairobi, Kenya.

2.3. Extraction and isolation of compounds

The air dried root barks (105 g) were powdered and extracted successively with 700 ml of *n*-hexane, chloroform, ethyl acetate and *n*-butanol in cold percolation. The extracts were concentrated to dryness under reduced pressure and controlled temperature (40-60℃) to afford; 4 g (3.81% w/w) *n*-hexane extract (CVR-1), 12.8 g (12.19% w/w) chloroform extract (CVR-2), 15.5 g (14.76% w/w) ethyl acetate (CVR-3) and 5.1 g (4.86% w/w) *n*-butanol extract (CVR-4). The antioxidant activities of the four extracts were determined using the enzymatic and non- enzymatic methods.

A portion of crude CVR-3 (10 g) was subjected to column chromatography on silica gel (200 g), eluted sequentially with *n*-hexane and increasing polarity with EtOAc to give six fractions (E1-E6). Fraction E2 afforded caesaldekarin C (**4**) as white amorphous solid (56 mg). Fractional crystallization in MeOH of E3 (2.4 g) afforded triacontanyl-(E)-ferrulic acid ester (**1**) as white crystalline solid (534 mg) and the mother liquor was passed through a small CC on silica gel to yield more of **1** (20 mg) and **4** (67 mg). The components of E4 and F5 (1.76 g) were comparable, thus were combined and passed through Sephadex LH-20 to afford two fractions. The first sub-fraction afforded more of **4** (43 mg) while the second sub-fraction yielded 5-hydroxyvinhaticoic acid (**5**) from *n*-hexane/dichloromethane as white amorphous solid (65 mg). Triacontanyl-*E*-caffeate (**3**) was obtained from E6 as yellowish brown solid (210 mg) as mixture of two compounds. Repeated fractional crystallization afforded **5** (106 mg) as colourless amorphous compound while preparative TLC yielded 30′-hydroxytriacontanyl-*E*-ferrulate (**2**) (54 mg).

Compound 1 (Triacontanyl-*E*-ferrulate): colourless amorphous solid, m.p 93-94℃ (uncorrected). IR (KBr) ν cm^{-1} 769, 934, 1461 (aromatic C=C), 1653 (C=C), 1730 (C=O), 3428 (OH). ^{1}H NMR (300 MHz, $CDCl_3$) δ_H: 0.90 (3H, t, *J* = 6.8 Hz, Me), 1.27 (76H, s, 38xCH_2), 3.95 (3H, s, OMe), 7.08 (1H, s, H-2), 4.21 (2H, t, J = 6.7 Hz, H-1′), 5.87 (1H, s, Ø OH), 6.31 (1H, d, *J* = 16 Hz, H-8), 6.93 (1H, d, *J* = 8.1 Hz, H-6), 7.05 (1H, d, *J* = 8.1 Hz, H-5), 7.63 (1H, d, *J* = 16 Hz, H-7). ^{13}C NMR (75 MHz, $CDCl_3$) δ_C: 14.1 (Me), 22.6-31.9 (CH_2)28, 56.1 (OMe), 64.8 (C-1′), 114.3 (C-2), 115.4 (C-8), 115.5 (C-5), 122.3 (C-6), 129.9 (C-1), 144.1 (C-7), 144.9 (C-3), 148.6 (C-4), 167.9 (C-9). HRESIMS, m/z (rel.int); 614.5274 ([M+H]+(65) $C_{40}H_{70}O_4$, 437.0 (15), 192 (10).

Compound 2 (30′-Hydroxytriacontanyl-*E*-ferrulate) brown amorphous solid, m.p 97-99℃(uncorrected), IR (KBr) ν cm^{-1} 3440, 2910, 1712, 1687, 1500, 960. ^{1}H NMR (300 MHz, $CDCl_3$) δ_H: 1.16 (56H, s, 28xCH_2), 3.66 (2H, t, *J*= 6.6 Hz, H-30′), 3.96 (3H, s, OMe), 4.21(2H, t, *J*= 6.5 Hz, H-1′), 5.88 (1H, s, Ø OH), 6.31 (1H, d, *J* = 15.7 Hz, H-8), 6.93 (1H, d, *J*= 8.1 Hz, H-6), 7.05 (1H, s, H-2), 7.09 (1H, d, *J*= 7.7 Hz, H-5), 7.63 (1H, d, *J*= 15.8 Hz, H-7). ^{13}C NMR (75 MHz, $CDCl_3$) δC: 22.7-31.9 (CH_2)28, 56.8 (OMe), 63.1 (C-30′), 64.8 (C-1′), 114.3 (C-2), 115.5 (C-5), 115.8 (C-8), 122.3 (C-6), 129.3 (C-1),144.1 (C-7), 146.4 (C-4), 148.6 (C-3), 169.9 (C-9). HRESIMS, m/z (rel. int. %) 600.5118 [M+H$^+$] (40), $C_{40}H_{70}O_5$, 194.9 (40), 176.9 (20).

Compound 3 (Triacontanyl-*E*-caffeate): yellowish brown solid m.p 113-115℃ (uncorrected). IR (KBr) ν cm^{-1}; 962, 1264 (C-O), 1513 (aromatic C=C), 1731 (C=O), 1625 (C=C), 3443, 3381 (OH). ^{1}H NMR (300 MHz, $CDCl_3$) δH: 0.89 (3H, t, *J* = 6.8 Hz, Me), 1.27 (54H, s, 27xCH_2), 1.72 (2H, quin, *J* = 6.7 Hz, H-2′), 4.20 (2H, t, *J* = 6.7 Hz, H-1′), 5.48 (1H, s, Ø OH), 6.26 (1H, d, *J* = 16 Hz, H-8), 6.87 (1H, d, *J* = 8 Hz, H-5), 6.99 (d, *J* = 8 Hz, H-6), 7.10 (1H, br s, H-2), 7.57 (1H, d, *J* = 16 Hz, H-7). ^{13}C NMR (75 MHz, $CDCl_3$) δ_C: 14.5 (Me), 22.6-30.1 $(CH_2)_{27}$, 31.9 (C-2′), 65.2 (C-1′), 100.9 (C-2), 114.0 (C-5), 115.6 (C-8), 122.4 (C-6), 127.4 (C-1), 144.1 (C-7), 145.4 (C-3), 146.4 (C-4), 167.9 (C-9). HRESIMS m/z (rel. int. %) 630.5223 [M+H$^+$] (69); $C_{39}H_{68}O_4$, 435.3 (20), 192.2 (68), 176.5 (32), 162.2 [caffeoyl]$^+$(15).

2.4. Superoxide anion scavenging activity assay

Superoxide anions activity was performed according to the method described by Martinez *et al*. [11] using xanthine-xanthine oxidase systems. About 0.1 ml of xanthine (160 µM) and 0.1 ml of nitro blue tetrazolium (320 µM) solution were added to

0.5 ml of the test samples (100 and 200 µg /ml) and standard drug (allopurinol, 20 µg/ml). The volume was made up to 1 ml with phosphate buffer (100 µM, pH 8.2). About 50 µl of xanthine-oxidase (0.04 units) was added to the system and sonicated well to start the reaction and incubated at 37°C for 30 min in water bath then stopped by addition of 0.5 ml glacial acetic acid. The amount of formazone formed was measured at 560 nm on a spectrophotometer.

2.5. Hydroxyl radical inhibition assay

Hydroxyl radical inhibition was assayed as described by Halliwell *et al*. [12]. The assay was based on quantification of the degradation product of 2-deoxyribose by condensation with thiobarbituric acid (TBA). Hydroxyl radical was generated by the Fe^{3+}-ascorbate-EDTA-H_2O_2 system (the Fenton reaction). The reaction mixture contained, in a volume of 1 ml, 2-deoxy-2-ribose (2.8 µM); KH_2PO_4-KOH buffer (20 µM, pH 7.4); $Fe_2SO_4.7H_2O$ (100 M); EDTA (100 M); H_2O_2(1.0 M); ascorbic acid (100 µM) and various concentrations of the test samples (100 and 200 µg/ml) or standard drug (mannitol, 100 µ g/ml). After incubation for 1 h at 37°C, 0.5 ml of the reaction mixture was added to 1 ml of 2.8% trichloroacetic acid (TCA), followed by 1 ml of 1% aqueous TBA and the mixture incubated at 90°C for 15 min to develop colour. After cooling to 20°C, the absorbance was measured at 532 nm against the control (reaction mixture without test sample). Percentage inhibition was evaluated based on the difference between the test sample and control.

2.6. Microsomal lipid peroxidation assay

The fractions and pure isolates were tested for their inhibitory action against microsomal lipid peroxidation in*vitro*by non-enzymatic inducers using TBA[13]. Different samples concentrations (100 and 200 µg/ml) and standard drug (α-tocopherol, 100 µg/ml) was added to the liver homogenate. Lipid peroxidation was initiated by addition of 1.5 ml of 20% aqueous acetic acid, 0.2 g of sodium dodecylsulphate and 1.5 ml TBA (1% in acetic acid). The volume of the mixture was made up to 4.0 ml with distilled water, followed by incubation at 95°C in a water bath for 60 min. After incubation the tubes were cooled to room temperature (25-27°C) and final volume adjusted to 5 ml with distilled water in each tube. Five (5.0) ml *n*-butanol-pyridine (15:1) mixture was added and the content centrifuged at 3000 rpm for 10 min. The organic upper layer was taken and optical density (O.D) of test sample tubes and control (reaction mixture without test samples) were read at 532 nm spectrophotometrically.

2.7. Statistical analyses

Results are presented as means ± standard deviation (SD). The total variation present between control and the samples and standard drugs were analyzed by one-way analysis of variance (ANOVA) using the Graph pad INSTAT and statistical significance considered at $p \leq 0.05$.

3. Results and Discussion

3.1. Phytochemical analysis

Chromatographic separation and purification of CV3 the most potent antioxidant fraction afforded triacontanyl-*E*-ferrulate(**1**),triacontanyl-**E**-caffeate (**2**), 30´-hydroxytricontanyl-**E**-ferrulate (**3**), caesaldekarin C (**4**), and 5-hydroxyvinhaticoic acid (**5**) Fig. 1. The structure of compound **4**and **5** were established based on the identical spectral data of caesaldekarin C[4]and 5-hydroxyvinhaticoic acid[4], respectively. Compounds **1**, **2**and **3**displayed the molecular structural requirement for antioxidant potential and were investigated further against the assays described earlier.

Triacontanyl-*E*-ferrulate (**1**) was obtained as a colourless amorphous solid, m.p 93-94˚C. The molecular formula was determined as $C_{40}H_{70}O_4$ on the basis of high resolution electron mass spectrometry $[M+H]^+$ m/z 614.5274. The IR spectrum of the compound indicated the presence of alcoholic and ester groups at 3428 and 1730 cm^{-1}, respectively. The presence of an absorption band at 1653 cm^{-1} suggested the presence of a conjugated group, which was supported by absorptions at 1464 and 960 cm^{-1} (conjugated double bonds). The ^1H NMR spectrum exhibited characteristic aromatic proton signals with an ABX spin system alongside a pair of downfield doublets for transvinylic protons typical of ferrulic acid moiety. In the aliphatic region, a singlet observed at δ_H 5.87 was assigned to phenolic hydroxyl proton while methoxylprotons appeared as a singlet at δ_H 3.95. Signals for a deshielded methylene (δ_H4.21, t, *J*= 6.7 Hz), a methylene envelope (δ_H1.27, s) and a methyl triplet (δ_H0.90, s), indicated the presence of a long alkyl chain. The ^{13}C NMR confirmed the presence of a 4-hydroxy-3-methoxy cinnamic derivative with resonance attributable to a carbonyl group (δ_C167.9), two deshielded oxygen bearing quaternary carbons, five methine carbons, a shielded aromatic quaternary carbon, a methoxyl carbon and an oxymethylene carbon. Subtraction of the elements of4-hydroxy-3-methoxy cinnamic ($C_{10}H_9O_4$) from the *m/z*614 left an alkyl chain of *m/z*421 equivalents to the C 40 *n*-alkyl. Therefore, the structure of compound **1**was established as triacontanyl-*E*-ferrulate, reported as new natural product.

The HRESIMS analysis of compound **2**showed $[M+H]^+$ion at *m/z*600.5118, suggesting a molecular weight of 600 equivalent to $C_{39}H_{68}O_4$and consistent with the structure of tricontanyl-*E*-

caffeate. In spite of the apparent difference between compound **1** and **2**, the ^{1}H and ^{13}C NMR spectra were almost similar except for the absence of methoxyl group in **2**.

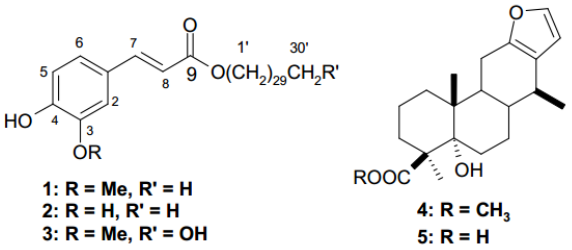

Figure 1. Compounds isolated from the ethyl acetate extract of *C. Volkensii* root bark

The spectroscopic data were in good agreement with published data for triacontanyl-*E*-caffaete (**2**)[14]. The molecular formula of 30´-hydroxytriacontanyl-*E*-ferulate (**3**) was determined from the HRESIMS spectrum as *m/z* 630.5223 which was 16 a.m.u higher than mass for **1**, which suggested additional OH group to the skeleton of **1**. Similarly, the^{1}H NMR data for **3** were comparable to that of **1** except the absence of the up field triplet for the terminal methyl and presence of two triplets of almost equal intensity and coupling constants at δ_H 4.21 and δ_H 3.66 (*J*= 6.6 Hz each) indicating two oxymethylene groups, ascribed to a methylene attached to ester linkage (Ar-OC-O-CH_2-R) and a methylene protons attached to hydroxyl groups (-CH_2OH), respectively. The signal for –OH group appeared at δ_H 3.51 (s) and a broad singlet at δ_H 1.16 showed the presence of the remaining 56H atoms for the $(CH_2)_{28}$ groups. The ^{13}C NMR was in agreement with data of 30´-hydroxytriacontanyl-*E*-ferulate[15] that confirmed the structure **3**.

3.2. Antioxidant activities

3.1.1. Antioxidant activities of the crude extracts

Antioxidant activities of the fractions from the root bark extracts of *C. Volkensii* were performed using different enzymatic and non-ezymatic assays. The effects of the test samples on superoxide anion ($O_2^{\cdot-}$) concentration was performed against xanthine-xanthine oxidase (XO) activity (enzymatic)which catalyses the generation of $O_2^{\cdot-}$and uric acid from hypoxanthine and xanthine[16,17]. The extent of XO activity was determined by the amount of uric acid formed per minute while $O_2^{\cdot-}$scavenging activity measured both enzymatically and non-enzymatically by observing the amount of formazon formed per minute[18,19]. The result for XO inhibition and $O_2^{\cdot-}$scavenging activities by *C. volkensii*extracts are summarized in Table 1. *n*-Hexane (CVR-1) and chloroform (CVR-2) exhibited significant (P≤0.05) reduction in uric acid production with an almost equivalent reduction in superoxide anion generation, though to a lesser extent compared to the ethyl acetate (CVR-3) and *n*-butanol (CVR-4). CVR-3 and CVR-4 fractions displayed significant (p≤0.05) inhibition of XO activity and $O_2^{\cdot-}$anion scavenging in the enzymatic and non-enzymatic systems, since an additional reduction of $O_2^{\cdot-}$concentration was observed from the fact that less formazon was formed in the presence of the two extracts i.e the corresponding scavenging percentage was high for the two fractions (CVR-3 and CVR-4). Inhibition of the activities of XO implies no or less $O_2^{\cdot-}$accumulation, consequently less uric acid generated. Suppose the rate of uric acid reduction equals the rate of superoxide reduction then it implies the test samples inhibit the actions of XO without any additional $O_2^{\cdot-}$scavenging activity. In case $O_2^{\cdot-}$scavenging activities predominates over inhibition of XO, then less formazon chromophores are formed ($O_2^{\cdot-}$anions are reduced) but less inhibition of uric acid (relatively high concentration) is observed.

The extracts of *C. volkensii* were examined for their ability to acts as hydroxyl radical scavenging agent. Ferric-EDTA was incubated with H_2O_2 and ascorbic acid at pH 7.4; hydroxyl radicals ($^{\cdot}OH$) were generated in free solution and detected by their ability to degrade 2-deoxy-2-ribose into metabolites that on heating with TBA and at low pH forms a pink chromogen[12]. The extracts, CVR-2, CVR-3 and CVR-4 except CVR-1 exhibited significant (P≤0.05) moderate to strong scavenging activity of hydroxyl radical (Table 1). The polar extracts CVR-3 and CVR-4 showed the highest percent (45 and 21%, respectively) scavenging activity.

Lipid peroxidation is a complex process and occurs in multiple stages. Antioxidants retard lipid peroxidation in foods andbiological systems. In the course of this investigation, TBA assay method[13]was used to detect lipid oxidation by measuring the extent of malondialdehyde (MDA) formation as the split product of an endoperoxide of unsaturated fatty acids resulting from oxidation of a lipid substrate. The results for lipid peroxidation inhibition of liver tissue (measured by the colour intensity of MDA-TBA-complex), were excellent and in the order of CVR-3>CVR-4>CVR-2>CVR-1, although CVR-1 showed insignificant (P≤0.05) reduction in MDA formed per hour per mg protein (Table 1).

Table 1.Effects of *the C. volkensii*root bark extracts and compounds on the generationof superoxide anions, hydroxyl radicals and lipid peroxidation in microsomes

Extracts (100 µg/ml)	Xanthine inhibition (XO)[a]	Superoxide anion($O_2^{\cdot-}$)		Hydroxyl Radicals ($^{\cdot}OH$)[c]	Microsomal lipid peroxidation[c]
		enzymatic[b]	Non-enzymatic[b]		
Control	223.32 ± 7.42	97.68 ± 6.14	88.95 ± 5.12	76.41 ± 5.30	87.39 ± 6.48
CVR-1	196.52 ± 5.43* (12)	84.69±6.33* (13)	77.85 ± 5.18* (12)	70.55 ± 6.00[NS] (8)	78.66 ± 5.32* (10)
CVR-2	180.89 ± 6.56 * (19)	80.14±4.88* (18)	67.73 ± 4.29* (24)	67.60±5.32* (11)	70.37 ± 5.22*(19)
CVR-3	167.49 ± 7.12* (25)	55.22±3.14* (43)	50.30 ± 2.88* (43)	42.12±4.00* (45)	57.77 ± 5.00*(34)
CVR-4	178.66 ± 7.35* (20)	70.23±5.14* (28)	63.82 ± 3.72* (29)	60.41±3.89* (21)	58.48 ± 3.97*(33)
Standard drug	103. 43 ± 6.49* (54)[d]	21.63±1.62* (78)[d]	25.43 ± 2.32* (71)[d]	40.66±2.64* (47)[e]	42.29 ± 2.84*(52)[f]
Compounds	**IC_{50} (µM)**				**[100 µM]**
1	2.08±0.03*	0.55±0.00*	0.63±0.00*	1.83±0.01*	51.06 ± 1.64(42)*
2	1.74±0.01*	0.33±0.00*	0.84±0.00*	1.65±0.01*	53.55 ± 3.09(39)*
3	2.06±0.02*	0.23±0.00*	0.87±0.00*	1.12±0.00*	50.63 ± 2.55(42)*
Standard drugs	1.34±0.00*[d]	0.20±0.00*[d]	0.51±0.00*[d]	1.85±0.01*[e]	42.29 ± 2.84(51)*[f]

Units: [a]µmol uric acid formed/min; [b]nmol formazone formed/min; [c] nmol MDA formed/h/mg protein, [d], [e] and [f] designate the standard drugs used, allopurinol (20 µg/ml), mannit ol (100 µg/ml), α-tocopherol (100 µg/ml), respectively. Values in parenthesis are percentage inhibition of free radical generation. Each value is means ± SE of six values; *values are comparable to control positive control at P≤0.05; NS are insignificant compared to control. CVR-1, CVR-2, CVR-3 and CVR-4 are *n*-hexane, chloroform, ethyl acetate and *n*-butanol crude extracts, respectively.

3.1.2. Antioxidant activities of the pure compounds

Compounds **1**, **2** and **3** exhibited strong XO inhibition at IC_{50} values 2.38, 1.74 and 2.76 µM, respectively and also showed $O_2^{\cdot-}$ scavenging activity in the enzymatic system (IC_{50} values 0.55, 0.33 and 0.23 µM, respectively) comparable to those of the standards drug allopurinol (a XO inhibitor as well as $O_2^{\cdot-}$anion scavenger, Table 1). Since the corresponding IC_{50} values of the compounds for $O_2^{\cdot-}$anion were lower than those for uric acid generation (xanthine inhibition), the compounds were considered as radical scavengers as well as XO inhibitors[17]. The higher IC_{50} values observed for the non-enzymatic system compared to the lower values in enzymatic systems indicated two-fold effects of the compounds against pro-oxidant and reactive $O_2^{\cdot-}$species.

When the three triacontanyl-*E*-cinnamoates [**1**, **2** and **3**] and mannitol were added to the reaction mixture in varying concentration, scavenging effects of ($^{\cdot}OH$) radical and prevention of the degradation of 2-deoxy-2-ribose was evidenced by the low IC_{50} values 1.83, 1.65 and 1.12 µM, respectively, comparable to the IC_{50} of mannitol (1.85 µM, standard drug) (Table 1). These results indicate that triacontanyl-*E*-cinnamoates from *C. volkensii* are the primary antioxidants compounds, which react aggressive with free radicals, particularly ($^{\cdot}OH$), thereby terminating the radical-chain reactions and retard the formation of hydroperoxides[20]. The triacontanyl-*E*-cinnamoates [**1**, **2**and **3**] isolated from CVR-3 showed inhibition of lipid peroxidation evidenced by significant (P≤0.05) reduction of MDA/h/mg protein formation on the liver homogenate reaction mixture (Table 24). The compounds [**1**, **2**and **3**] and α-tocopherol can transfer their phenolic hydrogen to a peroxy free radical of a peroxidized polyunsaturated fatty acid (PUFA), thereby breaking the radical chain reaction and preventing further peroxidation of PUFA in cellular and sub cellular membrane phospholipids[21].

The relatively antioxidant activity of these triacontanyl-*E*-cinnamoates can be attributed to the formation of stable antioxidation product from the caffeic acid moiety possessing an *O*-dihydroxy and α, β-unsaturated carbonyl that can form stabilized quinonoid intermediates[22]. The structural features of the *C. volkensii* phenolics are therefore excellent antioxidants

constituents as radical scavengers via hydrogen donation to lipid peroxyl radicals' comparable to known natural phenolic antioxidants such as quercetin, rutin or catechins[23]. Ferrulic acid esters **2**and **3**have been noted to undergo hydrogen donation to a radical and produce ferrulate radicals that couple to produce stable dihydrobenzofuran structure[22]. These facts are thus considered as the major contributors to the observed activities. However, the fatty alcohol chain effects to the polarity of the compounds might have imposed a negative influence for the assays performed in aqueous conditions. The antioxidant property of this plant has not been previously reported but the antioxidant activities in related species (*Caesalpinia sappan and Caesalpinia benthamiania*) have been documented[10,24]. This study is the first report of the presence of tricontanyl-*E*-cinnamoates in this plant alongside known cassane-type diterpenoids, phytochemically elaborated by several species of *Caesalpinia* genus.

4. Conclusions

The antioxidant activities of *n*-alkyl cinnamic acid esters observed in this study provide baseline information towards understanding the biological significance of lipophilic extract of *Caesalpinia volkensii* as antioxidants against free radical-mediated damage in the aetiology of human diseases.The result from this study thus demonstrated phyto-pharmacuetical potential of the plants as additional benefits towards its application in management of the other ailments mentioned earlier.

Acknowledgments

This research was supported by TWAS-CSIR post graduate sandwich fellowship programme. The Authors are grateful to Central Drug Research Institutes-SAIF for running the ESIMS and NMR analyses of the isolated compounds.

References

1. Beentje, H.J. (1994),*Kenya Trees, Shrubs and Lianas*; National Museums of Kenya: Nairobi, Kenya, 1994; pp 234.
2. Kuria, K.A.; De Coster, S.; Muriuki, G.; Masengo, W.; Kibwage, I.; Hoogmartens, J.; Laekeman, G.M. (2001). Antimalarial activity of *Ajuga remota*Benth (Labiatae) and *Caesalpinia volkensii*Harms (Caesalpiniaceae); in vitro confirmation of ethnopharmacological use. *J Ethnopharmcol*., 74, 141-148.
3. Ochieng, C.O.; Owuor P.O.;Manguro, L.A.O.; Akala, H.; Ishola, I.O. (2012). Antinociceptive and antiplasmodial activities of cassane furanoditerpenes from *Caesalpinia volkensii* H. root bark. *Fitoterapia.*, 83, 74-80.
4. Ochieng, C.O.; Manguro, L.A.O.; Owuor, P.O.; Akala, H. (2013) Voulkensin C–E, new 11-oxocassane-type diterpenoids and a steroid glycoside from *Caesalpinia volkensii* stem bark and their antiplasmodial activities. *Bioorg Med ChemLett.*,23, 3088–3095.
5. Kokwaro, J.O. (2009). *Medicinal plants of East Africa*; (3rdEd pg 152) University of Nairobi Press: Nairobi, Kenya,pp 218.
6. Kitagawa, I.; Simanjuntak, P.; Mahmud, T.; Kobayahi, M.; Fujii, S.; Uji, T.; Shibuya, H. (1996). Indonesian medicinal plants XII: chemical structure of caesadekarins c, d, and e, three additional cassane-type furanoditerpenes from the roots of *Caesalpinia major*(Fabaceae). Several interesting reaction products of caesadekarin a provided by N bromosuccinimide treatment. *Chem Pharma Bull*., 44, 1157-1161.
7. Bahia, M.V.; David, J.P.; David, J.M. (2010). Occurrence ofbiflavones in leaves of *Caesalpinia pyramidalis*specimens. *Quim Nova.*,33, 1297-1300.
8. Das, B.; Srinivas, Y.; Sudhakar, C.; Mahender, I.; Laxminarayana, K. (2010). New diterpenoids from *Caesalpinia*species and their cytotoxic activity. *Bioorg Med Chem Lett*., 20, 2847-2850.
9. Yodsaoue, O.; Karalai, C.; Ponglimanont, C.; Tewtrakul, S.; Chantrapromma, S. (2011). Potential anti-inflammatory diterpenoids from the roots of *Caesalpinia mimosoides* Lamk. *Phytochemistry*. 71, 1756-1764.
10. Dickson, R.A.; Houghton, P.J.; Hylands, P.J. (2007). Antibacterial and antioxidant cassane diterpenoids from *Caeaslpinia benthamiana*. *Phytochemistry*.68, 1436-1441.
11. Martinez, A.C.; Marcelo, E.L.; Marco, A.O.; Moacyr,M. (2001). Differential responses of superoxide dismutase in freezing resistant *Solanum curtibolum* and freezing sensitive *Solanum tuberosum*subjected to oxidative and water stress. *Plant Sci*., 160, 505-515.
12. Halliwell, B.; Gutteridge, J.M.C.; Aruoma, O. (1987). The deoxyribose method: A simple test tube assay for determination of rate constants for reaction of OH radicals. *Anal Biochem*., 165, 215-220.
13. Okhawa, H.; Qohishi, N.; Yagi, K. (1979) Assay for lipid peroxides in animal tissues by thiobarbituric acid reaction. *Anal Biochem*., 95, 351-358.
14. Saha, M.M.; Malik, U.K.; Malik, A.K. (1991). A chromenoflavanone and two caffeic esters from *Pongamia glabra*. *Phytochemistry.* 30, 3834-3836.

15. Doghal, M.P.; Aidroos, M.H.; Sharma, M.C.; Joshi, B.C. (1999). Ferrulic acid esters from *Plumeria bicolor*. *Phytochemistry*. 51, 319-321.
16. Salaris, S.C.; Babbs, C.F.; Voorhees, W.D. (1991). Methylene blues as an inhibitor of superoxide generation by xanthine oxidase: A potential new drug for the attenuation of ischemia/reperfusion injury. *J Biochem Pharmacol*., 42, 499-506.
17. Cos, P.; Ying, L.; Calomme, M.; Hu, J.P.; Cimanga, K.; Poel, B.V.; Pieters, L.; Vlietinck, A.J.; Berghe, D.V. (1998). Structure-activity relationship and classification of flavonoids as inhibitors of xanthine oxidase and superoxide scavengers. *J Nat Prod*., 61, 71-76.
18. Leong, C.N.A.; Tako, M.; Hanashiro, I.; Tamaki, H. (2008). Antioxidant flavonoid glycosides from the leaves of *Ficus pumila*L. *Food Chem*., 109, 415-420.
19. Bindoli, A.; Valenle, M.; Cavallin, I. (1985). Inhibition of xanthine oxidase and xanthine dehydrogenase activity. *Pharmacol Res Comm.*, 17, 831-39.
20. Frankel, E.N. (1991). Recent advances in lipid oxidation. *J Sci Food Agric*., 54, 495-511.
21. Lampi, A.; Kataja, L.; Kamal-Eldin, A.; Piironen, V. (1999). Antioxidant activities of α- and δ-tocopherols in the oxidation of rapeseed oil triacylglycerols. *J Am Oil Chem Soc*., 76, 749-755.
22. Masuda, T.; Yamada, K.; Maekawa, T.; Takeda, T.; Yamaguchi, H. (2006). Antioxidant mechanism studies on ferrulic acid: isolation and structure identification of the main antioxidation product from methyl ferrulate. *Food Sci Technol Res*., 12, 173-177.
23. Ameho, C.K.; Oliver-Chen, C.Y.; Smith, D.; S′anchez-Moreno, C.; Milbury, P.E.; Blumberg, J.B. (2008). Antioxidant activity and metabolite profile of quercetin in vitamin-E-depleted rats. *J Nutr Biochem*., 19, 467-474.
24. Badami, S; Moorkoth, S; Rai, R.S; Kannan, E; Bhojraj, S. (2003). Antioxidant activity of Caesalpinia *sappan*heartwood. *Biol Pharm Bull.*,26, 1534-1537

Available online at www.kenchemsoc.org

Journal of the Kenya Chemical Society 10-1 (2017), 10-13

JOURNAL OF THE KENYA CHEMICAL SOCIETY

Green synthesis of silver nanoparticles using *Euphorbia tirucalli* and *Catha edulis* extract

Geoffrey Otieno*, Simon Adede
Department of Chemical Science and Technology, The Technical University of Kenya
P.O. Box 52428-00200 Nairobi, Kenya
Corresponding Author: Email geoffrey.otieno@tukenya.ac.ke*, geoffrey.otieno@gmail.com

Abstract

Silver nanoparticles were synthesized using a rapid green biosynthetic method. Aqueous extract of *catha edulis* and *euphorbia tirucalli* were used in reducing silver ions to crystalline silver nanoparticles. Characterisation of silver nanoparticles was done using UV-Vis absorption spectroscopy and X-ray fluorescence. The nanoparticle diameter of silver was calculated using Mie scattering equation and found to be 35 nm and 56 nm for *euphorbia tirucalli* and *catha edulis* extracts respectively. The peak absorption wavelengths of the silver particles were found to be 425 nm for *euphorbia tirucalli* extract and 489nm from *catha edulis* extract. X-ray fluorescence analysis was used to identify elemental silver present in the sample which confirms the result that silver nanoparticles were synthesized. The total acidity of the extract were determined from potentiometric titration and were found to be 1.3×10^{-4} M for catha edulis extract and 1.5×10^{-4} M for Euphorbia extract suggesting that the higher the acidic groups in the extract the smaller the nanoparticles. This work clearly demonstrates that the method yields faster and stable silver nanoparticles and can be utilized in synthesizing this nanoparticle.

Keywords: Green Synthesis, Nanoparticles, Mie Equation

1. Introduction

Nanotechnology entails designing of chemical, physical and biological activities of substances at atomic levels (1-100 nm). Research in this area has attracted a lot of attention because nanoparticles have been found to have exceedingly better characteristics compared to their microscale counterparts (Phanjom *et al.*, 2012; Rucha *et al*., 2012) in several applications. This is due to their high surface area to volume ratio. To this end, nanoparticles have found lots of application in areas such as biomedical, optical and electrical fields (Meyer *et al*., 2009).

The methods for production of nanoparticles are generally classified as either a "bottom up" approach or a "top down" approach. In top-down synthesis, the nanoparticles are produced by size reduction of suitable starting materials (Meyer *et al*., 2009; Sepeur, 2008). Size reduction is achieved by various physical as well as chemical methods. Problems associated with top down production methods include imperfections in the surface structure of the resulting product. This pose a major limitation since the surface chemistry as well as the other physical properties of nanoparticles are mainly dependent on the surface structure (Thakkar *et al*., 2010).

In bottom up synthesis, the various nanoparticles are built up from smaller entities such as molecules, atoms and smaller particles (Shimomura and Sawadaishi, 2001). During synthesis, the nanoparticles building blocks are formed first followed by assembling to produce the final product (Thakkar *et al*., 2010). This type of synthesis mostly relies on the use of chemical as well as biological methods of production.

Optimizing nanoparticle synthesis is an immense prolific area of research. Controlling shape, distribution and size is an elegant process that depends on many variables like reactant concentration, solubility, reaction rate, reduction potential, temperature and time.

Use of chemicals in the reduction of metal ions in the liquid phase has received special attention as it results into monodispersed particles (Thakkar *et al*., 2010). Chemical reductants that are commonly used include borohydrides, aluminohydrides, formaldehyde, hypophosphites, oxalic salts and tartaric acids. Organic solvents are also employed in the chemical synthesis where they act as reducing and stabilizing functions (Shimomura and Sawadaishi, 2001). Such solvents play a key role during the synthesis of nanoparticles by binding to the surface of growing nanocrystals through the polar groups thus forming complexes with species in solutions

thereby controlling their chemical reactivity and stabilizing the formed nanoparticles. These methods of preparing nanoparticles are however, expensive and involve use of environmentally unfriendly reductants (Phanjom *et al.,* 2012). Researchers are now seeking cheaper methods of preparing these nanoparticles (Rodríguez-León *et al*., 2013; Phanjom *et al.,* 2012; Ruch*aet al*., 2012). One such option is the green synthesis route.

The use of plants in synthesis of nanoparticles are becoming the most preferred method as they are considerable rapid and often single step protocol (Dhillon *et al*., 2012;Kavitha *et al*., 2013). Moreover, according to Raveendran et al. (2003), biosynthetic routes provide nanoparticles of better defined sizes and morphology as compared to other physicochemical methods of producing nanoparticles. Additionally, nanoparticles prepared using plant extract as reducing agents as well as stabilizing agents have been found to be nontoxic and can be employed in medicine application.

Some commonly used plants in synthesis of nanoparticles have beenfound to contain therapeutic compounds (Phanjom *et al.,* 2012). Some of these compounds include broad range of water soluble plant biomolecules such as alkaloids, co-enzymes, tannins, quinines, flavonoids, phenols, and terpernoids. These biomolecules are known to mediate the reduction of ions to nanoparticles and in the stabilization of the same nanoparticles (Kavitha *et al.,* 2013). This biogenic reduction of metal ion to metal nanoparticles is quite rapid, environmentally friendly, easily scaled up and can be conducted at room temperature and pressure (Iravani, 2011). The enormous plant diversity thus presents a wide research area that requires exploitation.

In this work, silver nanoparticles were synthesized using a rapid green biosynthetic method. Aqueous extract of *catha edulis*and *euphorbia tirucalli*were used in reducing silver ions to crystalline silver nanoparticles. Characterisation of silver nanoparticles was done using UV-Vis absorption spectroscopy and X-ray fluorescence.

2. Methodology

2.1. Extraction of Plants Extracts

Fresh leaves of *catha edulis* and *euphorbia tirucalli stems* were dried in open air and crushed using a motar and pestle in the laboratory into fine powder. 100g of the powder was weighed and transferred into a conical flask. 250mls of distilled water was added and the mixture soaked at 60^{o}C for12 hours. The solution was then filtered using a Whatman filter paper then decolourised using activated carbon to obtain a clear filtrate. The total acidity of the two extracts were determined using potentiometric titrations to indicate the total reducing and stabilizing biomolecules present which are the suggested stabilizing biomolecules. The titrations were done using 0.1M NaOH.

2.2. Synthesis and Characterization of Silver Nanoparticles

1ml of 0.01M silver nitrate solution was added to 5ml of the extract to produce the nanoparticles.

The Ag nanoparticles solution also analysed in UV-Vis absorption spectroscopy, X-ray fluorescence. XRF was used to verify that the nanoparticles formed were of Ag. Uv-Vis absorption result was applied to calculate the size of the silver nanoparticles using Mie scattering theory using the equation below.

$$w = \frac{\left(\varepsilon_0 + 2n^2\right)cmu_f}{2N_c e^2 D}$$

Where;

w= full width at half maxima of the peak which follows Lorentz shape

ε_0= the frequency independent part of complex form of dielectric constant

n= refractive index of water

c= the speed of light

m= mass of electron

u_f=electron velocity at Fermi energy

N_c= number of electrons per unit volume

e^2= electron charge

D= diameter of the particle

3. Results and Discussion

3.1. Formation of Silver Nanoparticles

The formation of Ag nanoparticles was observed immediately after silver nitrate solution was introduced in *cathaedulis* and *euphorbia tiracalli* extract with the color changing from clear, to milky/cloudy and finally to brown indicating formation of the silver nanoparticles as shown in figure 1.

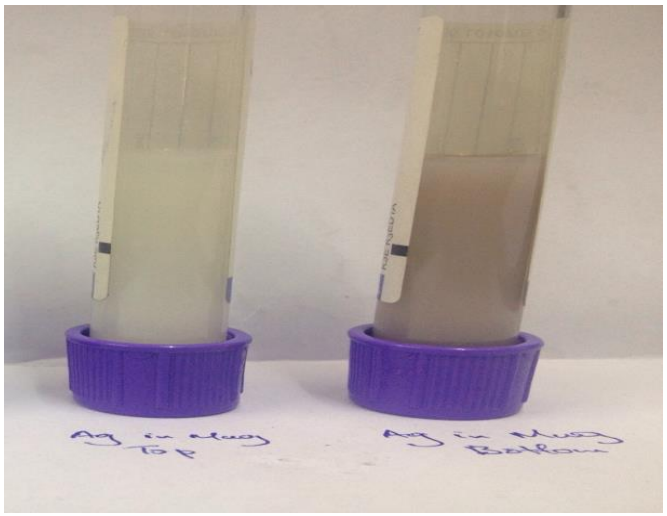

Figure 1: Image of Ag nanoparticles synthesized using *catha edulis* extract

XRF results showed an absorption peak at 2.96 *KeV*. This is the typical absorption energy for silver which further confirms formation of Ag nanoparticles.

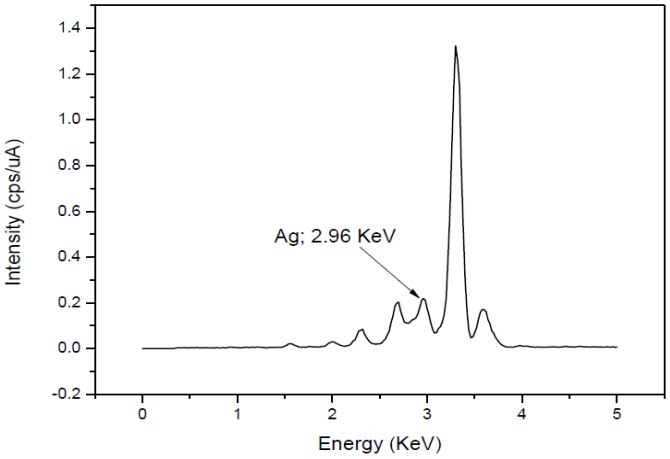

Figure 2: XRF spectrum of synthesised Ag Nanoparticle

The synthesized Ag nanoparticles formed absorb radiation in the visible region. The UV-vis spectrum (Figure 3) shows a distinct peak, centered at 425 nm for *Euphorbia tirucalli* and a similar absorption peak for *Catha edulis* was observed at 489 nm. The characteristic absorption peaks in the 400 nm region indicates the successful synthesis of Ag nanoparticles which is in good agreement with previous work reported by Rodríguez-León *et al*., 2013 and Phanjom *et al.*, 2012. From the UV-vis absorption peaks, the full width at half maximum was used in the Mie equation and the average sizes of the nanoparticles produced were determined and are presented in table 1.

Table 1: Particles sizes computed using the Mie equation

Plant extract	Calculated Diameter (nm)
Catha edulis	56±5
Euphorbia tiracalli	35±6

The results show that *Catha edulis* aqueous extract produced silver nanoparticles approximately 1.6 times larger diameter size compared to those of *Euphorbia tiracalli*. The difference was due to the types of stabilizing and reducing molecules and their concentrations.

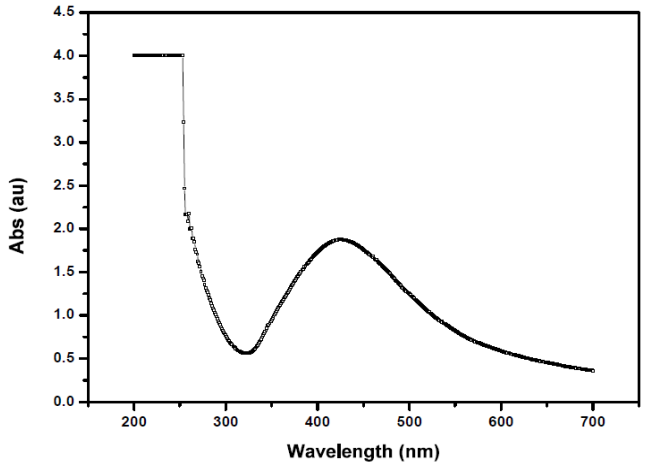

Figure 3: Absorption peak of Ag Nanoparticles synthesised using *Euphorbia tirucalli* extract

A typical potentiometic titrations curve used to determine the end-point of the titration is shown in figure 4.

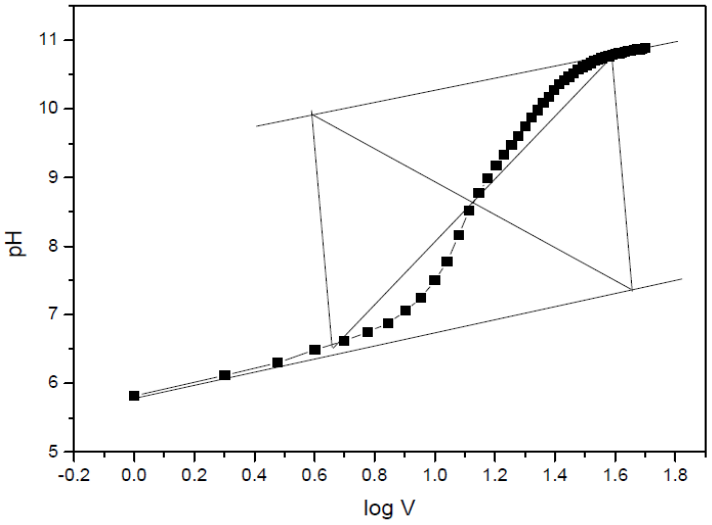

Figure 4: Potentiometric titration curve of *Euphorbia tirucalli* plants extract

From the curve, the endpoint was determined and used to determine the total acidity as shown in table 2. The results showed that the total acidity in *Euphorbia tirucalli* was higher compared to that of *Catha edulis*. This indicates that the stabilizing biomolecules such as phenols were more in *Euphorbia tiracalli* compared to that of *Catha edulis* extract.

Table 2: Potentiometric titration results for the plant extracts.

Plant Extract	Total Acidity (Molarity)
Catha edulis	$1.3\times10^{-4}\ M$
Euphorbia	$1.5\times10^{-4}\ M$

4. Conclusion

In this work we have synthesized and characterized silver nanoparticles using the plant extract of *euphorbia tirucalli* and *catha edulis* as reducing agent. The silver nanoparticle diameter was calculated using Mie scattering equation and found to be 35 nm and 56 nm for *euphorbia tirucalli* and *catha edulis* extracts respectively. The peak absorption wavelengths of the silver particles were found to be 425 nm for *euphorbia tirucalli* extract and 489 nm from *catha edulis* extract. X-ray fluorescence analysis was used to identify silver present in the sample which confirms the result that silver nanoparticles were synthesized. The total acidity of the extract were determined from potentiometric titration and were found to be 1.3×10^{-4} M for *catha edulis* extract and 1.5×10^{-4} M for *euphorbia tiracalli* extract suggesting that the higher the acidic groups in the extract the smaller the nanoparticles.

The study demonstrates that this method yields faster and stable silver nanoparticles and can be utilized in synthesizing this nanoparticle. The study recommends that further work be done on characterization of Ag nanoparticles including use of complementary methods of SEM and TEM.

References

1. Dhillon, G. S., Brar, S. K., Kaur, S., & Verma, M. (2012) Green approach for nanoparticle biosynthesis by fungi: current trends and applications *Critical reviews in biotechnology*, **32**: 49-73
2. Iravani, S. (2011) Green synthesis of metal nanoparticles using plants *Green Chemistry*, **13**: 2638-2650.
3. Kavitha, K. S., Syed, B., Rakshith, D., Kavitha, H. U., Yashwantha, R. H. C., Harini, B. P., & Satish, S. (2013) Plants as green source towards synthesis of nanoparticles. *Int. Res. J. Bio. Sci*, **2**: 66-76.
4. Meyer, D. E., Curran, M. A., and Gonzalez, M. A. (2009) An examination of existing data for the industrial manufacture and use of nanocomponents and their role in the life cycle impact of nanoproducts. *Environmental Science and Technology*, **43**: 1256-1263.
5. Phanjom, P., Sultana, A., Sarma, H., Ramchiary, J., Goswami, K. And Baishya, P. (2012), Plant-Mediated Synthesis of Silver Nanoparticles using *Elaeagnus Latifolia* Leaf Extract,*Digest Journal of Nanomaterials And Biostructures*, 7(3); 1117 – 1123.
6. Rucha Desai, Venu Mankad, Sanjeev K. Gupta, and Prafulla K. Jha. Size Distribution of Silver Nanoparticles: UV-Visible Spectroscopic Assessment. Nanoscience and Nanotechnology Letters (2012) Vol. 4, 30–34.
7. Raveendran, P., Fu, J., & Wallen, S. L. (2003) Completely "green" synthesis and stabilization of metal nanoparticles. *Journal of the American Chemical Society*, **125**: 13940-13941.
8. Sepeur, S. (2008) *Nanotechnology: technical basics and applications* Vincentz Network GmbH & Co KG.
9. Shimomura, M., & Sawadaishi, T. (2001) Bottom-up strategy of materials fabrication: a new trend in nanotechnology of soft materials *Current opinion in colloid & interface science*, **6**: 11-16.
10. Thakkar, K. N., Mhatre, S. S., & Parikh, R. Y. (2010) Biological synthesis of metallic nanoparticles *Nanomedicine: Nanotechnology, Biology and Medicine*, ***6***: 257-262.

Available online at www.kenchemsoc.org

Journal of the Kenya Chemical Society 10-1 (2017), 14-23

JOURNAL OF THE KENYA CHEMICAL SOCIETY

A Study of Elemental composition of biomass fuel from Kenyan grown Chamomile flowers extract

Joseph M. Mwaniki*, Hezron Ogutu and Kevin Gituauki.
Department of Chemistry, School of Physical Sciences,
College of Biological and Physical Sciences, University of Nairobi,
P.O. Box 30197-00100, Nairobi, Kenya.
Corresponding Author: Email*jmwaniki@uonbi.ac.ke

Abstract

The analysis of environmental emissions from the biomass fuel was done through tracing of the elemental concentration of two crucial alkali earth metals (potassium and calcium), four transition elements responsible for pollution (zinc, copper, manganese and iron), one heavy metal (lead), six trace elements (rubidium, strontium, yttrium ,Germanium, zirconium and niobium), nitrogen, phosphorus and one halogen gas (bromine) by colorimetric analysis (N-P-K), and XRF (all other elements). The elemental concentrations was analyzed in the waste flowers, compact pelletized biomass carbonized fuel and ash residue.. Concentrations of the element lead in ash implies higher than normal amount of what is expected of bottom ash, but comparable to concentrations found in fly ash of woody biomass fuels. NPK analysis suggests that chamomile biomass flowers found at Kibwezi are high in potassium (3.5%) and nitrogen content (2.6%).

Keywords: Carbonized, chamomile, XRF, colorimetry, NPK, trace elements

1.0. Introduction

1.1. Chamomile– a useful medicinal plant

Chamomile (a herbaceous plant) is a common name for three plants; German Chamomile, Roman/English Chamomile and Moroccan chamomile, all being members of the daisy family. Naturally, it grows by the roadsides and waste places. German Chamomile is quick and easy to grow, prefers full sun, grows well in poor, clay soils. Commercial cultivation is best in light, sandy loam soil with high levels of potassium. The medicinal part of the plant is the flower. Specific extracts from the flowers by steam distillation and solvent extraction have useful medical properties like anti-cancer activity [1-6], antiviral activity[7-8], antispasmodic activity[9] and sedative activity[10], anti-inflammatory activity[11], antiphlogistic[12], antiulcerogenic[13], antispasmodic[14], anti-oxidant activity[15-16], sedative effect[17]. Enhanced therapy involving combined extracts from the flowers has also been reported[18-28].

A number of products where Chamomile has been incorporated are available in the world market[29]. These include: cosmetic cream (protection and nurturing the skin-sensitive and dry, irritating skin, improves blood circulation and skin regeneration), herbal balm, gel, lipstick, hand cream, emollient foot cream, shampoo, cosmetic soap, wet towels, toothpaste, mouth wash, cosmetic tonic, cosmetic facial cream, bath salt, bath gel, herbal alcohol solution, instant tea and herbal tea

1.2. Biomass as a useful energy source

Biomass is the name given to any organic matter which is derived from plants such as wood from forests, crops, seaweed. Organic material left over from agricultural and forestry processes, and organic industrial, human and animal wastes can also be termed as biomass. It is made up of carbohydrates, contains varying amounts of cellulose, hemicellulose, lignin and small amounts of lipids, proteins, simple sugars and starches. Biomass absorbs carbon dioxide to form carbohydrates during the growing stage.

$6H_2O + 6CO_2 + \text{Radiant energy} \rightarrow C_6H_{12}O + 6O_2$

When it is burned, or used after converting it to other types of fuel such as solid, liquid, and gaseous fuels (for example charcoal, ethanol, methane), the biomass carbon reacts with

oxygen in the air to form carbon dioxide which is released into the atmosphere. If fully combusted the amount of carbon dioxide produced is equal to the amount which was taken from the atmosphere during the growing stage, so the input and output carbon is the same. As such, biomass is said to be carbon-neutral as it does not lead to increase in net carbon dioxide emissions. It is classified as a renewable energy, as it can be produced at a rate greater than it is depleted. Compared to other renewable technologies such as solar, geothermal, ocean tide or wind, biomass has few problems with energy storage. As such biomass is classified as combustible materials that can be used as an energy source. Moreover, biomass is a versatile fuel that can produce biogas (through anaerobic digestion), liquid fuels (by pyrolisis and liquefaction) and electricity (from turbines turned by pressurized steam from controlled biomass combustion). Sometimes biomass is classified as combustible materials that can be used as an energy source. Biomass is a renewable energy source because its supplies are not limited. When used as a domestic or an industrial energy source, biomass is referred to as "biofuel", short for "**bio**mass-**fuel**".

1.3. Environmental effects of biomass fuel

The emission of carbon monoxide, Volatile Organic Compounds (VOC) and methane, affect the oxidation (or self-cleaning) capacity of the troposphere by reacting with hydroxyl radicals 30.). Trace elements such as Cadmium, Cobalt, Chromium, Copper, Mercury, Manganese, *Molybdenum*, Nickel, Lead, Tin, Vanadium and Zinc, present in some biomass fuels can create a great environmental concern for heavy metal emissions when the biomass is combusted. The resulting ash can be classified into either bottom ash or fly ash. The fly ash is the one formed on boiler pipes etc while the bottom ash is found at the grate of incinerator and is non-volatile. The concentrations of each element in the fuel depends upon the source of biomass. For example, for agricultural biomass, age of plant, growing site, distance from the source of pollution generally determine the trace element fraction in the fuel while for others such as wood used in construction, past processing of the source is relevant. Volatile ash forming elements such as Chlorine, Sulphur, Sodium, Potassium, Arsenic, Cadmium, Mercury, Lead and Zinc play a major role regarding gaseous and especially aerosol (very small sized particles with diameters less than one micrometer formed during the combustion of biomass fuels) emissions as well as concerning deposit formation, corrosion and ash utilization/disposal. Ash deposits high in chlorine may cause corrosion of boiler tubes. The formation of inorganic gases and particulate matter may lead to health problems especially in rural homes of less developed countries. The gases that are formed and emitted to the atmosphere include environmentally harmful gases such as suphur dioxide and hydrogen chloride. The formation of particular matter causes deposit formation on biolers, which in turn leads to a reduction of the heat transfer efficiency to the steam system and may cause corrosion of the metallic tubes. Biomass fuels are frequently used in rural areas of the developing world, particularly Africa for cooking, compared to natural gas, kerosene and electricity. It has been reported that the use of these biomass fuels indoor causes hazardous effects on the body 31-44. The health effects of biomass smoke inhalation may not be restricted to the lungs because biomass smoke contains fine and ultra fine particles that readily cross the alveolar-capillary barrier and reach vital organs of the body through circulation and this could lead to systemic health impairment.45- 52.

1.4. Chamomile Biomass fuel.

Chamomile biomass fuel (made from the flowers of chamomile herb) was synthesized on a laboratory scale by some of the authors 53. They determined a number of parameters including the Higher and Lower calorific value of the carbonized fuel (more than 26KJ/Kg), which is higher than the typical value of uncharred biomass fuels (8-19 KJ/kg) reported in literature 54, but comparable to that of charred biofuels of between 22-30 KJ/kg 55-57. Table 1 below shows useful parameters related to the carbonized chamomile fuel From previous observations [53], the waste chamomile flowers from the solvent extraction process were noted to attract anobiid beetles during storage after the flowers were mixed with water in order to press them into shapes, in preparation for the manufacture of biomass fuel. It is therefore crucial to quantify the amounts of potassium (K), phosphorus (P) and nitrogen (N) present in the waste chamomile flowers so as to compare with the contents present in organic compost and deduce if the waste chamomile flowers (after solvent extraction) can be used as compost or organic fertilizer. Given the fact that a great deal of flowers are produced annually worldwide for aromatherapy, this research explores NPK elemental composition of the chamomile flowers and trace elemental composition of carbonized biofuel and ash.

Table 1: Data on the carbonized Chamomile biomass from previous studies[53]

Parameter	**Value**
HHV	29,379 KJ/Kg
LHV	26,662 KJ/g
Wet basis Moisture content	9.3%* (computed)
Volatile matter	71% (estimation)
Ash	13%

* Computed from the equation LHV = HHV(1-M)-2.447M [58] which can be rearranged to M = (HHV-LHV) /(HHV + 2.447) Since LHV and HHV are known.

= (estimated from the biomass weight reduction after subtracting the weight of carbonized biomass from the uncarbonized one).

2.0. Experimental

2.1. Digestion of chamomile biomass flowers.

Wet sample digestion method using 'Pyrex' glassware on an electric hot plate in a fume hood.

Procedure

1. 0.3 g of dry well ground dry chamomile flower was weighed into a clean dry 125 ml conical flask.
2. 4ml of concentrated H_2SO_4 was added and the flask swirled to ensure that all the sample was wetted.
3. This was the heated in a fume hood, the flask (and contents) on an electric hot plate set at "medium" heat setting.
4. The flask was removed cooled and 10 drops of 30% H_2O_2 were added, 3-4 drops at a time, to avoid vigorous reaction of the contents.
5. The flask was swirled, keeping contents at the bottom of the flask. It then reheated.
6. The flask was again cooled and 6 more drops of H_2O_2 were added until there was a colour change , from black to dark brown.
7. The heater was then set to high setting on the hot plate , while cooling, adding 6 drops of H_2O_2 and heating again.
8. This was done till the solution was colourless on cooling, where the last drops of hydrogen peroxide were added. A slight colouration of the digest was noticed where it was treated with activated charcoal. This then filtered and transferred into 50 ml volumetric flasks.

2.2. Determination Of Total Phosphorus content with Ph Adjustment

Reagents

1. Ammonium molybdate. $(NH_4)_2MoO_4$
2. Ammonium vanadate (NH_4VO_3)
3. Conc. HNO_3
4. Paranitrophenol
5. Conc. Ammonium solution
6. K_2PO_4

Working Solutions

1. Ammonium molybdate/Ammonium vanadate mixed reagent
2. 0.5% w/v paranitrophenol
3. 1N Nitric acid.
4. 6N aqueous ammonia.
5. Standard phosphorus solution. (1000ppm).

Procedure

1. Ammonium molybdate/Ammonium vanadate mixed reagent

2g Ammonium molybdate was dissolved in about 40 ml of distilled water warmed to about 50^0c. 0.1g ammonium vanadate was also dissolved in boiling water, cooled, and finally 1.4 ml of conc. Nitric acid was added. The two solutions were quantitatively mixed to 100ml with distilled water.

2. Para-nitro Phenol indicator

0.25g p-nitroPhenol was weighed and dissolved in distilled water and made to 50ml.

3. 1N Nitric acid

3.15ml of conc. Nitric acid was diluted to 50 ml with distilled water.

4. 6N Aqueous Ammonia

21ml of conc. Ammonia solution was diluted to 50ml using distilled water.

5. 1000ppm standard phosphorus stock solution.

1.0967g of oven dried K_2PO_4 was dissolved and made to 250ml with distilled water.

6. 10ppm P working solution

1ml of the 1000ppm standard solution was dissolved in 100ml with distilled water

Phosphorus Standards

0, 5, 10, 15, 20 and 35 ml of the standard 10ppm P solution was pipetted into a clean set of 50 ml volumetric flasks. The standard series in addition to the 2 blanks and 3 samples were treated through the steps (1-8) below. The standard P solution contains 0, 1, 2, 3, 4, 5 ppm P

Procedure

1. 2.5ml of the wet digest was pipetted into a 50 ml volumetric flask.
2. 0.2ml of 0.5% p-nitroPhenol indicator solution was added.
3. The solution was just made alkaline (yellow colour) with 6N NH3 solution by drop wise addition and gentle shaking.
4. 1N HNO_3 was added drop wise with shaking until just colourless.
5. 5ml Ammonium molybdate/Ammonium vanadate mixed reagent was added.
6. The solutions were made to 50 ml with distilled water stoppered and mixed well.
7. The absorptions were measured after 30 minutes using a colorimeter at 400nm wavelength setting.

2.3 Determination of Nitrogen Content

Reagents

1. 6M NaOH
2. Conc. H_2SO_4
3. NH_4Cl
4. Distilled water

Working Solutions

1. 1000PM N solution
2. Nesslers reagent (dipotassium tetraiodomercurate (II) in dilute sodium hydroxide)

Procedure

(a) Digestion for Nitrogen analysis

0.2 g each of well ground, oven dried chamomile flowers were placed in 3 different round-bottomed flasks and anti bumping chips added.

(b) 1000ppm N working solution

0.5107g of NH_4Cl was dissolved and made to 100ml in a volumetric flask with distilled water

(c) 10ppm working solution

1ml of the 1000 ppm N solution was pipetted into a 100 ml volumetric flask and made to the mark using distilled water.

(d) Standards

2.5, 5.0, 7.5, 10, 12.5ml of the standard 10 ppm working solution were pipetted into a clean set of 50 ml volumetric flasks. All these were treated through the Nesslerization process. The volumetric flasks after treatment contained 0.5, 1.0, 1.5, and 2.0, 2.5 ppms respectively.

(e) Direct Nesslerization

0.5 ml of digest was put into 3 different volumetric flasks.

2 drops of 6M NaOH was added followed by 2ml of nesslers reagent and made to the mark using distilled water. The absorptions of the solutions were measured using a colorimeter at 425nm after full development of blue color.

2.4. Determination of Potassium Content

Reagents

1. Stock Potassium solution –1000ppm

0.47675g (100ºC, 2hr) of dried potassium chloride was dissolved in distilled water in a 250ml volumetric flask.

2. 100ppm K working solution

10ml of the1000ppm stock solution was diluted to 100ml in a volumetric flask.

3. Standard solutions

0,0.5, 1, 2, 3, 4, 5, of the 100ppm working solution was pipetted in a set of 50ml volumetric flasks and filled to the mark using distilled water.

Procedure

3 sets of 2ml of the wet digested sample solution as pipetted into 50m volumetric flasks in addition to 2 blanks. The samples were sprayed into the flame photometer at 765.5nm starting with the standards, sample, and blank solutions. The results were taken and recorded.

2.5. Preparation Of Chamomile Fuel

The waste flowers from either steam distillation or solvent extraction of the chamomile flowers are sticky like clay if a correct amount of water is added to (or drained from) them and can therefore be molded into shapes. The biomass flowers (figure 1) used for the preparation of chamomile fuel were obtained from solvent extraction method. Controlled evaporation of the water in the biomass leaves a hard solid (figure 2) which must be stored in a sealed container as the solid is highly hygroscopic. Controlled carbonization of the biomass results in the black char (figure 3), which burns efficiently to give the ash (figure 4).

Sample procedure:

70 grams of the dried ground flower were passed through a sieve to get rid of the petals or small stones. The fine dust of the chamomile was mixed with 140ml of water then pressed into a cylindrical shape as shown in Figure 2 (using an equipment fabricated by a tinsmith). The resultant shape is the fused flower that is then dried and kept in a polythene bag to avoid absorption of excess moisture.

2.6. Analysis of the elemental concentration using XRF.

In order to ensure the data read from the XRF machine were valid, a Certified reference Material **Soil7 SRM** supplied through the International Atomic Energy Agency was run. This was to ensure that values quoted are not lower than the accepted detection limit of the machine, and also the error of the elemental concentration of the chamomile samples was within the 10% error limit.

Sample Preparation For XRF Analysis

The fused flowers, carbonized fuel and ash samples were grounded into small particles then pulverized for 15 minutes. The finely ground flowers were then passed through a sieve and the different weights taken between 0.4-0.5 grams and pressure system to 15 atmosphere with each resulting pellet having the same surface area of 4.9087 cm^2. Results are tabulated as shown in Table 6.

Figure 1: Waste Chamomile biomass from solvent extraction.

Figure 2: Compacted chamomile biomass.

Figure 3: Carbonised Chamomile fuel.

Figure 4: Ash residue.

3. Results and Discussion

3.1. N P, K, Values of Chamomile Biomass

3.1.1. Phosphorus Content

Graph 1: Calibration curve for Phosphorus

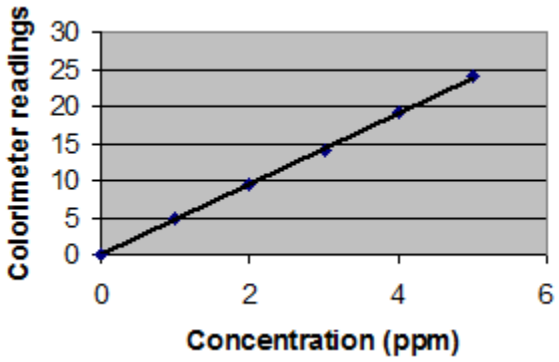

$$\textit{Ion}\ \% = \frac{\textit{Graph ppm}\ x\ 10^{-6}\ x\ \textit{Dilution Factor}\ x\ \textit{Volume of sample}}{\textit{Weight of Sample}}\ x\ 100 \quad (1)^{59}$$

Where graph ppm =concentration of ion in digest; - concentration of blank in digest

Average concentration of P in ppm =0.94, Dilution Factor = 20, Volume = 50, weight = 0.3. Therefore using equation (1) gives % P in sample as 0.313%

3.1.2. Nitrogen Content

Graph 2: Calibration curve for Nitrogen

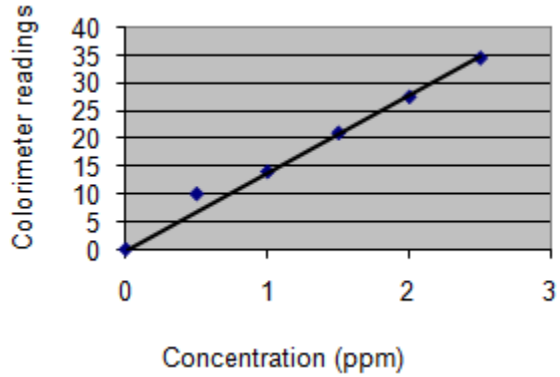

Average concentration of N in ppm =1.56, Dilution Factor = 100, Volume = 50, weight = 0.3. Therefore using equation (1) gives % N in sample as 2.6 %

3.1.3. Potassium Content

Average concentration of K in ppm =8.42, Dilution Factor = 25, Volume = 50, weight = 0.3. Therefore using equation (1) gives % K in sample as 3.5%

Comparison of N-P-K values of chamomile biomass (2.6% N, 0.313% P and 3.5% K) and other organic fertilizers (Table 2) show that chamomile flowers are rich in nitrogen and potassium.

Graph 3: Calibration curve for Potassium

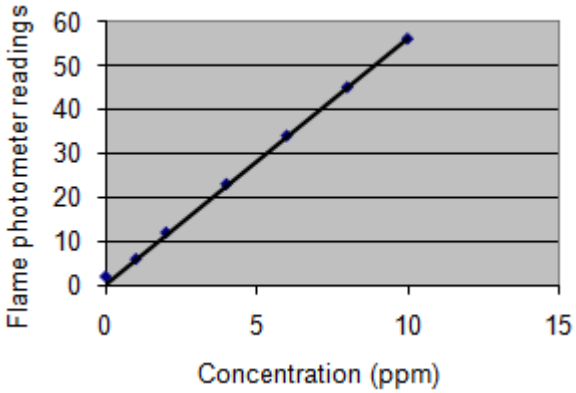

Table 2 Ref [60]– NPK values of selected organic fertilizers

Material	%N	%P	%K
Alfalfa	2.5	0.5	2
Compost	1.5 to 3.5	0.5 to 1	1 to 2
Soybean Meal (dry)	6.5	1.5	2.4
Sawdust	0.1	0.05 to 0.1	2 to 4
Mushroom Compost	0.5 to 0.8	40 to 55	0.5 to 0.8
Fish Scrap (dry)	3.5 to 12	1 to 12	1 to 1.5
Cattle Manure	0.5 to 1.5	0.2 to 0.7	0.5 to 2
Goat manure	4	0.6	1 to 2.8
Horse manure	0.7 to 1.5	0.2 to 0.7	0.6 to 0.8
Poultry manure (30% water)	3 to 4	2.5	1.5

This means that when chamomile flowers have been used for extraction of essential oil and other useful products, the use of waste flowers as organic fertilizer would greatly increase the percentage of potassium and nitrogen to the soil relative to other common organic fertilizers.

3.2. XRF Data

Table 3: Weights of biomass samples for XRF analysis

Fused flower	
Sample number	Weights (g)
1	0.4377
2	0.454
3	0.4357
Carbonized samples	
4	0.4319
5	0.434
6	0.4335
Ash samples	
7	0.4405
8	0.442
9	0.4496

Table 4: Chamomile Biomass ground Flowers

Element	Flow1 ppm	Flow2 ppm	Flow3 ppm	Avg ppm	StDev ppm
Ca	5780.00	5340.00	5640.00	5590.00	224.80
Mn	46.20	49.70	47.90	47.90	1.75
Fe	396.00	391.00	403.00	397.00	6.03
Cu	18.90	14.90	16.80	16.90	2.00
Zn	37.90	33.80	35.90	35.90	2.05
Pb	7.31	5.00	6.68	6.33	1.19
Br	19.50	17.00	17.20	17.90	1.39
Rb	8.31	6.71	7.42	7.48	0.80
Sr	32.40	30.50	31.50	31.50	0.95
Zr	6.16	3.28	4.79	4.74	1.44

Table 5: Chamomile Fused Flowers

EL	Pellet 1 ppm	Pellet 2 ppm	Pellet 3 ppm	Avg ppm	StDev ppm
Ca	4600	4430	5750	4930	718
Mn	39.60	38.40	51.10	43.00	7.01
Fe	278.00	245.00	274.00	266.00	18.01
Cu	14.50	16.10	12.00	14.20	2.07
Zn	45.80	52.70	49.50	49.30	3.45
Pb	6.52	5.02	4.10	5.21	1.22
Br	20.90	18.70	19.90	19.80	1.10
Rb	7.30	7.53	7.49	7.44	0.12
Sr	32.80	33.50	33.80	33.40	0.51
Zr	2.18	3.76	2.57	2.84	0.82

Table 6: Chamomile Biomass Carbonized fuel

Element	Pellet 1 pm	Pellet 2 ppm	Pellet 3 ppm	Avg ppm	StDev ppm
Ca	4400	5100	7050	5520	1373
Mn	58.20	41.10	78.90	59.40	18.93
Fe	501	482	739	574	143
Cu	15.50	20.70	25.00	20.40	4.76
Zn	73.90	66.70	101.00	80.50	18.09
Pb	5.97	5.67	8.81	6.82	1.73
Br	33.30	29.60	45.20	36.00	8.15
Rb	12.70	11.70	18.30	14.20	3.56
Sr	50.90	44.80	72.80	56.20	14.72
Zr	4.39	3.50	5.12	4.34	0.81

The concentration in ppm of Pb in ashed samples is comparable with that obtained of woody ash in general[61]. Other studies on woody bottom and fly ash indicate that in general, there is a significantly higher concentration of Pb in fly ash than in bottom ash [62].

Table 7: Chamomile ash

Ele	Pellet 1 ppm	Pellet 2 ppm	Pellet 3 ppm	Avg ppm	StDev ppm
Ca	87500	84700	85600	85900	1429
Mn	687	493	535	572	102
Fe	8830	10100	9930	9620	689
Cu	123.00	120.00	137.00	127.00	9.07
Zn	1970	2180	2210	2120	130.80
Pb	36.50	41.90	41.40	39.90	2.98
Br	161.00	163.00	166.00	163.00	2.52
Rb	76.00	715.00	447.00	413.00	320.90
Sr	329.00	313.00	319.00	320.00	8.08
Zr	43.60	51.40	49.90	48.30	4.14

Table 8: Chamomile Ash concentration when compared with woody bottom and fly ash.

Element (ppm)	Woody Bottom Ash [62] (ppm)	Woody Fly Ash [62] (ppm)	Chamomile Ash (ppm)
Pb	<3.0	33	39.9
Mn	492	2,383	572
Cu	12.2	98	127
Zn	348	671	2120
Fe	7,633	71,167	9620

As such care should be taken that should chamomile carbonized biomass fuel be used for household heating and cooking due to its high Net caloric value (or Lower heat Value) of 26 KJ/g, enough air should be present to avoid inhaling gases from inorganic elements such as lead, zinc and manganese.

4.0. Conclusion

The high value of potassium (3.5%) compared to organic fertilizers shows that chamomile waste can be composted, or can be sprinkled on plants with a deficiency of potassium. The elemental concentration of nitrogen and phosphorus is within range of organic fertilizers. The chamomile waste flowers had enough nitrogen and potassium quantities to be composted, so as to be used as an organic fertilizer. The manganese values (12%) are slightly above the acceptable 10% range of the SRM values, and as such should be treated with some caution. Concentration of the heavy metals especially lead in ash is comparable to what is expected in fly ash (39ppm) but higher than concentrations found in bottom ash (less than 10ppm). This means that sufficient air should be present when commercial quantities of carbonized chamomile biofuel are used for domestic cooking purposes.

Acknowledgements:

The authors would like to thank the Institute of Nuclear Science, University of Nairobi for the XRF analysis of the

chamomile samples and the Department of Chemistry for other instrumental analyses.

References

1. Birt, DF, Mitchell, D. Gold, B., Pour, P. and Pinch, HC , (1997), 'Inhibition of ultraviolet light induced skin carcinogenesis in SKH-1 mice by apigenin, a plant flavonoid.' *Anticancer Res*. **17(1A)**, 85-91.
2. Lepley DM, Li B, Birt DF and Pelling JC, (1996), 'The chemopreventive flavonoid apigenin induces G2/M arrest in keratinocytes.' Carcinogenesis. **17(11)**, 2367-75.
3. Lepley DM, Pelling JC, (1997), 'Induction of p21/WAF1 and G1 cell-cycle arrest by the chemopreventive agent apigenin.' *Mol-Carcinog*., **19(2)**,74-82.
4. Wei H, Tye L, Bresnick E and Birt DF, (1990), 'Inhibitory effect of apigenin, a plant flavonoid, on epidermal orthinine decarboxylase and skin tumour production in mice.' *Cancer Res*, **50(3)**, 499-502.
5. Panes J, Gerritsen ME, Anderson DC, Miyasaka M and Granger DN, (1996), 'Apigenin inhibits tumor necrosis factorinduced intercellular adhesion molecule-1 upregulation in vivo.' *Microcirculation*. , **3(3)**, 279-86.
6. Sato F, Matsukawa Y, Matsumoto K, Nishino H and Sakai T., (1994), 'Apigenin induces morphological differentiation and G2-M arrest in rat neuronal cells.' *Biochem-Biophys-Res-Commun*., **204(2)**, 578-84.
7. Musci I, Gyulai Z, Beladi I, (1992), 'Combined effect of Flavonoids and acyclovir against herpesviruses in cell cultures', *Acta Microbiol Hung*, **39(2)**, 137-47.
8. Critchfield JW, Butera ST, Folks TM, (1996), 'Inhibition of HIV activation in latently infected cells by flavonoid compounds', *AIDS-Res-Hum-Retroviruses*, **12(1)**, 39-46.
9. Achterrath-Tuckermann U, Kunde R, Flaskamp E, Isaac O and Thiemer K, (1980), 'Pharmacological investigations with compounds of chamomile. V. Investigations on the spasmolytic effect of compounds of chamomile and Kamillosan on the isolated guinea pig lieum', *Planta Med*, **39(1)**, 38-50.
10. Viola, H, Wasowski, C, Levi de Stein, M, Wolfman C, Silveira R, Dajas F, Medina JH and Paladini AC, (1995), 'Apigenin, a component of Matricaria recutita flowers, is a central benzodiazepene receptors-ligand with anxiolytic effects', *Planta Med*, **61(3)**, 213-15.
11. Della Loggia, R., Tubaro, A., Dri, P., Zilli, C., Del Negro, P., (1986), 'The role of flavonoids in the antiinflammatory activity of Chamomilla recutita' in *Plant Flavonoids and Medicine*. *Biochemical, Pharmacological and Structure-Activity Relationships*, Alan R Liss Inc, 481-484, Università di Trieste, Italia.
12. Jakovlev V, Isaac O, Thiemer K and Kunde R, (1979), 'Pharmacological investigations with compounds of chamomile. II. New investigations on the antiphlogistic effects of (-)-alphabisabolols and bisabolol oxides', *Planta Med*, **35(2)**, 125-40.
13. Szelenyi I, Isaac O, Theimer K, (1979), 'Pharmacological experiments with compounds of chamomile. III. Experimental studies of the ulceroprotective effect of chamomile', *Planta Med*, **35(3)**, 218-2.
14. Achterrath-Tuckermann U, Kunde R, Flaskamp E, Isaac O and Thiemer K , (1980), 'Pharmacological investigations with compounds of chamomile. V. Investigations on the spasmolytic effect of compounds of chamomile and Kamillosan on the isolated guinea pig lieum', *Planta Med*, **39(1)**, 38-50.
15. Safayhi H, Sabieraj J, Sailer ER and Ammon HP, (1994), 'Chamazulene: An antioxidant-type inhibitor of leukotriene B4 formation', *Planta Med*, **60(5)**, 410-3.
16. Rekka EA, Kourounakis AP, Koiurounakis PN, (1996), 'Investigation of the effect of chamazulene on lipid peroxidation and free radical processes', *Res Commun Mol Pathol Pharmacol*, **92(3)**, 361-4.
17. Gould L, Reddy CV, Gomprecht RF, (1973), 'Cardiac effects of chamomile tea', *J Clin Pharmacol*, **13(11)**, 475-9.
18. Tubaro, A, Zilli, C, Redaelli, C and Della Loggia R, (1984), 'Evaluation of anti-inflammatory activity of chamomile extract after topical application' *Planta Med*, **50(4)**, 359.
19. Della-Loggia, R, Tubaro, A, Redaelli, C, (1981), 'Evaluation of the activity on the mouse CNS of several plant extracts and a combination of them', *Riv Neurol*, **51(5)**, 297-310.
20. Loggia, RD, Traversa, U, Scarcia, V, Tubaro A, 1982, 'Depressive effects of Chamomilla recutita (L.) Rausch, tubular flowers, on central nervous system in mice', *Pharmacol Res Commun*, 14(2), 153-62.
21. Pasechnik, IK, (1966), 'Choleretic action of Matricaria officinalis', *Farmakol Toksikol*, **29(4)**, 468-9.
22. Kliachko LL, Ankhimova ES, Svitina NN and Iaremenko KV, (1994), 'The effect of medicinal herbs on lymphocyte rosetteforming function', *Vestn-Otorinolaringol*, Mar-Apr(2), 31-3.
23. Shipochliev T, (1981), 'Uterotonic action of extracts from a group of medicinal plants', *Vet-Med-Nauki*, **18(4)**, 94-8.
24. de la Motte S, Bose O'Reilly S, Heinisch M and Harrison F, (1997), 'Double-blind comparison of an

apple pectin-chamomile extract preparation with placebo in children with diarrhoea', *Arzneimittelforschung*, **47(11)**, 1247-9.

25. Roberts A, Williams JM, (1992), 'The effect of olfactory stimulation on fluency, vividness of imagery and associated mood: A preliminary study', *Br J Med Psychol*, **65(2)**, 197-99.
26. Nissen HP, Biltz H, Kreysel HW, (1988), 'Profilometry, a method for the assessment of the therapeutic effectiveness of Kamillosan ointment', *Z Hautkr*, **63(3)**, 184-90.
27. Aertgeerts P, Albring M, Klaschka F, Nasemann T, Patzelt-Wenczler R, Rauhut K, and Weigl B, (1985), 'Comparative testing of Kamillosan cream and steroidal (0.25% hydrocortisone, 0.75% fluocortin butyl ester) and non-steroidal (5% bufexamac) dermatologic agents in maintenance therapy of eczematous diseases', *Z Hautkr*, **60(3)**, 270-7.
28. Glowania HJ, Raulin C, Swoboda M, (1987), 'Effect of chamomile on wound healing - a clinical double-blind study', *Z Hautkr*, **62(17)**, 1262, 1267-71.
29. Bo B, (1999)University-Industry Cooperation, Chamomile Project in Kenya, UNESCO Report, 101-106.
30. Koppmann R., , von Czapiewski K. and J. S. Reid (2005), A review of biomass burning emissions, part I: gaseous emissions of carbon monoxide, methane, volatile organic compounds, and nitrogen containing compounds, *Atmos. Chem. Phys. Discuss.*, **5**, 10455–1051.)
31. Mishra V K, Retherford R D and Smith K R, (1999), Biomass cooking fuels and prevalence of blindness in India, *Journal of Environmental Medicine*, **1(4)**, 189 - 199
32. Morten A. Schei, Jens O. Hessen, Kirk R. Smith, Nigel Bruce,C John Mccrackenc, and Victorina Lopez, (2004), Childhood asthma and indoor woodsmoke from cooking in Guatemala, *Journal of Exposure Analysis and Environmental Epidemiology*, **14**, 110–S117
33. Kiraz K, Kart L, Demir R, Oymak S, Gulmez I, Unalacak M, and Ozesmi M, (2003), Chronic Pulmonary disease in rural women exposed to biomass fumes, *Clin Invest Med*, **26(5)**, 243-8.
34. Mishra V, Retherford R D, and Smith KR, (2005), Cooking smoke and tobacco smoke as risk factors for stillbirth, *International Journal of Environmental Health Research*, **15(6)**, 397 – 410
35. Işık B, Işık R S, Akyıldız L, and Topçu F, (2005), Does Biomass Exposure Affect Serum MDA Levels In Women?, *Inhalation Toxicology*, **17**, 695–697,
36. Gustafson P, Barregard L, Strandberg B and Sällsten G, (2007), The impact of domestic wood burning on personal, indoor and outdoor levels of 1,3-butadiene, benzene, formaldehyde and acetaldehyde, *J. Environ. Monit*., **9**, 23–32
37. Sharpe M, (2004), Safe as houses? Indoor air pollution and health , *J . Environ . Monit*., **6**, 46-49.
38. Ezzati M and Kammen D M (2001), Indoor air pollution from biomass combustion and acute respiratory infections in Kenya: an exposure-response study, *Lancet*; **358**, 619–24
39. See S W, Karthikeyana S and Balasubramanian R, (2006), Health risk assessment of occupational exposure to particulate-phase polycyclic aromatic hydrocarbons associated with Chinese, Malay and Indian cooking, *J. Environ. Monit.*, 8, 369–376
40. Judith T. Zelikoff, Lung Chi Chen, Mitchell D. Cohen, Richard B. Schlesinger (2002), The Toxicology Of Inhaled Woodsmoke , *Journal of Toxicology and Environmental Health, Part B*, **5**, 269–282.
41. Mishra V, , Dai X, Smith KR, Mika L (2004), Maternal exposure to biomass smoke and reduced birth weight in Zimbabwe, *Annals of Epidemiology*; **14(10)**, 740-747.
42. Ekici A, Ekici M, , Kurtipek E, Akin A, Arslan M, Kara T, Apaydin Z, Demir S, (2005), Obstructive airway diseases in women exposed to biomass smoke , *Environmental Research*;**99(1)**, 93-98
43. Neufeld LM; Haas JD; Ruel MT; Grajeda R; Naeher LP (2004), Smoky indoor cooking fires are associated with elevated hemoglobin concentration in iron-deficient women, *Pan American Journal Of Public Health*, **15 (2)**, 110-8
44. Naeher L P, Brauer M, Lipsett M, Zelikoff J T, Simpson C D, Koenig J Q, Smith K R. (2007), Woodsmoke Health Effects: A Review, *Inhalation Toxicology*, **19(1)**, 67-106,
45. Bruce, N., Perez-Padilla, R., Albalak, R., (2000), Indoor air pollution in developing countries: a major environmental and public health challenge for the new millennium, *Bulletin of the World Health Org.*, **78**, 1078-1092.
46. Albalak, R., Frisancho, AR., Keeler, G.J., (1999), Domestic biomass fuel combustion and chronic bronchitis in two rural Bolivian villages. *Thorax*, **54**, 1004-1008.
47. Fujii, T., Hayashi, S., Hogg, J.C., Vincent, R., Van Eeden, S.F., (2001), Particulate matter induces cytokine expression in human bronchial epithelial cells, *American journal of respiratory cell and molecular biology*, **25**, 265-271.

48. Honicky, R.E., Osborne, J.S., Akpom, C.A., (1985), Symptoms of respiratory illness in young children and the use of wood burning stoves for indoor heating, *Pediatrics*, **75**, 587-593.
49. Smith, K.R., Samet, J.M., Romieu, I., Bruce, N., (2000), Indoor air pollution in developing countries and acute respiratory infections in children, *Thorax*, **55**, 518-532.
50. Zhang, J., Smith, K.R., (1996), Hydrocarbon emissions and health risks from cook stoves in developing countries, *Journal of Exposure Analysis and Environmental Epidemiology*, **6**, 147-161.
51. Tesfaigzi, Y., Singh, S.P, Foster, J.E., Kubatko, J., Barr, E.B., Fine, P.M., McDonald, J.D., Hahn, F.F., Mauderly, J.L., (2002), Health effects of subchronic exposure to low levels of wood smoke in the rats, *Toxicological sciences*, **65 (1)**, 115-25.
52. Nemmar, A., Hoet, P.H., Vanquickenborne, B., Dinsdale, D., Thomeer, M., Hoylaerts , M.F., Vanbilloen, H., Mortelmans, L., Nemery, B.,(2002), Passage of inhaled particles into the blood circulation in humans, *Circulation*, **105**, 411-414.
53. Mwaniki J. M., Mbugua S. N. and Gituauki K. M., (2005), Biomass Fuel from Chamomile Waste Flowers, *International Journal of BioChemiPhysics*, **14 (1)**, 7-14
54. T. Daniela, (2004), Report, Wood Energy Programme, FAO Forestry Department, 22.
55. J. A. Fuwape and , S. O. Akindele, (1997), Biomass and Bioenergy, 12, 101-106.
56. A. E. Ghaly, A. Ergüdenler and E. Laufer, (1993), Biomass and Bioenergy, **5(6)**, 467-480.
57. A. Lucchesi and G. Maschio, (1983), Proceedings EC Contractors meeting, 289-296
58. Shariff, A, Aziz, N S M and Abdullah N, (2014) Slow Pyrolysis of Oil Palm Empty Fruit Bunches for Biochar Production and Characterisation, *Journal of Physical Science*, **25(2)**, 97-112.
59. Meghalatha, R, Ashok C, Nataraja S and Krishnappa M, (2014), Studies on chemical composition and proximate analysis of wild mushrooms, *World J Pharm Sci* , **2(4)**, 357-363
60. Penhallegon, R (2003) Nitrogen, Phosphorus, Potassium Values Of Organic Fertilizers**,** LC437 (Report)**,** Oregon State University., 1-3.
61. Pan, H. and Eberhardt, T L. (2011). "Fly ash as soil amendment," BioResources **6(4),** 3987-4004.)
62. Poykio,R., Manskinen, K., Dahl, O., Makela, M., and Nurmesniemi, H., Release of Elements in Bottom Ash and Fly Ash from Incineration of Peat- and Wood-Residues using a Sequential Extraction Procedure, Engineering and Technology 60, 1417-1421 (2011)

Appendix

Table 9: Phosphorus colorimetry data

Concentration	Reading
0 PPM	0
1 PPM	5
2 PPM	9.5
3 PPM	14.2
4 PPM	19.2
5 PPM	24.0
Blank 1	12
Blank 2	12
Sample 1	14
Sample 2	14.5
Sample 3	14.5

Table 10: Nitrogen colorimetry data

Concentration	Reading
0 PPM	0
0.5 PPM	10
1.0 PPM	14.0
1.5 PPM	21
2.0 PPM	27.5
2.5 PPM	34.5
Blank 1	0
Blank 2	0
Sample 1	18.2
Sample 2	16.0
Sample 3	16.0

Table 11: Potassium colorimetry data

Concentration	Reading
0 PPM	2
1 PPM	6
2 PPM	12
4 PPM	23
6 PPM	34
8 PPM	45
10 PPM	56
Blank 1	0
Blank 2	0
Sample 1	43
Sample 2	44
Sample 3	44

Table 12: Determination of the detection limit of the XRF machine.

Element	Peak Area	Background	Experimental	Certified	root Bg	DL EXPT	DL CERT	AVG DL
Ca	65570	4219	156000	163000	64.95383	463.6021	484.4048	474.0035
Mn	1828	2998	534	631	54.754	47.98463	56.70094	52.34278
Fe	126249	3196	22800	25700	56.53318	30.62891	34.52469	32.5768
Zn	1817	1932	93.2	104	43.95452	6.763723	7.547502	7.155612
Br	717	2480	10.3	7	49.7996	2.146175	1.458566	1.80237
Rb	4024	3018	47	51	54.93633	1.924956	2.088782	2.006869
Sr	10526	3204	104	108	56.60389	1.67779	1.74232	1.710055
Y	2336	3601	20.4	21	60.00833	1.572136	1.618375	1.595256
Zr	22215	4606	181	185	67.86752	1.658882	1.695542	1.677212
Nb	1085	5162	8.1	12	71.84706	1.609109	2.383866	1.996487
Pb	2036	2081	58.6	60	45.61798	3.93892	4.033024	3.985972

DL = Detection Limit; CERT = Certified Reference Material

Table 13: Determination of elemental error

	Soil7 SRM				
Element	**Expt'l**	**Certified LL**	**Certified UL**	**SRM Mean**	**% Change**
Ca	1.56E+01	1.57E+01	1.74E+01	1.66E+01	6%
Mn	5.34E-02	6.04E-02	6.50E-02	6.27E-02	12%
Fe	2.28E+00	2.52E+00	2.63E+00	2.58E+00	10%
Zn	9.32E-05	1.01E-04	1.13E-04	1.07E-04	8%
Pb	5.86E-05	5.50E-05	7.10E-05	6.30E-05	7%
Br	1.03E-05	3.00E-06	1.00E-05	6.50E-06	-3%
Rb	4.70E-05	4.70E-05	5.60E-05	5.15E-05	9%
Sr	1.04E-04	1.03E-04	1.14E-04	1.09E-04	4%
Zr	1.81E-04	1.80E-04	2.01E-04	1.91E-04	-1%

Available online at www.kenchemsoc.org

Journal of the Kenya Chemical Society 10-1 (2017), 24-34

JOURNAL OF THE KENYA CHEMICAL SOCIETY

Kinetics and Isothermal studies of Lambda Cyhalothrin sorption on Eburru soil in Kenya

G. A. Waswa[a], D. Andala[b] , A. O. Aluoch[c], G. N. Kamau[a],I. Michira[a] and J. K. Mbugua[a]

[a]Department of Chemistry, University of Nairobi, P.O. Box 30197-00100, Nairobi, Kenya

[b]Department of Chemistry, Multimedia University of Kenya,P.O. Box 15653- 00503, Nairobi, Kenya

[c]Department of Chemical Scienceand Technology, Technical University of Kenya, P.O. Box 52428 - 00200Nairobi-Kenya

Corresponding author's E-mail address: waswagabriel@gmail.com

Abstract

A kinetic and mechanistic study on adsorption of Lambda cyhalothrin on Eburru soils in Kenya was carried out using adsorption isothermal model. The study was carried out to predict adsorption mechanisms on Kenya soil. In this paper, Freundlich, Langmuir, Quasi-Langmuir and Temkin isotherm models were employed to correlate data from the batch mode experiments. Kinetic investigation was done under pseudo first-order conditions and fitted to second-order and intrapartical diffusion models. The results show a linearized good fit to the employed models with correlation coefficient (r^2) in the range of 0.984 – 0.999

Keywords: *Lambda-cyhalothrin, sorption, equilibrium constant, free energ*.

1. Introduction

Lambda-cyhalothrin is a pyrethroid insecticide active ingredient found in several brand name products like scimitar, warrior, matador and icon, applied in agriculture to aphids, coleopterous and lepidopterous pests, as well as in public health to control cockroaches, mosquitoes, flies and ticks. This compound,was first reported by Robson and Crosby [1], is synthesized from pyrethrum chrysanthemum flowers and photostabilized bysubstitution reactions [2,3].

The structure of Lambda-cyhalothrin shown in (Figure 1) is a 1:1 mixture of two isomers: (*S*)-α-cyano-3-phenoxybenzyl-(*Z*)-(1*R*, 3R)-3-(2-chloro-3,3,3-trifluoroprop-1-enyl)-2,2-dimethyl cyclopropanecarboxylate ('a')and (*R*)-α-cyano-3-phenoxybenzyl-(*Z*) -(1*S*,3*S*)- 3-(2-chloro-3, 3,3-trifluoroprop-1-enyl)-2,2-dimethylcyclopropanecarboxylate ('b') [4].
The compound acts as a pesticide by binding to a protein that regulates the voltage-gated sodium channel of the nervous system, preventing them from closing normally which results in continuous nerve stimulation and tremors leading to paralysis and death [5,6,7,8].

When introduced into the environment, like many other organic compounds, Lambda-cyhalothrinundergoes a number of processes, including adsorption on soils and dissipation in water, which contribute to its pollution effect. Studies on ecotoxicity of Lambda-cyhalothrin reveals it has slight to high toxicity levels to terrestrial and aquatic animals [9]. It is highly toxic to a number of fish and shellfish, the LC_{50} (96 hrs) is 210ng/L for bluegill sunfish and 0.8ng/L for sheepshead minnow [10, 11]. Weston et al., [12] studied Lambda-cyhalothrin sediment toxicity, with the median lethal concentration LC_{50} residue being 0.45µg/g which corresponds to 1.4 ng/L for pore water concentration [13].

Hence, there is need to mitigate the environmental contamination associated with the wide range use of this pesticide. The main significance of this study is to analyze the sorption properties of Eburru soils on Lambda-cyhalothrin, which could be applied as carrier materials for smart delivery of the pesticide to minimize the related environmental contamination effects.

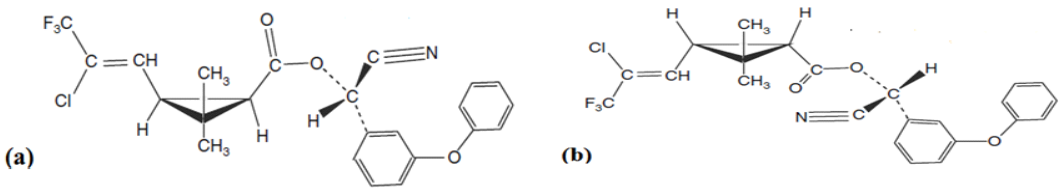

Figure 1: Structures of Lambda-cyhalothrin; (a) (S)-alcohol(Z)-(1R)-*cis*-acid, (b) (R) - alcohol (Z) - (1S) - *cis*– acid.

Sorption models

Freundlich, Langmuir, Quasi-Langmuir and Temkin models were used to assess the adsorption of Lambda-cyhalothrin onto the Eburru soils of Kenya.

Freundlich Equation

The Freundlich [14] equation is an empirical equation based on adsorption on a heterogeneous surface. The equation is commonly represented as shown in equation (1).

$$q_e = K_F C_e^{1/n} 1) \quad \text{.....(1)}$$

This can be rearranged linearly by equation 2.

$$\ln q_e = \ln K_F + \frac{1}{n} \ln C_e \quad \text{.....(2)}$$

Where C_e(mg/L) is the equilibrium concentration and q_e(mg/g) is the amount of adsorbed pesticide per unit mass of the adsorbent. The constant n is the Freundlich equation exponent that represents the parameter characterizing quasi-Gaussian energetic heterogeneity of the adsorption surface [15].K_F (L/g) is the Freundlich constant indicative of the relative adsorption capacity of the adsorbent.

Langmuir model

This model assumes that adsorption of sorbate molecules occurs on a homogeneous surface to form a monolayer with no interactions between the adsorbed molecules [16].

The Langmuir equation is representedby equation 3 as:

$$q_e = \frac{q_m K_L C_e}{1+K_L C_e} \quad \text{.....(3)}$$

Which can be expressed in a linear form as:

$$\frac{C_e}{q_e} = \frac{1}{q_m K_L} + \frac{C_e}{q_m} \quad \text{.....(4)}$$

Where: q_e (mg/g) is the amount adsorbed, C_e (mg/L) is the concentration of sorbate molecules, q_m (mg/g) is the maximum amount of adsorbed sorbate molecules per unit mass of sorbent corresponding to complete coverage of the adsorptive sites and K_L(L/mg) is the Langmuir constant related to the energy of adsorption.

Quasi-Langmuir Model

Quasi-Langmuir model is used as a compromise between Langmuir and Freundlichmodels, which is givenin equation (5) [17]:

$$q_e = \frac{K_c C_e}{1+ \alpha_c C_e^{\beta}} \quad \text{.....(5)}$$

This can be expressed in its linear form as:

$$\frac{1}{q_e} = \frac{1}{K_c C_e} + \frac{\alpha_c}{K_c} \quad \text{.....(6)}$$

Where K_c(L/g), α_c(L/mol) and β are Quasi-Langmuir constants. The value of β lies between 0 and 1. Hence plots of $1/q_e$ versus $1/C_e$from equation 6 are linear.

Temkin Isotherm Equation

The Temkin isotherm equation assumes that the heat of adsorption of all the molecules in layer decreases linearly with coverage due to adsorbent-adsorbate interactions, and that the adsorption is characterized by a uniform distribution of the bonding energies, up to some maximum binding energy [18]. The Temkin isotherm is represented by equation (7).

$$q_e = \frac{RT}{b} \ln(K_T C_e) \quad \text{.....(7)}$$

Taking $B_T = RT/b$, this can be rearranged linearly as:

$$q_e = B_T \ln K_T + B_T \ln C_e \quad \text{.....(8)}$$

Where T is the absolute temperature (K), R is the universal gas constant (8.314J/mol. K), K_T is the equilibrium binding constant (L/mg), $b$is the variation of adsorption energy (kJ/mol) and $B_T$is Temkin constant, which is related to the heat of adsorption (kJ/mol).

Therefore, plots of q_e against ln$C_e$from equation 8 should be linear.

2. Materials and methods

The following instruments, materials and reagents were used: UV-Visible spectrometer (UV-1700 model, Shimadzu Corporation, Kyoto, Japan), Analytical balance (Fischer A-160), Orbital shaker (fitted with timer), Lambda cyhalothrin pesticide (analytical standard 99% pure from IOBA Chemie), distilled water and soil samples from Eburru crater, Rift valley, Kenya (0.63S, 36.23E).

The soil samples were prepared for analysis by air drying in natural sunlight at room temperature for four days to prevent nutrient transformation, crashing, sieved using 0.85mm sieve size and stored in plastic sampling bags.

The dried soil samples were analyzed for Na, Ca and K using a flame photometer while P, Mg and Mn were analyzed calorimetrically, using theMehlich Double Acid Method [19,20].

Other trace elements Fe, Zn, and Cu and exchangeableCa and Mgwere determined by Atomic Absorbance Spectrophotometer [21].

Total organic carbon (C) was determined by calorimetric method [22]. Total nitrogen was determined by Kjeldahl method [23]. Soil pH was determined using a pH meter on a 1:1 (w/v) soil-water suspension. Exchangeable Na and K were determined by flame photometer after leaching with 1M KCl. Cation Exchange Capacity (CEC) was determined on the leachate at pH 7.0 by distillation followed by titration with 0.01 M HCl [24,25].

To carry out sorption studies, standard concentrations of Lambda-cyhalothrin pesticide were prepared by varying concentrations from 2.0, 4.0, 6.0, 8.0, 10.0, 20.0, 40.0, 60.0, 80.0 and 100.0 ppm in aqueous medium. They were scanned between 200-900nm wavelengths on the UV-Visible Spectrophotometer to determine the maximum absorption wavelength of the pesticide, which was obtained at 218 nm. Calibration curves at218nm were used to determine concentrations of other pesticide solutions. Studies on variation of time and concentrations were done by treating 1.00g of the soil with 10ml aqueous solutions each containing 10.0, 20.0, 30.0, 40.0 and 50.0ppm concentrations of Lambda-cyhalothrin pesticide. The media were shaken at room temperature for 15, 30, 45 and 60 minutes each, and then centrifuged at 10,000rpm for 10 minutes. The supernatants were then filtered using 0.22µm what-man papers and equilibrium concentration determined. Varying masses was conducted using 0.10, 0.20, 0.50, 1.0, 1.5, and 2.0 g of soil suspended in 10ml pesticide solution of concentration 50ppm, shaken for 24 hours and equilibrium concentration determined. Procedures modified from Manikandan and Subramanian (2014) [26].

To load the pesticide into the soil pores, 15g of soil was spiked with 25ml of 100ppm Lambda- cyhalothrin pesticide solution, shaken at room temperature for 24 hours, then equilibrium concentration of the remaining pesticide determined .The difference between initial concentration and equilibrium concentration gave the amount loaded in the samples. The resulting soil was dried at 100^0C for 24 hours to obtain the pesticide loaded soil samples. Desorption studies were conducted by placing 15g of pesticide loaded soil samples in 250ml separating funnels and 50ml distilled water infiltrated through at an approximate flow rate of 0.1667ml/min. 50ml distilled water was refilled every 24 hours to infiltrate the same samples for 18 days. Modified from Bansiwal*et. al.*, (2006) [27].The filtrates/elutes were collected on a daily basis prior to refilling, filtered using 0.22 µm what- man papers and equilibrium concentration determined.

The amount of Lambda-cyhalothrin pesticide adsorbed (mg/g) was calculated using equation (9)reported by Vanderborght and van Greikenm [28].

$$q_e = \frac{v(C_i - C_e)}{W} \quad \text{.....(9)}$$

Where $q_e$is the amount of solute adsorbed from the solution, v is the volume of the adsorbate, $C_i$is the concentration before adsorption, C_e is the concentration after adsorption, and w is the weight in grams of the adsorbent.

3. Results and discussion

Soil analysis

The nature of the soil greatly influences its adsorption characteristics. Table 1 shows the pH (8.38) of the soil being basic, while the low percentage of organic carbon (0.94%) supports the low degree of adsorption of Lambda-cyhalothrin onto the soil.

Table 1: Properties of the soils used in adsorption experiment

Properties	**Description**
Soil pH	8.38
Total Nitrogen %	0.10
Total Org. Carbon %	0.94
Phosphorus (Olsen) ppm	3.40
Potassium me%	0.62
Calcium me%	4.70
Magnesium me%	0.59
Manganese me%	0.20
Copper ppm	1.36
Iron ppm	13.34
Zinc ppm	10.22
Sodium me%	0.84
Electrical conductivity (mS/cm)	0.23

Absorbance curves

The absorbance curves at 218 nm for Lambda-cyhalothrin obeyed Beer's law at lower concentrations (2-10ppm) as shown in Figure 2.

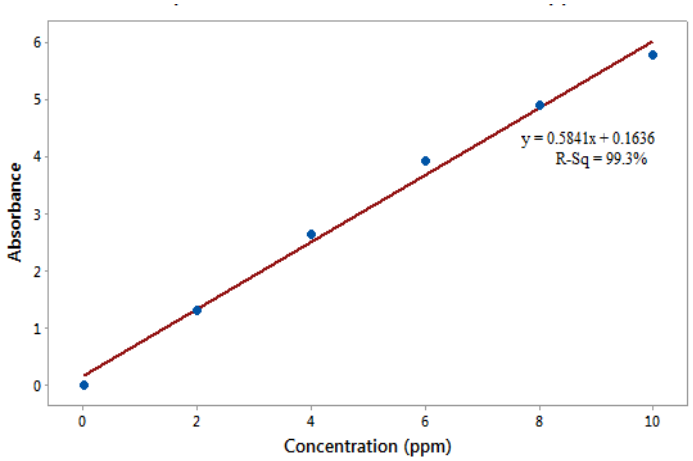

Sorption studies

Figure 3 shows the plots of Lambda-cyhalothrin varying concentration versus different shaking time.

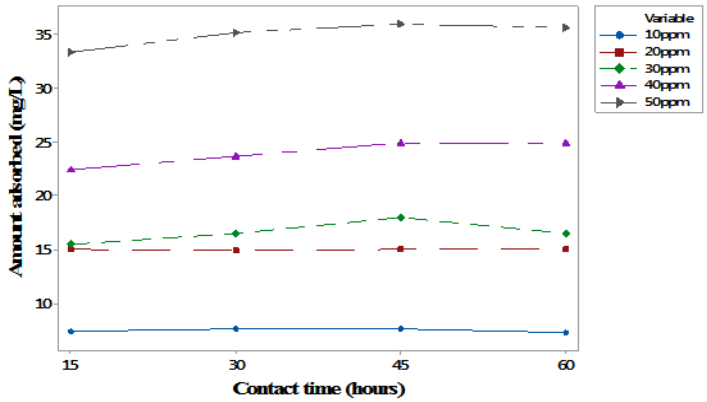

Figure 3: Concentration versus time on Lambda-cyhalothrin adsorption.

The amount of pesticide adsorbed on the soil surface increases with increase in spiking levels. This is due to the presence of the high number of vacant adsorption sites, leading to increase in concentration gradient between adsorbate in solution and the adsorbent surface. The equilibration time depends on the initial concentration of the pesticide. The lower the concentration, the shorter the time to equilibrate due to higher adsorbent surface site ratio to pesticide molecules per unit volume. Therefore increasing the initial pesticide concentration increases the amount of pesticide molecules uptake per unit mass of the soil. Variation in masses of soil reported overall positive gradient on amounts of Lambda-cyhalothrin molecules adsorbed, as shown in Figure 4.Increase in amount of soil decreased the concentration of the pesticide.

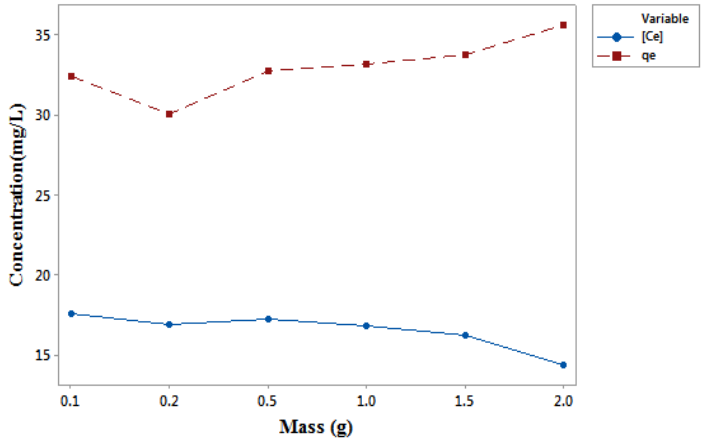

Figure 4: Effect of varying mass of soil with concentrationon Lambda-cyhalothrin adsorption

Similarly, percentage of pesticide removed from aqueous medium increased from 65 – 70% when the mass of the soil increased from about 0.2 – 2.0g (Figure 5). Increasing amounts of soil relates to increasing number of adsorption sites which generates higher adsorption gradient.

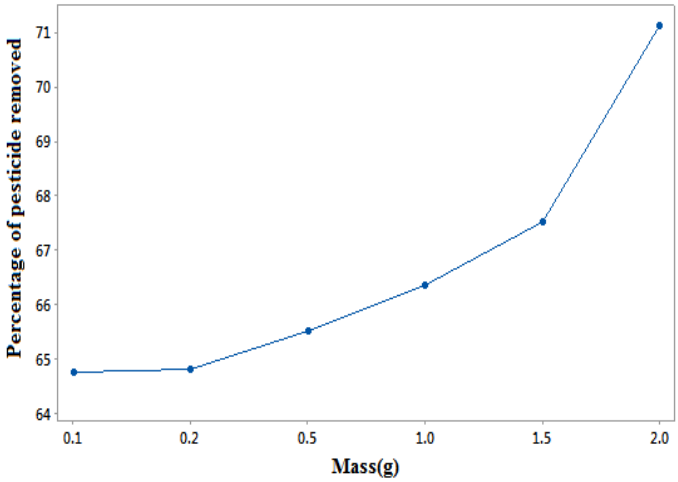

Figure 5: Percentage of pesticide removed by varying the mass of the soil

Desorption studies of Lambda cyhalothrin indicated a rapid discharge of pesticide molecules into the aqueous medium (Figure 6), with more than half of the loaded amounts desorbed within the first four days. Although the literature reported soil adsorption (Koc) for Lambdacyhalothrin (247,000 – 330,000 cm3g-1)(Table 6) is a high value, which is indicative of high preferential affinity to organic matter, only 0.94% of the soil used was the total organic content. This low organic

composition could be strongly attributed to the high initial desorption rates.

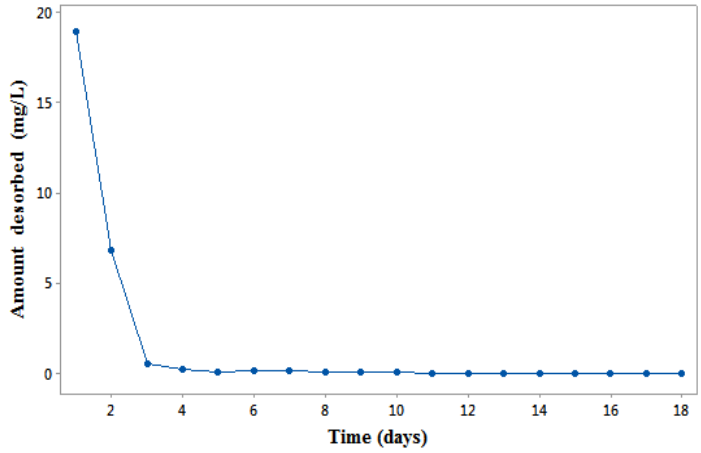

Figure 6: Variation ofamount of pesticidedesorbed with time

Adsorption isotherms

Freundlich isotherms

The Freundlich model was chosen to estimate the adsorption intensity of the sorbate on the sorbent surface. The experimental data from the batch sorption study of the Lambda-cyhalothrin pesticide on Eburru soils of Kenya were plotted logarithmically using the linear Freundlich isotherm equation as shown in Figure7 below.

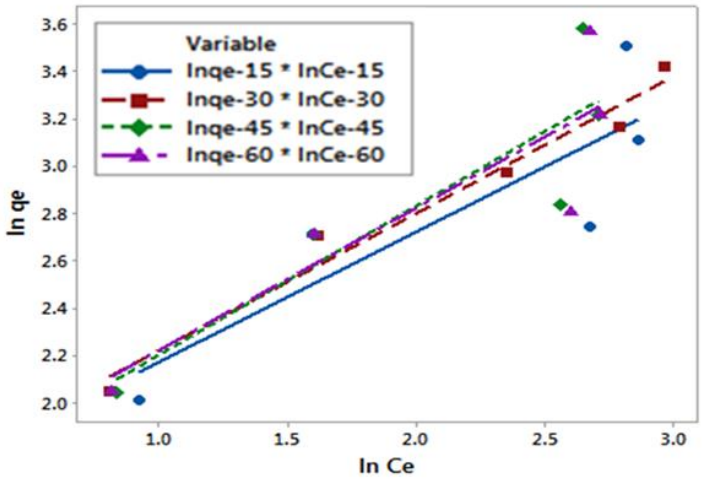

Figure 7: Linear Freundlich isotherm plot

The linear Freundlich isotherm constants for Lambda-cyhalothrin pesticide on Eburrusoils are presented in Table 2. The average Gibb's free energy of -3.9864 kJmol^{-1}indicates spontaneity in the adsorption process. Adsorption non-linearity parameter (n), which also indicates the quasi-Guassian energetic heterogeneity obtained was an average of 1.6949, while R^2 values ranged from 0.753 to 0.970, comparatively making Freundlich isotherm better definitive of lambda-cyhalothrin adsorption on Eburru soils.

Table 2: Freundlich isotherm parameters for Lambda-cyhalothrin

Time (min.)	n	K_F (L/g)	R^2	ΔG (kJmol^{-1})
15	1.8089	5.0128	0.753	-3.9938
30	1.7209	5.1397	0.970	-4.0559
45	1.5893	4.8163	0.804	-3.8947
60	1.6606	5.0279	0.786	-4.0013

Langmuir isotherms

The Langmuir model was used for a homogenous monolayer adsorption without any interaction between adsorbed molecules and uniform energies of adsorption, whose plots generated Figure 8 below.

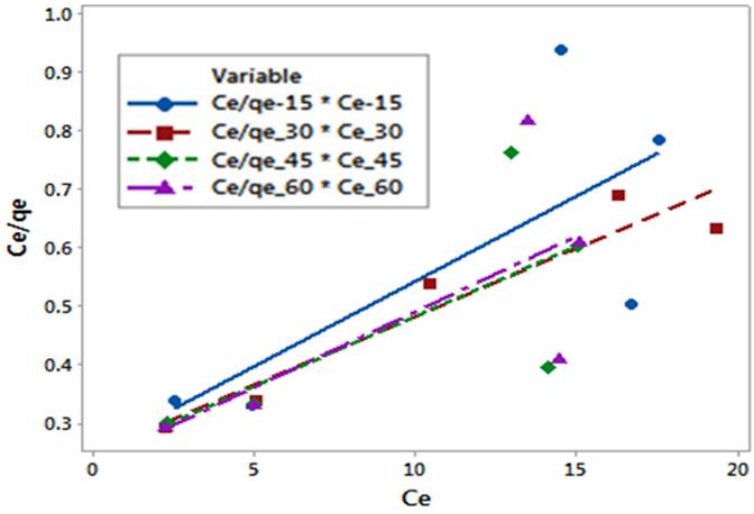

Figure 8: Linear Langmuir isotherm plots

The assumption made is that the adsorbed chemical species do not react with one another. From figure 8 above, the following constants were calculated.

Table 3 Langmuir isotherm parameters for Lambda-cyhalothrin

Time (min.)	$1/q_m$	$1/q_mK_L$	K_L(L/mg)	R^2
15	0.02910	0.2506	0.11610	0.5611
30	0.02325	0.2488	0.09344	0.9110
45	0.02490	0.2475	0.10061	0.9313
60	0.02572	0.2321	0.11081	0.4990

R^2 values ranged from 0.4990 to 0.9313, while the average value of K_L constant was 0.1052, as obtained from Table 3 above.

Quasi Langmuir isotherms

This was used as a compromise between Langmuir and Freundlich models, whose linear plots of $1/q_e$ versus $1/C_e$obtained are shown below.

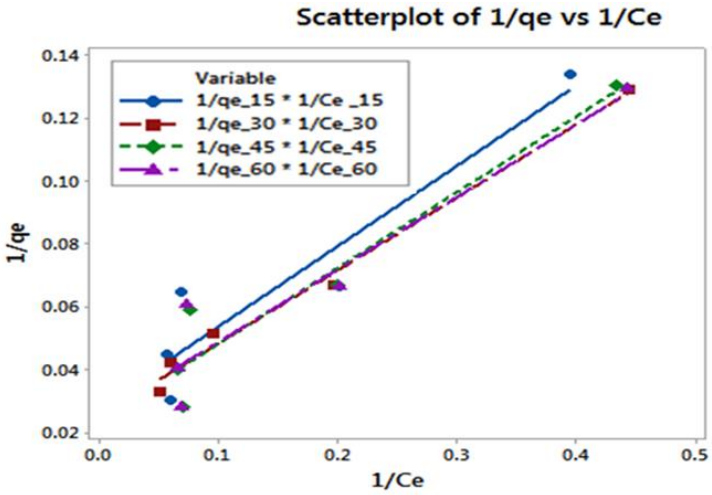

Table 4 shows the Quasi-Langmuir equilibrium constant values from the plots.

Table 4: Quasi-Langmuir isotherm parameters for Lambda-cyhalothrin

Time	$1/K_cc_e$	$1/c_e$	K_{RP} (L/g)	R^2
15	0.02910	0.2506	8.6117	0.5611
30	0.02325	0.2488	10.7011	0.9110
45	0.02697	0.2387	8.8506	0.8910
60	0.02572	0.2321	9.0241	0.4990

Quasi-Langmuir average K_c value was 9.2969, while the R^2 values ranged from 0.4990 to 0.9110 as obtained from Table 4 above.

Temkin isotherms

This was used to assume the linear decrease in the heat of adsorption of all the molecules with layer coverage, and that the adsorption is characterized by a uniform distribution of the bondingenergies.Plots of q_e against $\ln C_e$were linear.

The data in table 5 shows the Temkin equilibrium constant values from the plots.

The average equilibrium binding constant,K_T, obtained was 1.0815Lmg^{-1}, while the average Temkin constant,B_T, related to heat of adsorption was9.6253k$Jmol^{-1}$.

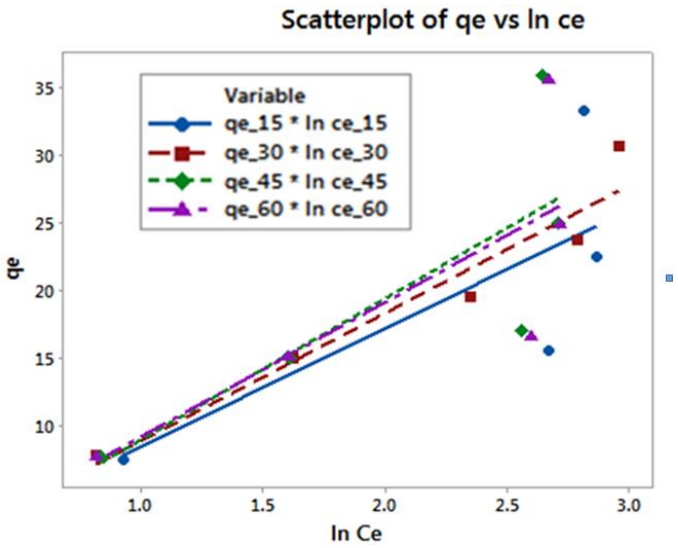

Figure 10: Linear Temkin isotherm plots

Table 5: Temkin isotherm parameters for Lambda-cyhalothrin

Time in minutes	B_T(kJ/mol)	B_TInK_T	K_T(L/mg)	R^2
15	8.740	0.284	1.033	0.614
30	9.398	0.502	1.059	0.934
45	10.42	1.487	1.153	0.640
60	9.943	0.774	1.081	0.625

Physicochemical properties

Table 6 below gives a summary of the physical, chemical and environmental properties of Lambda-cyhalothrin.

Table 6: Physicochemical properties of Lambda-cyhalothrin [4]

Properties	Description
Molecular formula	$C_{23}H_{19}ClF_3NO_3$
Molecular weight (g/mol)	449.9
Density (g/mL at 25°C)	1.33
Melting point (°C)	49.2
Boiling point (°C at 0.2 mmHg)	187–190
Water solubility (mg/L at 20°C)	0.005
Octanol–water partitioning (log *K*ow at 20°C)	7.00
Hydrolysis half-life (d): pH 5 pH 7 pH 9	 Stable Stable 8.66
Photolysis half-life (d): Water at pH 5 and 25°C Soil	 24.5 53.7
Bioconcentration factor (BCF) (fish)	2,240
Soil adsorption *K*oc (cm^3/g)	247,000–330,000
Soil degradation half-life (d)	

Aerobic soil	42.6
Aquatic degradation half-life (d) aerobic aquatic 21.9	 21.9
State at room temperature	solid
Colour: Solid solution	 Colourless yellow
CAS number	91465-08-6
US EPA PC Code	128897

Thelow water solubility and relative stability at neutral conditionscould contribute to its persistence , the high octanol-water partition coefficient (K_{ow}) indicates greater lipid partitions, while the high mean water-soil organic carbon partition coefficient (K_{oc}) indicates preferential affinity to organic matter and higher adsorption rates to particles (sediments), an aspect that may reduce its degradation rate due to unavailability to micro-organisms and sunlight when introduced in streams and rivers; but also may form the mechanisms of sediment sorption removal and mitigation of toxicity in water. A number of studies have been reported on adsorption of Lambda-cyhalothrin on different types of soils, sediments and varied contact time. Most of these data was found to fit theFreundlich isotherm. The extent of adsorption was dependent on the amount of organic matter in these soils, contact time and soil type [29,30,31,32,33,34,35].

Adsorption Kinetics

Kinetic studies was used to analyze sorption dynamics and mechanisms while pseudo-first and secondorders were used to determine the rate constants and orders of sorption processes.

Pseudo-First-Order Model

Pseudo-first-order Kinetic model of Lagergren [36] is based on the solid capacity forsorption analysis and is expressed as given in equation 10.

$$\frac{dq_t}{dt} = kf(q_e - q_t) \quad \text{.....(10)}$$

where qt is the amount of adsorbate adsorbed at time t (mg/g), kfis the rate constant ofpseudo-first-order kinetics (min) and t is the time (min). The integration of equation 10 withthe initial condition, qt =0 at t = 0 leads to the pseudo-first-order rate equation:

$$\ln(q_e - q_t) = lnq_e - kft \quad \text{.....(11)}$$

A straight line of ln(qe −qt) versus t suggests the applicability of this kinetic model.Pseudo-first-order rate constant (kf) (1/min) can be determined from the slope of the plot.Figure 11and Table 7shows plotsfrom experimental data.

Table 7: *Pseudo*-first order kinetic parameter

Concentration(ppm)	$\ln q_e$	K_f	R^2
100	0.3872	0.02939	0.996
200	1.240	0.03338	0.831
300	1.828	0.03652	0.746
400	2.162	0.07138	0.957
500	2.929	0.07230	0.980

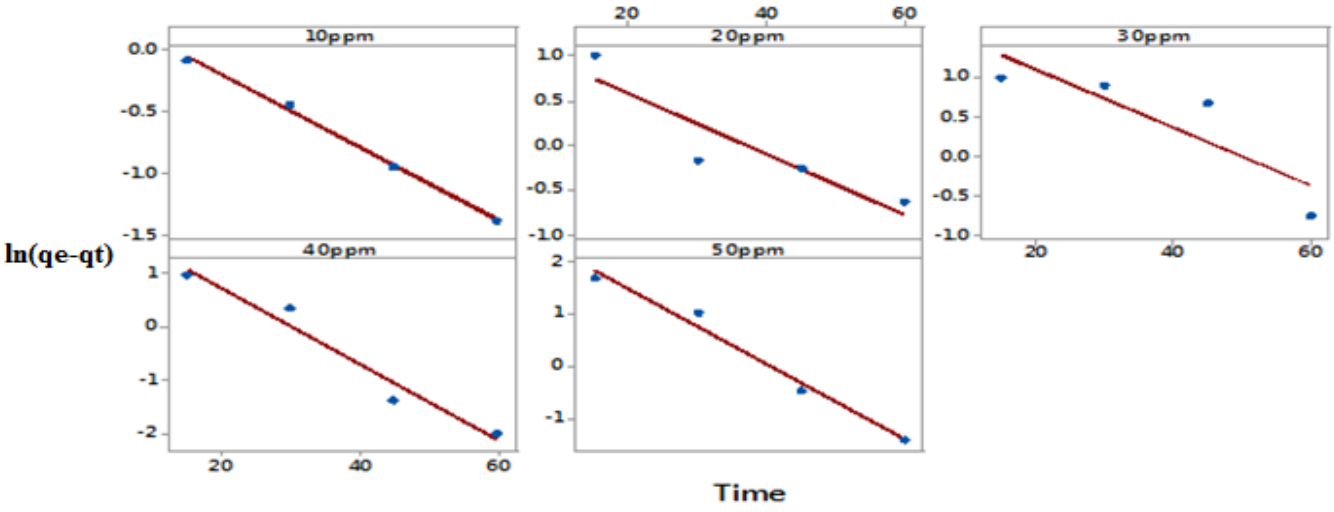

Figure 11: *Pseudo*-first order model plot

Pseudo-second-Order Model

The pseudo-second order reaction kinetic model based on the sorption equilibriumcapacity can be expressed by equation 12[37],

$$\frac{dq_t}{d_t} = ks(q_e - q_t) \quad \text{.....(12)}$$

where k_S is the pseudo-second-order rate constant (g/mg min). Integrating equation 12 andnoting that q_t =0 at t = 0, the following equation is obtained:

$$\frac{t}{q_t} = \frac{1}{ksq_e} + \frac{1}{q_e t} \quad \text{.....(13)}$$

The plot t/qt versus t gives a straight line if second-order kinetics are applicable,whereqe and ks can be determined from the slope and intercept of the plot, respectively. Theinitial sorption rate, h (mg/g min), as $t \rightarrow 0$ can be defined as

$$h = ksq_e^2 \quad \text{.....(14)}$$

The straight line plot for the *pseudo*-first-order sorption kinetic model betweenln($q_e - q_t$) vs. t was plotted (Figure11) for sorption of Lambda cyhalothrin. The value of the rate constantcalculated from the slope of plotsranged from 0.02939 to 0.07230 min^{-1}. The linear plots of *pseudo*-second-order kinetic model was also plotted between t/qt. vs. t, and sorption capacity and *pseudo*-second-order rate constants q_e and $k_s$werecalculated from the slope and intercept of the plot (Figure 12).

Table 8: *Pseudo*-second-order kinetic parameter

Conc.(ppm)	$1/k_sq_e$	$1/q_e$	k_s(g/mg min)	h(mg/g min)	R^2
100	0.06786	0.1281	1.8877	115.0363	0.999
200	0.03781	0.0665	1.7588	397.7161	0.997
300	0.0782	0.06061	0.7751	210.9935	0.984
400	0.09594	0.03846	0.4009	271.0301	0.999
500	0.09525	0.026682	0.2801	393.4380	0.987

The *pseudo*-second-orderkinetic constant $k_s$and sorption capacity $q_e$ranged from1.8877 to 0.280 $gmg^{-1}min^{-1}$ and 7.8064 to 37.47845 mgg^{-1} between 100 to 500ppm respectively. Coefficient of determination values ranged from 0.984 to0.999, a good illustration of the pesticide adsorption having followed *pseudo*-second-orderrate expression. Additionally, initial sorption rates, h,increased from 115.0363 – 393.438 $mgg^{-1}min^{-1}$between 100 to 500ppm respectively, as shown in Table 8.

Intraparticle Diffusion Model

Theintra-particle diffusion was determinedusing the intra-particlediffusion modelgiven in equation (15).

$$q_t = k_{id}t^{\frac{1}{2}} + I \quad \text{.....(15)}$$

where k_{id} is the intra-particle diffusion rate constant. According to equation 15, a plot of $q_t$versus $t^{1/2}$should be a straight line with a slope k_{id} and intercept I when adsorptionmechanism follows the intra-particle diffusion process as shown in Figure 13.

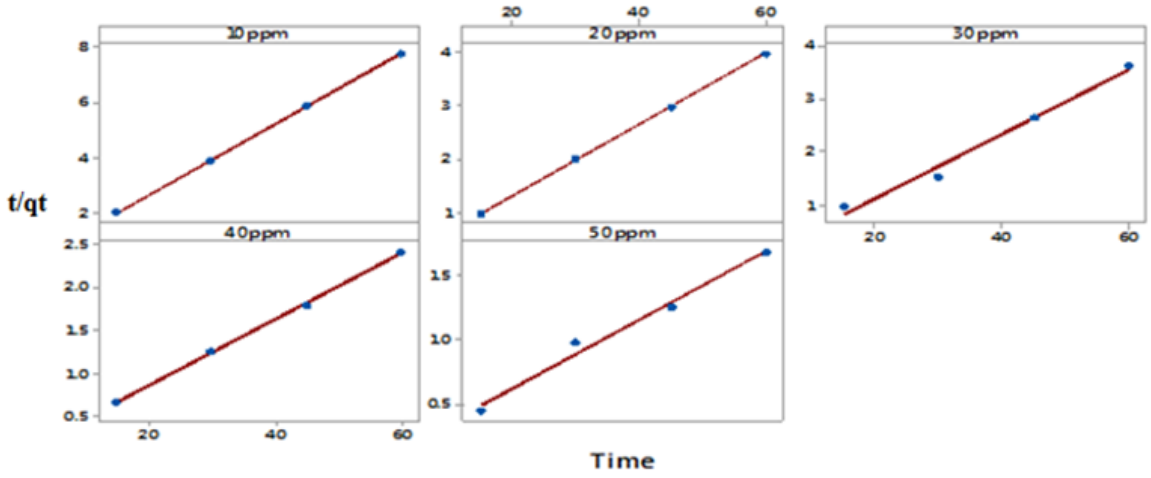

Figure 12: Pseudo second order model plot

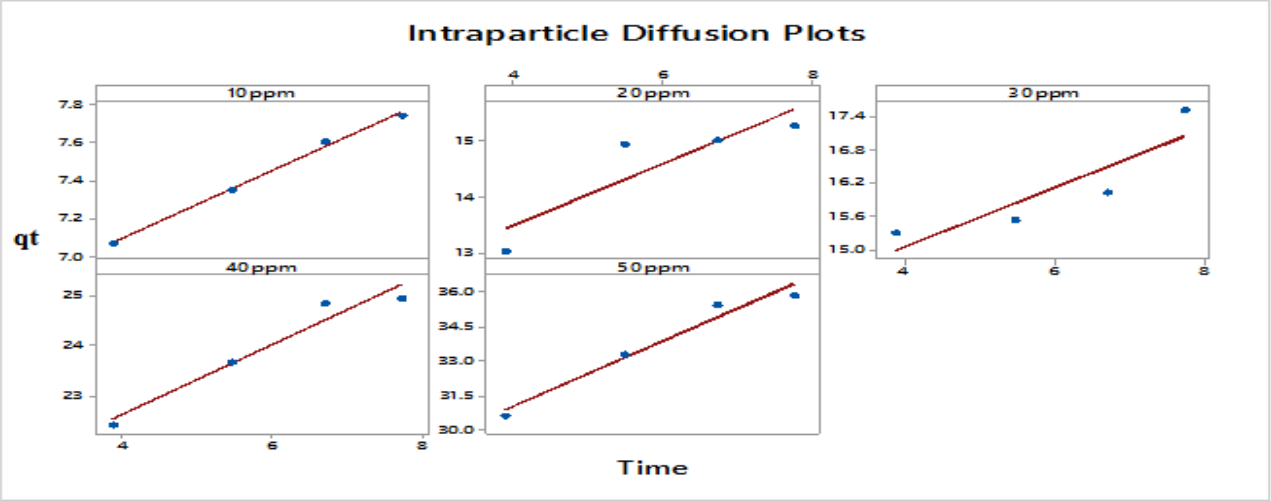

Figure 13: intra-particle diffusion model

The data obtained from the plots in Figure 13 above are summarized in Table 9.

Table 9: Intra-particle diffusion model parameters

Concentration(ppm)	I	k_{id}	R^2
100	6.386	0.1770	0.995
200	11.32	0.5458	0.796
300	12.90	0.5357	0.787
400	19.84	0.6953	0.953
500	25.37	1.4200	0.961

Lower regression values were obtained with the plots not passing the origin. The values for k_{id} and *I* were in a range of 0.177 – 1.42 and 6.386 – 25.37 respectively. *'I'*values are usually directly proportional to the thickness of the boundary layer[38]. Deviation of the lines from the origin is attributed tothe differences in the rate of mass transfer in the initial and final stages of adsorption, indicating that pore diffusion may not be the only rate controlling step [39].

4. Conclusion

The present study has shown that Lambda-cyhalothrin has a moderateadsorption capacity on Eburrusoils. This weak adsorption capacity is due to its low organic content. Also this adsorption behavior of Lambda-cyhalothrin depends significantly on the properties of the soil; like organic carbon, clay contents, organic matter and pH.The negativefree energydemonstrated by the Freundlich isotherm illustrates that the pesticide adsorbs onto Eburru soils spontaneously, althoughit's also shown to be affected by the solute concentration. In conclusion, the study recommends Eburru soil to be used for carrier materials in smart delivery of Lambda-cyhalothrin pesticide for improved agronomic practice.

Acknowledgement

The authors thank Kenya Bureau of Standards for availing the Lambda-cyhalothrin standard, Kenya Agricultural and Livestock Research Organization for soil analysis and the University of Nairobi, where this analysis was conducted.

References

1.Robson M. J and Crosby J., (1984). Insecticidal product and preparation thereof.European Patent Office.Patent Number EU 106469. UK.

2.Spurlock F., (2006). Synthetic pyrethroids and California surface water: use patterns, properties, and unique aspects. http://wwwcdprcagov/docs/sw/swposters/spurlock_acs06pdf.

3.Syngenta (2007). KARATE. http://wwwsyngentacom/en/products_services/karate_pageaspx .

4.Li-Ming H., John T., Albert W and Kean G., (2008). Environmental Chemistry, Ecotoxicity, and Fate of Lambda-Cyhalothrin.*Reviews of Environmental Contamination and Toxicology*.71 .Springer.

5.Bradbury S. P and Coats J. R., (1989). Toxicokinetics and toxicodynamics of pyrethroid insecticides in fish. Environ ToxicolChem 8:373–380.

6.Shafer T. J and Meyer D. A., (2004). Effects of pyrethroids on voltage-sensitive calcium channels: a critical evaluation of

strengths, weaknesses, data needs, and relationship to assessment of cumulative neurotoxicity. ToxicolApplPharmacol 196:303–318.

7.Burr S. A and Ray D. E., (2004).Structure-activity and interaction effects of 14 different pyrethroids on voltage-gated chloride ion channels.ToxicolSci 77:341–346.

8.Fernandez-Alvarez M, Sanchez-Prado L, Lores M, Llompart M., Garcia-Jares C, Cela R., (2007).Alternative sample preparation method for photochemical studies based on solid phase microextraction: synthetic pyrethroid photochemistry. J Chromatogr A Adv Sample Prep 1152:156–167.

9.Roessink I, Arts G. H. P, Belgers J. D. M, Bransen F, Maund S. J, Brock T. C. M., (2005). Effects of lambdacyhalothrin in two ditch microcosm systems of different trophic status. Environ ToxicolChem 24:1684–1696.

10.USDA, (2007). USDA-ARS Pesticide Properties Database: http://www.ars.usda.gov/Services/docs. htm?docid=14199.

11.USEPA, (2007). ECOTOX database.http://cfpubepagov/ecotox/quick_queryhtm.

12.Weston D. P, You J. C and Lydy M. J., (2004). Distribution and toxicity of sediment-associated pesticides in agriculture-dominated water bodies of California's Central Valley. Environ Sci Technol. 38:2752–2759.

13.Amweg E. L, Weston D. P, You J and Lydy M. J., (2006). Pyrethroid insecticides and sediment toxicity in urban creeks from California and Tennessee. Environ SciTechnol 40:1700–1706.

14.Freundlich H.M.F., (1906). Over the adsorption in solution. J. Phys. Chem. 57, 385–470.

15.Bansal R.C and Goyal M., (2005). Activated Carbon Adsorption, Boca Raton, Crc Press Taylor Francis Group.

16.Langmuir I (1918). The Adsorption of Gases on Plane Surfaces of Glass, Mica, and Platinum. J.A.M. Chem. Soc. 40, 1361-1403.

17.Redlich O. and Peterson D.L., (1959). A useful adsorption isotherm. J. Phys. Chem. 63, 1024–1029.

18.Temkin M. J and Pyzhev V., (1940). Kinetics of ammonia synthesis on promoted iron catalysts. ActaPhysiochim.Urs. 12, 217-222.

19.Mehlich A., (1953). Determination of P, Ca, Mg, K, Na, and NH4. North Carolina Soil Test Division (Mimeo 1953); 23-89.

20.Tran T. S and Simard R. R., (1993). Mehlich III-Extractable Elements. In: M. R. Carter, Ed. Soil Sampling and Methods of Analysis: 43-49.

21.Yang S.Y and Chang W.L., (2005). Soil Sci., 170, 55.

22.Gislason E.A and Craig N.C., (2005). Cementing the foundations of thermodynamics:comparison of system-based and surroundings-based definitions of work and heat, J. Chem.Thermodynamics 37: 954-966.

23.Jan-Åke P, Mårten W and Stephen O., (2008). Handbook for Kjeldahl Digestion:11- 42.

24.Carrolland Dorothy "Ion exchange in clays and other minerals". Geological Society of America Bulletin 70 (6): 749-780 (1959).

25.Turner R. C and Clark J. S., (1966). Lime potential in acid clay and soil suspensions. Trans. Comm. II & IV Int. Soc. Soil Science, pp. 208-215.

26.Manikandan A and Subramanian K. S. (2014). Fabrication and characterization of nanoporous zeolite based N fertilizer. African Journal of Agricultural Researc. Vol. 9(2): 276-284.

27.Bansiwal A. K; Rayalu S. S; Labhasetwar N. K; Juwarkar A. A and Devotta S (2006).Surfactant-modified zeolites as slow release fertilizer for phosphorus. J. Agri. Food Chem. 54:4773-4779.

28.Vanderborght M and Van Grieken E., (1997). "Enrichment of trace metals in water by adsorption on activated carbon," *Analytical Chemistry*, vol. 49, no. 2, pp. 311–316.

29.Gupta S, Handa S. K and Sharma K. K., (1998). A new spray reagent for the detection of synthetic pyrethroids containing a nitrile group on thin-layer plates.Talanta 45:1111–1114.

30.Wang S, Kimber L, and Kennedy I. R., (1997). The dissipation of lambda-cyhalothrin from cotton production systems. J Environ Sci Health B B32:335–352.

31.European-Commission, (2001). Review report for the active substance lambda-cyhalothrin. 7572/VI/97-final.http://ec.europa.eu/food/plant/protection/evaluation/existactive/list1-24_en.pdf.

32.Ali M. A and Baugh P. J., (2003). Sorption-desorption studies of six pyrethroids and mirex on soils using GC/MS-NICI. Int J Environ Anal Chem 83:923–933.

33.Oudo H, Hansen H. C., (2002). Sorption of lambda-cyhalothrin, cypermethrin, deltamethrin and fenvalerate to quartz, corundum, kaolinite and montmorillonite. Chemosphere 49:1285–1294.

34.Zhou J. L, Rowland S and Mantoura C., (1995). Partition of synthetic pyrethroid insecticides between dissolved and particulate phases. Water Res 29:1023–1031.

35.Bondarenko S, Putt A, Kavanaugh S, Poletika N and Gan J. Y., (2006). Time dependence of phase distribution of pyrethroid insecticides in sediment. Environ ToxicolChem 25:3148–3154.

36.Lagergren S., "ZurTheorie der sogenannten Adsorption gelosterStoffe," KungligaSvenskaVetenkapsakademiens, Handlingar 24, 1-39 (1898).

37.Ho Y. S., (2006). "Review of second order models for adsorption systems," *J. Hazard.Mater*. 136, 681-689.

38.Anirudhan T.S and Suchithra P.S., (2012). "equilibrium, kinetic and thermodynamic modelling for the adsorption of heavy metals onto chemically modified hydrotactile', Ind. J. Chem. Technol, vol.17, pp.247-259.

39.Kannan K, and Sundaram M. M., (2001). "Kinetics and mechanism of removal ofmethylene blue by adsorption on various carbons e a comparative study," *DyesPigments* 51, 25

Available online at www.kenchemsoc.org

Journal of the Kenya Chemical Society 10-1 (2017), 35-39

JOURNAL OF THE KENYA CHEMICAL SOCIETY

Concentration of Selected Nutrients and Heavy Metals in river Nyamasogota, Kisii County-Kenya

Omwancha Priscilla Nyaboke, Jane Igoki Murungi, Alphonse Wanyonyi Wafula

[1]Department of Chemistry, Kenyatta Univeristy, P.O. Box 43844-00100 Nairobi, Kenya

*Correspondence author:*E-Mail: wafula.alphonse@ku.ac.ke*

Abstract

Water contamination and hence quality deterioration in Kenya is becoming more and more a menace to the natural water resources due to modern methods of farming and industrialization. River Nyamasogota, a source of water for domestic purposes and growing crops, passes through areas that have many tea farms where fertilizers are heavily used and drainage end up from tea factories was investigated for possible pollution by inorganic, organic and microbial substances. This was done by determining the levels of lead, copper and nutrients in river water and compared with the limits set by World Health Organization and Kenya Bureau of Standards. Two heavy metals (lead and copper) were investigated in river Nyamasogota during dry and wet seasons using atomic absorption spectrophotometry techniques. Samples were obtained three times each season in water from river Nyamasogota. The levels of nitrates and phosphates were determined using UV-VIS spectrophotometer. The results for levels for heavy metals in river Nyamasogota ranged from 0.100±0.015 to 0.202±0.034in mg/L for lead with dry season having highest levels. The copper levels in mg/L ranged from 0.127±0.016 to 0.312±0.013 and were significantly higher than the recommended level of 0.05 mg/L. Nitrates, concentration in river water for both seasons in mg/L ranged from 0.206±0.021 to 0.358±0.015; p = 0.605. Nitrate levels remained within acceptable limits for both seasons. Phosphate concentration for both seasons in river Nyamasogota in mg/L ranged from 0.232±0.021 to 0.524±0.023. Levels of phosphates were significantly higher than the standard value during wet season ($p<0.05$). Results showed high levels of copper and phosphates in river Nyamasogota water which may cause eutrophication to the river with time and have negative health implications to human and animals. Based on the findings of this study, strategies should be put in place to prevent further contamination of water in river Nyamasogota in Kisii County, especially during wet season.

Keywords: heavy metals, phosphate, nitrate and eutrophication

1. Introduction

Majority of problems that mankind is confronting in the 21st century is identified with water quantity and water quality. Water pollution is among the most substantial environmental problems (Carson et al., 2002). Water pollution is the deteriorating quality of water for example in rivers, lakes, streams, seasand groundwater. Ecological degradation of this type happens when contaminants are directly or indirectly released into water bodies with no satisfactory remedy to eliminate poisonous compounds (Goel, 2006). Boyd and David (2010) points out that there are more toxic chemical run offs dumped into water bodies every year. Some of these pollutants include nitrates, nitrites, phosphates and heavy metals such as copper, cadmium and lead which are introduced into rivers through industrial effluents and agricultural run-offs (Prabodanie et al., 2010).

Water resources in Kenya are continuously being polluted by inorganic, organic and microbial matter (Kithiia, 2006). The effect of contamination on water resources is evidenced by the poor water quality which gives rise to water noxiousness to mammals and marine life; loss of artistic value by becoming unfit for recreational activities, waterborne illnesses, high charge of water purification, eutrophication, deoxygenation, acid rain and habitat modification (Palaniappan et al., 2010)

It is estimated that approximately half of all patients admitted to African hospital beds experience the ill effects of water-borne ailments because of lack of access to treated water and sanitation (Nagajyoti et al., 2010). Prone or exposed

subpopulations may face substantial health problems from water-related diseases at reduced levels of introduction to waterborne pollutants than the overall community (United Nations Centre for Human Settlements, 1995). The quality of water is worsening because of inorganic anions and cations being discharged from residential and modern effluent, by the year 2030 when Kenya is envisaged to have achieved an industrial economy, industrial and domestic water will be a rare asset. The vast majority of the groundwater will be profoundly contaminated and a portion of the water bodies will be covered by vegetation as an outcome of eutrophication and render the water unfit for human consumption (Kithiia and Khroda, 2011).

Gathumbi et al., (2013) found out that most farmers apply large amounts of fertilizers and pesticides which contributes to elevated levels of lead and copper in the river water hence harmful to human consumption. This was according to a study conducted in Kirinyaga South District, to measure the levels of copper (Cu) and lead (Pb) in fish and soil deposits from areas growing horticultural produces. While doing a study on impacts of fertilizer residues on river Kuywa, Omwoma et al., (2011) established that fertilizer residues notably nitrates and phosphates get washed into river Kuywa during rainy season posing danger to the community. Magena area is located along river Nyamasogota and is known as a tea giant estate in Ogembo district. It produces 6 million kgs per year of green leaf taken to Ogembo tea factory which receives 15 million kgs of green leaf per year(KTDA, 2016).

In the upper lands, the major activities include animal production, garden weeding and spray, motor bike and car washing that contain high levels of heavy metals especially lead that are expected to be transported to the river water during rainy season (wet) as the land slopes towards Nyamasogota river. The land adjacent toriver Nyamasogota has less human activities due to the fact that most farmers have planted tea near the river. Near river Nyamasogota, fishing, car, motor bike washing and making of bricks are the major human activities conducted. In Magena area there is also Ogembo tea factory and Nyamache coffee factory which could attribute to release of effluents to river Nyamasogota. These activities could be sources of pollution to river Nyamasogota hence the need for this study.

2. Materials and Methods

The study area covered an area of 50 $km^2$with an estimated population of 30,000 people and the length of river Nyamasogota of about 29 km from Kiango to river Gucha. Three factor randomized block design was used in sampling where land above the tea farms, tea farms, adjacent land and river Nyamasogota were considered as separate blocks. Each block had three sampling points. 9 samples were obtained at every visit. Sampling was done thrice every season totalling to 36 samples. Samples were collected during the dry season in February 2016 and repeated during the wet season in April 2016 season. Water was sampled using 2 literplastic bucket with distances between sampling points of 200 m and 1 kmbetween sections at 50 cm depth below surface.

2.1. Preparation of samples

The water samples were mixed with 100 ml of concentrated nitric acid for preservation and to keep the metal in solution.Water samples were filtered using Whatman 4.5 µm filter paper. 20 ml of water from each sample was digested with 5 ml nitric acid in a beaker using a heating block digestion while adding a few drops of 30% of hydrogen peroxide and further heated until fumes ceases. The solution was filtered and topped to 100 ml mark of volumetric flask and solution was ready for analysis (Jackson, 1999). Analysis was done at Kenya Institute of Research and Development laboratories one day after preparation of samples.

2.2. Preparation of stock and standard solution

Copper standards were prepared by carefully weighing 1.901 g of copper nitrate of analytical grade and dissolved in deionized water and diluted to 1 litre in a volumetric flask. The resulting solution was completely acidified with 10 ml of 5M nitric acid and further diluted to 500 ppm standard solution then followed by diluting to 1 ppm, 2 ppm, 3 ppm, 4 ppm and 5 ppm.
Lead standards were prepared by carefully weighing 0.800 g of lead nitrate of analytical grade and dissolving it in deionized water and diluted to 1 litre in a volumetric flask. The resulting solution was completely acidified with 10 ml of 5M nitric acid and further diluted to 500 ppm standard solution then followed by diluting to 1 ppm, 2 ppm, 3 ppm, 4 ppm and 5 ppm.

All standards were run under the same conditions as the samples and used to prepare calibration curves of absorbance versus concentration which were used to determine the concentration of respective samples. Atomic Absorption spectroscopy (AA 6300 Shimadzu) was used for analysis of the heavy metals.It consists of hollow cathode lamp with a tungsten anode and a cylindrical cathode sealed in glass tube that is filled with neon and argon at a pressure of 1 to 5 torr. Ionization of the inert gas occurs when a potential of 300v was applied across the electrodes.A lead hollow cathode lamp was used as a radiation source, operated at a current of 5 MA, Slit

width of 0.1 nm, the wavelength was set at 324.7 nm resonance line. The fuel flow rate of air-acetylene flame was set at 4 L/min^{-1}

Phosphates were determined using molybdenum blue method where 100 ml of water sample was digested in a beaker at 150 ^{0}C with 1 ml concentrated sulfuric acid (H_2SO_4) and 5 ml concentrated nitric acid (HNO_3) and evaporated to dryness using sun bath for 30 minutes. The residue was then leached with 5 ml 1NHNO_3 and transferred to a 50 ml volumetric flask. A volume of 5 ml of 10% ammonium molybdate was added followed by addition of 5 ml of 0.25% ammonium vanadate in 6N HCl. The mixture was diluted to the mark with distilled water and left to cool for 10 minutes.

Phosphate standards were prepared by carefully weighing 2.200 g of A.R potassium dihydrogen phosphate (KH_2PO_4) in distilled water and diluted to 1 litre to give a solution containing 500 mg/L of phosphorous. 500 ml of phosphorous solution was diluted to prepare standards containing 10 mg/l phosphorous. 1,2, 5 and 10 ml aliquots of the 10mg/l phosphorous standards were taken to give 0.01, 0.02, 0.05 and 0.10 mg of phosphorous. The standards were treated in the same manner as the sample solution and were used to determine the molybdenum absorbance for the range of the phosphorous.

Nitrates were determined using spectrophotometric method with sodium salicylate where the nitrate ions and sodium salicylate reacted in an alkaline media to form a yellow sodiumnitrosalicylate which was determined spectrophotometrically at 420 nm. Reagents of analytical grade and only distilled water was used. 0.5g of AR grade sodium salicylate was dissolved in distilled water and diluted to 100 mlmark volumetric flask. Also 400g AR sodium hydroxide pellets and 16g AR potassium sodium tartrate was dissolved using distilled water in a plastic beaker then nitrate stock solution was prepared using 1.37 g AR sodium nitrate which was dissolved in distilled water topped to 1 litre.

The nitrate stock solution was prepared daily and disposed after use. The standard solutions in the range 1.0, 3.0, 6.0, 9.0 and 12.0 mg/ L in 50.0mlwere prepared in the same way and made to the mark of the 100 ml volumetric flasks. The solution was then transferred to 100 ml flask beakers. Blank solution was also prepared in similar manner containing 50 ml of distilled water and then analyzed using UV-VIS spectrophotometer.

The UV-VIS spectrophotometer consists of a light source, holder of the sample and diffraction grating in a monochromator to separate different wavelengths of light. Samples were placed in cuvettes of path length 10mm.

2.3. Procedure

UV-VIS spectrophotometer was set at a wavelength of 420 nm. 2 ml of sodium salicylate was added to standard solution and evaporated to dryness in an oven at 100±0.5^0 C. The residue was cooled in a desiccator, 2 ml of sulphuric acid was added and the solution allowed to stand for 10min. 15ml of distilled was added followed by 15 ml of sodium hydroxide solution cooled constantly and transferred to 100 ml one-mark volumetric flask topped with distilled water. Shaking was done and the absorbance of the solution were measured using a calibrated spectrophotometer at 420 nm after taking the zero reading using a blank test solution. The sample was also prepared in a similar manner without adding the nitrate solution and its absorbance was measured. Absorbance reading of the calibration standards were plotted against the concentrations.

One-way ANOVA was used to compare the means at 95% confidence level using SPSS 16 for windows.The paired sample test was used to compare the means in the levels of the copper, lead, nitrates and phosphates between dry season and wet season and between the four sections of sample collection.Whenever a significant difference existed the means were compared at p=0.05 significance levels which accounts for errors, using paired sample test and one sample t-test since a sample was used to represent a population (Salvador *et al*., 2007).

3. Results and Discussion

Tables 1.1 shows the levels of heavy metals in river Nyamasogota water.From table1.1levels of lead in river Nyamasogota water varied between seasons, with a mean of 0.109±0.016 mg/Land a range of 0.100±0.015 to0.169±0.017 mg/Lin the dry season and 0.084±0.032 mg/L and a range of 0.070±0.029 to0.202±0.034 mg/L in the wet season. However, levels in both seasons did not deviate significantly from the recommended value of 0.1 mg/L (p= 0.835 for the dry season and *p*= 0.711 for the wet season). The concentration of lead in water was therefore within the acceptable standards as shown in **figure 1.1**.Copper mean levels in water were 0.142±0.011 mg/L with a range of 0.127±0.016 to0.252±0.017 mg/ L with higher levels in

Table 1.1: Concentration of lead and copper in river Nyamasogota water

	Dry season				Wet season			
	N	Mean (mg/l)	Range	Variance	N	Mean (mg/l)	Range	Variance
Lead	9	0.109	0.100-0.169	0.004	9	0.084	0.070-0.202	0.014
Copper	9	0.142	0.127-0.252	0.013	9	0.175	0.156-0.312	0.019

Table 1.2 Concentrations of Nitrates and Phosphates in River Nyamasogota Water

	Dry season				Wet season			
Nutrient	N	Mean (mg/l)	Range	Variance	N	Mean (mg/l)	Range	Variance
Nitrates	9	0.248	0.206-0.291	0.002	9	0.256	0.216-0.358	0.01
Phosphates	9	0.288	0.232-0.524	0.056	9	0.319	0.279-0.518	0.04

Nyamasogota river water during the wet season as compared in the dry season. During the dry season, the levels of copper were not significantly higher than the recommended value ($p=0.053$). However, levels of copper in the wet season were significantly higher than the recommended value of 0.05 mg/L ($p=0.033$).This indicates that the runoff from farms may have contributed to the copper levels in Nyamasogota river.

Table 1.2 shows levels of nutrients in river Nyamasogota water. From table 1.2 The mean nitrate levels in Nyamasogota river water was 0.248±0.010 mg/L with a range of 0.206±0.021to0.291±0.019 mg/L during the dry season and a mean of 0.256±0.019 mg/L with a range of 0.216±0.019 to0.358±0.015 mg/L during wet season.The levels of nitrates in river Nyamasogota water did not vary significantly between the dry and wet seasons ($p=0.605$). Both dry and wet season means were significantly lower than the recommended value of 0.5mg/l ($p<0.05$) and were therefore within the acceptable limits as shown in figure 1.0. Levels of phosphates in river Nyamasogota water ranged from 0.232±0.021 to 0.524±0.023 mg/L with a mean of 0.288±0.024 during dry season and a range of 0.279±0.022 to 0.518±0.023 mg/L with a mean of 0.319±0.021 mg/L during wet season. phosphate levels were significantly higher in the wet season than the dry season ($p=0.045$). The levels of phosphates in wet season were significantly higher than the recommended value of 0.025mg/L ($p<0.05$) as shown in figure 1.2.

Table 1.3: Percentage recovery of copper, lead, phosphates and nitrates

Elements	Unspiked sample in ppm	Spiked sample in ppm	% Recovery
Pb	1.86	6.83	99.2
Cu	0.88	5.82	99.1
NO_3	0.14	5.03	99.4
PO_4	0.40	5.35	99.2

Table 1.3 shows the percentage recovery of copper, lead, phosphates and nitrates

The results show that the samples were well prepared, efficiently handled and without contamination and the instruments used for analysis were accurate since the percentage recovery was almost 100 %.

4. Conclusion

The results show evidence of the presence of selected nutrients and heavy metals in river Nyamasogota water. In particular from the results there is elevated levels of phosphates and copper in river Nyamasogota in wet season as compared to dry season. There is significant difference in the levels of copper during wet season as compared to recommended value of 0.05 mg/L ($p=0.033$). Higher levels of phosphates are present in river Nyamasogota as compared to recommended value of 0.025 mg/L ($P<0.05$). Although some of the levels were lower than those set by WHO and KEBS, these does not warrant safety for residents of Magena area since they can accumulate to levels that are detrimental to health. The findings show need to address the implications of elevated levels of copper and phosphates and initiate strategies to reduce to acceptable levels.

Acknowledgements

The authors thank the Research, Planning and Extension (RPE) of Kenyatta University (KU) for funding this work and as well the Chemistry department, KU for laboratory space.

References

1. Boyd, D. R. and David Suzuki Foundation. (2010). Dodging the Toxic Bullet: How to Protect Yourself from Everyday Environmental Health Hazards. *Vancouver Greystone Books*, 78-104.
2. Carson, R., Darling, L. and Darling, L. (2002). Silent Spring. Boston: Houghton Mifflin.

3. Gathumbi, J. K., Kanja, L. W., Maitho, T. E., Nduhiu, J. G., Gitau, F. K., Nderitu, J. G., Lucy, M.W. and Maloba, K. (2013). Assessment of Lead and Copper in Fish and Soil Sediments in Kirinyaga South District, Kenya. *Journal of Applied Sciences in Environmental Sanitation*, 145.
4. Goel, P. K. (2006). Water Pollution: Causes, Effects and Control. New Delhi: New Age International.
5. Jackson, S. J., (1999). Documentation of Variable Trace- and Rare-Earth-Element Abundances in Carbonates from Auriferous Quartz Veins in Meguma Lode-Gold Deposits, Nova Scotia. *Canadian Mineralogist*,**37**, 469-488.
6. Kithiia, S.M. and G.O. Khroda. (2011). Sediments Yields and Transport Within The Nairobi River Basins, Kenya: In River, Coastal and Estuarine Morphodynamics. Beijing: Tsinghua University Press.
7. KTDA. (2016). Ogembo Tea Factory Company Limited. Retrievedfrom http://www.ktdateas.com/index.php/factories-regions/230-ogembo-tea-factory-company-limited.html on December 2, 2016.
8. Omwoma, S, Wesley, N, Lalah, J.O, Ongeri M.K and Okinda P.O. (2011). Impact of Agronomic Inputs in Sugarcane Farming on River Kuywa Surface Water Quality Traversing Sugarcane Zones in Western Kenya. National Council for Science and Technology of Kenya Conference on Dissemination of Research Results, 05/2011.
9. Nagajyoti, P. C., Lee, K. D. and Sreekanth, T. V. M. (2010). Heavy Metals, Occurrence and Toxicity for Plants: A Review. *Environmental Chemistry Letters*,**8**(3), 199–216.
10. Palaniappan, M., Gleick, P. H., Allen, L., Cohen, M. J., Christian-Smith, J., Smith, C. and Ross, E. N. (2010). *Clearing the Waters: A Focus on Water Quality Solutions*. Retrieved from UNEP, Nairobi on August 8, 2016.
11. Prabodanie, R. A., Raffensperger, J. F. and Milke, M.W. (2010). A Pollution Offset System for Trading Nonpoint Source Water Pollution Permits. *Environmental and Resource Economics*,**66**, 68-70.
12. Salvador, R., Suckling, J., Schwarzbauer, C. and Bullmore, E. (2007). Undirected Graphs of Frequency-Dependent Functional Connectivity in Whole Brain Networks. *Philosophical Transactions of the Royal Society B: Biological Sciences*, **360**, 937–94610.1098/rstb.2005.1645.
13. United Nations Centre for Human Settlements. (1995). Habitat Debate. Nairobi, Kenya: UNCHS (Habitat).
14. World Health Organization, WHO (2006). Guidelines for Drinking Water Quality, Recommendation Geneva, Switzerland.

Available online at www.kenchemsoc.org

Journal of the Kenya Chemical Society 10-1 (2017), 40-57

JOURNAL OF THE KENYA CHEMICAL SOCIETY

Preliminary Studies for Evaluation of a Fibre Optical Nano Chemical Sensor for Selected Carcinogenic Compounds

Pamela Khakasa Butalanyi[1], Jackson Kiptoo[2], Anam Onditi[3], Dickson Andala[4], W. Bulimo[5], B. K Mwanza[6] and J. K. Muchuna[7]

Department of Chemistry, School of physical science[1, 2, 3, 7],
The Jomo Kenyatta University of Agriculture and Technology, P.O Box 62000-00100,
Nairobi; Multimedia University, Department of Chemistry[4], P.O Box Nairobi, Department of Biochemistry
University of Nairobi[5,6], P.O Box 30197 Nairobi..
E-mail: butalanyipk@googlemail.com
*Correspondence author:*E-Mail: butalanyipk@googlemail.com*

Abstract

Developing a suitable selective, optical nano chemical sensor for carcinogenic organic pollutants, namely anthracene (ANTH), benzo(a)pyrene(BaP), pyrene(PRN) and pyridine(py) found as constituents in cigarette smoke and vehicle exhaust dust has been considered. Two macromolecules, namely Florescein[1] (FLXN), 1, 10-Phenanthroline hydrochloride monohydrate[2] (phenCl) have been identified as possible sensing macromolecules for the pollutants mentioned above. These macromolecules have not been used before as sensors for Polycyclic Aromatic Hydrocarbons (PAHs) and py but for metal ions. It was envisaged that, the pollutants will change the way these sensor chemicals interact with the electromagnetic radiation by particularly altering their electromagnetic spectrum. These changes are desirable for these chemicals to qualify as sensors. These sensing molecules have been preliminarily evaluated through solution study and the results for solution study are presented in this paper. In solution study, there has been observed changes in the way these sensing molecules interact with the electromagnetic spectrum when made to react with the pollutant molecules. The mechanism of sensing was based on monitoring properties of fixed concentrations of sensing molecules (chemical sensors), with increasing concentrations of pollutants. Dilute solutions of known concentration in µM of neat pollutants, after interaction with the sensor chemicals were used to model calibration plots. The slopes, intercepts of the calibration plots obtained and signals of pollutants in environmental samples were applied in estimation of the amounts of ANTH, BaP, PRN and py, constituents of cigarette smoke and vehicle exhaust pipe dust sampled from Central Business District (CBD) of Nairobi city.

Keywords: Fluorescence, nano-sensor, carcinogenic organic pollutants, Fluorescein, and 1, 10-phenanthroline.

1. Introduction

Environmental pollution continues to be a major challenge to the wellbeing of humans, other living organisms and activities that have to be performed in order to sustain the balance of nature. Global warming, which is a threat to living organisms and their environment has resulted from pollution. The environmental contamination is caused by a massive presence of inorganic and organic compounds that have been released through industrialization and other natural processes.

The aim of this research therefore, was to develop a sensing system for detecting anthracene (ANTH), benzo(a)pyrene (BaP), pyrene (PRN) and pyridine (py) levels when released into the environment, before they reach amounts that are harmful to organisms as established by EPA and other environmental monitoring organizations. Vehicle exhaust pipe dust [Malgorzata et al 2013] and cigarette smoke [Schmeltz et al 1964] contain the above listed pollutants among other carcinogenic compounds. The enlisted compounds as presented in Figure 2 are known mutagens and carcinogens and therefore classified as hazardous compounds [NIOSH Manual for Analytical Methods (NMAM) July issue (1986)] and [OSHA Occupational Safety and Health Administration Manual (1996)]. These pollutants especially BaP have affinity for DNA and therefore form adducts with the DNA that mutate into cancerous growth [Kongati et al 2001].

Identified sensor chemicals Fluorescein (FLXN) and 1, 10-phenanthroline chloride monohydrate have not been used before as sensors for PAHs and py. However, they have been applied as sensors for heavy metal Ions[Zhihui et al 2012; Lin

et al 2016] and their derivatives used as sensors; fluorescein isothiocyanate as a gold nanosensor [Sironi et al 2009]; bis-chelated – 1,10 – Phenanthroline – azido – Copper(II)complex for selective sensing of aniline [Mistri et al 2013]; fluorescein derivative as a calorimetric chemosensor for detecting copper (II) ion [Li et al 2011]; a Porphyrin – related macrocycle with an embedded 1, 10 – Phenanthroline moiety: Fluorescent Magnesium (II) ion sensor [Ishida et al 2010]; Carbon nanotubes modified with fluorescein derivatives for pH sensing [Ghini et al 2013].

To achieve the goal of this study, it entailed searching for, and also synthesizing and developing chemicals that, when they interact with these polluting compounds, their resulting physical and chemical changes are monitored using optical fibre interface to novel instrumental analytical techniques including-VIS spectroscopy and fluorescence spectroscopy.

Chemical sensors identified for this study

The molecular structures of some of the sensing reagent molecules selected for this project are fluorescein abbreviated as FLXN and 1, 10-Phenanthroline hydrochloride monohydrate abbreviated as phenCl. These compounds whose results on studies carried out are presented in this paper are as shown in Figure1.

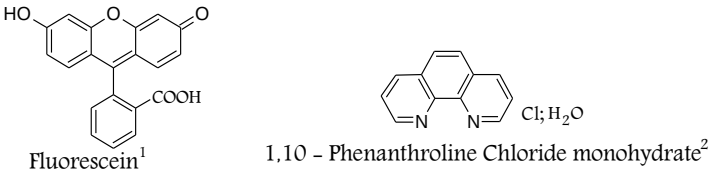

Fluorescein[1] 1,10 – Phenanthroline Chloride monohydrate[2]

Figure 1. Some of the sensing molecules of this study

The molecular structures for the pollutant molecules identified for this research are as presented in Figure 2.

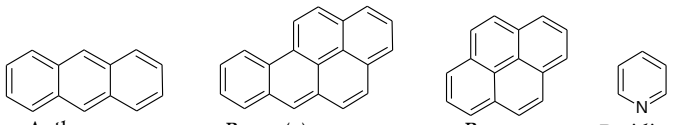

Anthracene Benzo(a)pyrene Pyrene Pyridine

Figure 2. Carcinogenic organic pollutants identified for this study.

In this study, preliminary solution experiments presented in this paper were carried out before eventually immobilising the sensor chemicals into solid thin films – results of which are not presented in this paper. Considerable research has previously been carried out on optical fibre based gas, vapour and solution sensing, for PAHs, which utilised chemical sensor films such as: porphyrin [Yusoff et al 2008], metallophthalocyanines [Granito et al 1996; Lloyd et al 1987; Spadaveccha et al 2004] inorganic metal oxides [Körber et al 2002; Niranjan et al 2002], semiconductors [Horrillo et al 1998], carbon nanotubes [Li et al 2003; Penza et al 2005; Quercia et al 2004], calixarenes [Kalchenko et al 2002; Koshets et al 2005], zeolites [Dubbe et al 2006; Mintova et al 2001; Vilaseca et al 2003; Zhang et al 2006], polymers [Fort et al 2005; Shepherd et al 2002; Sluszny et al 2004] and molecularly imprinted polymers [Chen et al 2004; Dickert et al 1998; Wolfbeis et al 1988]; molecularly imprinted polymers using PAHs as the template have been used for specificity of sensing BaP, PRN [Traviesa-Alvarez et al 2007; Lai et al 2004' Fernandez Sanchez et al 2004; Brylee et al 2016], Vapochromic cobalt complex – change in colour on exposure to pyridine vapour was developed by [Elosua et al 2008]]; a pyrene sensor based on Graphene–Cadmium Telluride Quantum Dot Nanocomposites has been developed [Wang et al 2015].There have been studies too to evaluate the specificity of sensor chemicals towards BaP using fluorescence spectroscopic technique [Fernandez et al 2004]. In this study, we explored the possibility of the developed sensors' specificity towards the enlisted pollutants among other constituents of cigarette smoke and vehicle exhaust pipe dust.

2. Materials and method development

2.1. Chemicals

Anthracene, benzo(a)pyrene, pyrene and Fluorescein were purchased from Sigma-Aldrich through Kobian Scientific as their agents in Kenya, while 1,10-Phenanthrolinium Chloride monohydrate and pyridine were sourced from R D HAEN through Kobian as their agents and ethanol was obtained from Manigate agencies ltd. These reagents were of analytical grade and therefore used as purchased without further purification

2.2. Apparatus

The apparatus used were readily available in the laboratory or purchased as required and these included; volumetric flasks for preparation of stock solutions, micropipettes (bought from Heathrow Scientific through Kobian as their agents) and tips (bought from GRENNIER through Kobian) for siphoning and delivery of liquids and solutions in micro volumes, weighing crucibles for holding reagents to be weighed and universal bottles (bought from UGB through Kobian) for dilutions and or mixing reagents, weighing micro-balances for taking weights of chemicals, cuvettes and other sample holders for handling solutions in the sample compartment of the instrument for measurement. Filter paper, whatman No, 1 was bought from Sigma-Aldrich through Kobian and syringe filter attached to a

acrodisc syringe filter - 0.2 μm HT Tuffryn membrane – provided by Professor Bulimo's research team at KEMRI.

2.3. Instruments

Instruments used for evaluation of sensors in this study were Shimadzu 1800 UV-VIS PC spectrophotometer for absorbance and Infinite M 1000 Tecan analyser, for fluorescence measurements.

2.4. Experimental methods for development of sensors

Absorption and fluorescence measurements were performed for the sensor molecules alone and fixed concentration of sensor molecules with varying concentration of pollutant molecules. Six replicate measurements were carried out on same concentrations for the sensing reagents alone and these sensors with the pollutants so as to establish repeatability of measurements. This approach gives representative data for evaluation and conclusions. Known concentrations of solutions for the sensing reagents and those of pollutant molecules were prepared as stocks in appropriate solvents and then dilutions made from them in µM concentrations. Method for preparation of the solutions is as presented in the next section. Absorption measurements are usually carried out within a scale of signals ranging from 0.0 to 1.0, because absorbance is a logarithmic ratio of the incident radiant energy to that of transmitted energy. Mostly recommended for linear calibration plots are measurements done within the signals ranging from 0.005 to 0.8 so that deviations from the limiting Beer-Lambert's law are contained Solutions for this study were prepared in known µM concentration and a series of measurements done however, to establish absorbance within 0.01 to 0.8 absorption ranges. This range gave linear calibration plots. The aim was to establish the highest concentration of the sensing reagent that can be fixed as the concentration for the pollutants are varied in order to monitor any changes to the signal of the sensor molecule. Absorption and fluorescence intensity scans were performed of the sensors and of sensors after interaction with pollutants.

2.5. Absorption measurements

During absorption measurements, signal(s) for a known fixed concentration for the sensor chemicals were obtained, by scanning the entire spectrum from 190 nm to 800 nm. The scanning enabled us establish the way the sensor chemicals interacted with the electromagnetic spectrum and the appearance of their spectra. After establishing the interaction pattern for the sensor chemicals with radiant energy and their main absorption peaks, known aliquot concentration for the pollutant chemicals were successively added and the pattern of interaction of the sensors with pollutants and any changes observed were then established. These changes were vital in establishing specific interaction of a given sensor with a particular pollutant and the characteristic peaks observed after such interaction. The characteristic peaks after interaction of the sensors with pollutants during study with environmental samples, could show if ANTH, BaP, PRN and py were present in cigarette smoke and vehicle exhaust pipe dust extracts.

2.6. Absorption measurements

A stock solution for FLXN containing 19.2 mg (0.0192 g) in absolute ethanol was prepared and this solution was an equivalent of 9.03 x 10^{-5} moles (90.3 μM) for FLXN of formula weight of 212.21 g/mol. From the stock solution, volumes for dilutions as desired were evaluated using equation 2 and prepared accordingly to give a range of µM dilute solutions required.

$$C_1V_1 = C_2V_2 \quad \ldots\ldots(1)$$

Where, C and V stand for concentration and volume respectively.

C_1 = concentration one, which is the concentration for stock solution

V_1 = the volume for stock solution to be diluted to get C_2

C_2 = the desired dilute concentration

V_2 = the volume of solvent to be used in diluting that from stock solution.

A set of dilutions were made by pipetting aliquots of known 10 µL-volume from the stock solution into a spotlessly clean cuvette, containing 2 ml of the solvent used in dissolving the reagents. Same amount in aliquots were added in succession as measurements were being performed. This ensured that the concentration was increasing in a certain given magnitude. To curb any solvent evaporation, the cuvette has a tight fitting stopper (lid). Every time the amount in volume of 10 µL from the stock solution earlier prepared as explained above were added to the cuvette. Thorough mixing was performed by shaking the Stoppard cuvette, then cleaning its external surface of any specs of dirt before reintroducing into the sample compartment of the instrument for measurement. From such dilutions, a fixed concentration for FLXN was established. This fixed concentration was established by visualisation of various measurements of different concentrations that had a signal $\leq$ 0.5 absorption units. Absorption units ≤ 0.5, gives allowance for increasing signal when the pollutant is added, such that the signal can be well below 1.0 absorption unit.

A scan ranging from 190 nm – 800 nm was performed on Shimadzu U- 1800 PC spectrophotometer, with a slit width of 1.5 nm, a scan speed of 400 nm/min in a 1 cm path length cuvette.

The procedure as employed to FLXN above was applied to the other sensor and pollutants. The results are as presented in the sections that follow below:

3. Results and discussion

3.1. Absorption spectra for the sensor chemicals.

The spectra for the sensor chemicals FLXN and phenCl are as presented in Figures 3. These spectra were obtained so that the interaction of the sensor chemicals with the electromagnetic spectrum could be established for comparison after they interacted with the pollutants, as explained in the previous section.

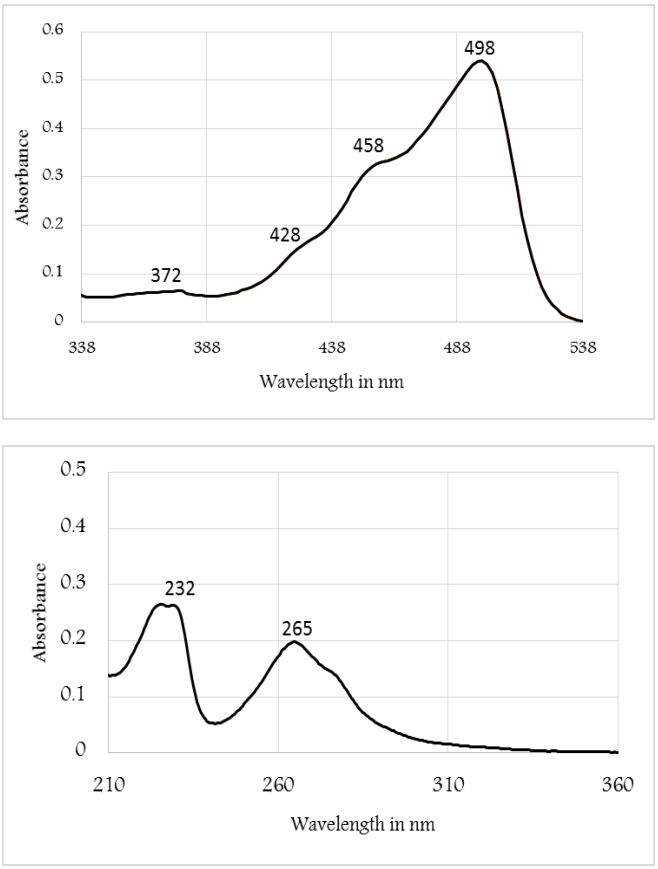

Figure 3. Absorption spectra for sensor reagents alone- on the top: [0.452]µM FLXN and on the bottom [0.903]µM phenCl in ethanol.

As it can be observed in Figure 3, FLXN has a main absorption peak at 498 nm; a minor one at 372 nm and shoulder peaks at 458 and 428 nm. The molar absorptivity for FLXN as calculated from measurements of this research, range from 10^3 – 10^4 L M^{-1} cm^{-1}. The absorption bands for phenCl are at 232 and 265 nm with molar absorptivity ranging from10^4 - 10^5L M^{-1} cm^{-1} as established in this research. Initially, as explained earlier, acquiring of absorbance and fluorescence for the sensor molecules alone and those of the pollutant molecules alone was quite necessary. These measurements revealed the pattern of interaction for these reagents with the electromagnetic spectrum. The individual pattern of interaction of the sensor molecules with the electromagnetic spectrum and that after they interacted with the pollutant molecules was used for comparison so as to establish the changes observed. This was also helpful in that, we observed characteristic peaks for individual pollutants after interaction with individual sensor chemicals. When these sensor chemicals were made to interact with the environmental samples, characteristic peaks revealed whether they reacted specifically with a given pollutant as it has been elaborated in the results and discussion section of this paper.

3.2. Absorption spectra for the pollutants

Measurements for the absorption spectra for the organic pollutants of this research were first performed following the procedure as explained previously above. Through visualisation and subsequent dilutions of the solutions, clear spectra absorbing below1.0 au were obtained. Presented in Figures 4 are absorption spectra for ANTH, BaP, PRN and Py. These spectra for the solutions of neat pollutants were also obtained so that their way of interaction with radiant energy of the electromagnetic spectrum is established for the same reason as explained of the sensor chemicals. As illustrated in Figure 4, ANTH absorbs strongly between 290 and 390 nm wavelength with six vibrational energy band levels. It has a high absorption coefficient of about 7 x 10^6 L mol^{-1} cm^{-1} and exists as white solid crystals. The appearance of BaP is yellow solid crystals. It absorbs strongly in the UV-VIS region of the electromagnetic spectrum with high molar absorptivities; 4.3 x10^5 L mol^{-1} cm^{-1}. Pyrene strongly absorbs in the UV-VIS region of the electromagnetic spectrum as illustrated in Figure 4. It has a high absorption coefficient, of 7.5 x 10^6 L mol^{-1} cm^{-1} and the crystals are greyish in colour. Pyridine exists as colourless liquid and absorbs strongly with molar absorptivity of1.75x10^3L mol^{-1} cm^{-1}, in the UV- region of the electromagnetic spectrum. A sensor which is selective towards these pollutants could extract them from a mixture of other pollutants. As explained previously, the purpose for obtaining the spectra for the pollutants and sensors alone was to observe their individual pattern of interaction with the electromagnetic spectrum and their characteristic peaks. After the sensors and neat pollutants interacted, the changes and resultant characteristic peaks were established. Subsequently, if the sensors then interacted with solutions of cigarette smoke and vehicle exhaust pipe extracts and the characteristic peaks

established of the sensors with pollutants were present, it can reveal if the enlisted pollutants are present as part of the constituents in the environmental samples.

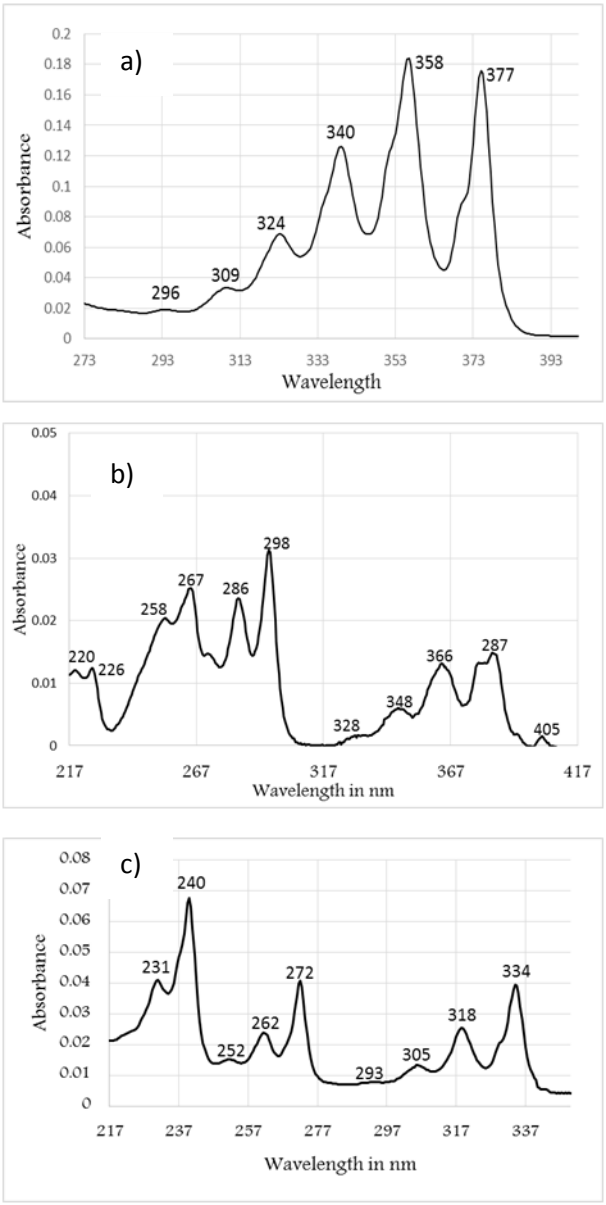

3.3. Absorption spectra for FLXN and phenCl with the pollutants

Absorption measurements were performed of fixed concentration for FLXN 9.03μM and of phenCl 9.03μM with increasing concentration of pollutant molecules as in PAHs 1.21 – 7.26μM and py 0.36 - 2.16 μM in absolute ethanol. The increasing concentration of pollutants was obtained from aliquots of 10 μL from the stock solutions – PAHs (90.3 μM) and py (72.05 μM). The increasing concentration of pollutants as subsequent measurements were performed facilitated a method of photo-titration. Initially, the absorption measurement for the sensor chemicals alone was performed – for comparison after interaction with pollutants. The absorption spectra for the sensor molecules enlisted above with the pollutants are as presented in Figure(s) 5.

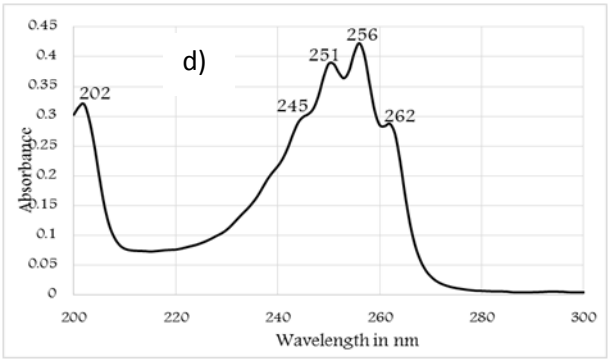

Figure 4. Absorption spectra for pollutant molecules (a) ANTH, (b) for BaP (b), for py in absolute ethanol (c) and PRN (d).

As it can be observed of Figure 5, the pollutant molecules have changed the way the sensor reagents interact with the electromagnetic spectrum. This has manifested in changing of the absorption spectra of the sensor reagents, by formation of new peaks and shifting of the spectrum mostly towards the blue end of the electromagnetic spectrum. Observing the spectra after interaction of FLXN with ANTH, the sensor spectrum appears as though the absorption bands have been split, giving the main absorption peak at 457 nm as opposed to the main absorption peak of this sensor reagent before interaction with ANTH which was at 498 nm – Figure 3. Another relatively intense peak can be observed at 485 nm and a shoulder absorption peak at 430 nm. It can clearly be seen that, the main absorption peak for this sensor chemical has shifted about 41 absorption units (a.u) towards the blue end of the electromagnetic spectrum. From the spectra of interaction of FLXN with ANTH, the absorption band for FLXN is reducing in absorbance while the characteristic band for ANTH is increasing in absorbance.

Observing the absorption bands for interaction of PAHs with FLXN, the pattern is consistently as - splitting of the absorption band of FLXN, shifting the main absorption peak to 457 nm, with a relatively intense peak at 485 nm and a shoulder peak at 430 nm. Aside the changes in absorption band for the sensor chemical, there appears characteristic peaks for each given PAH, with also slight changes in prominent peaks – as in ANTH, the peaks at 377 and 358, which have slightly shifted to 375 and 356 respectively, giving a shift of 2 a.u. those for BaP likewise have shifted the same magnitude also towards the blue end of the electromagnetic spectrum.

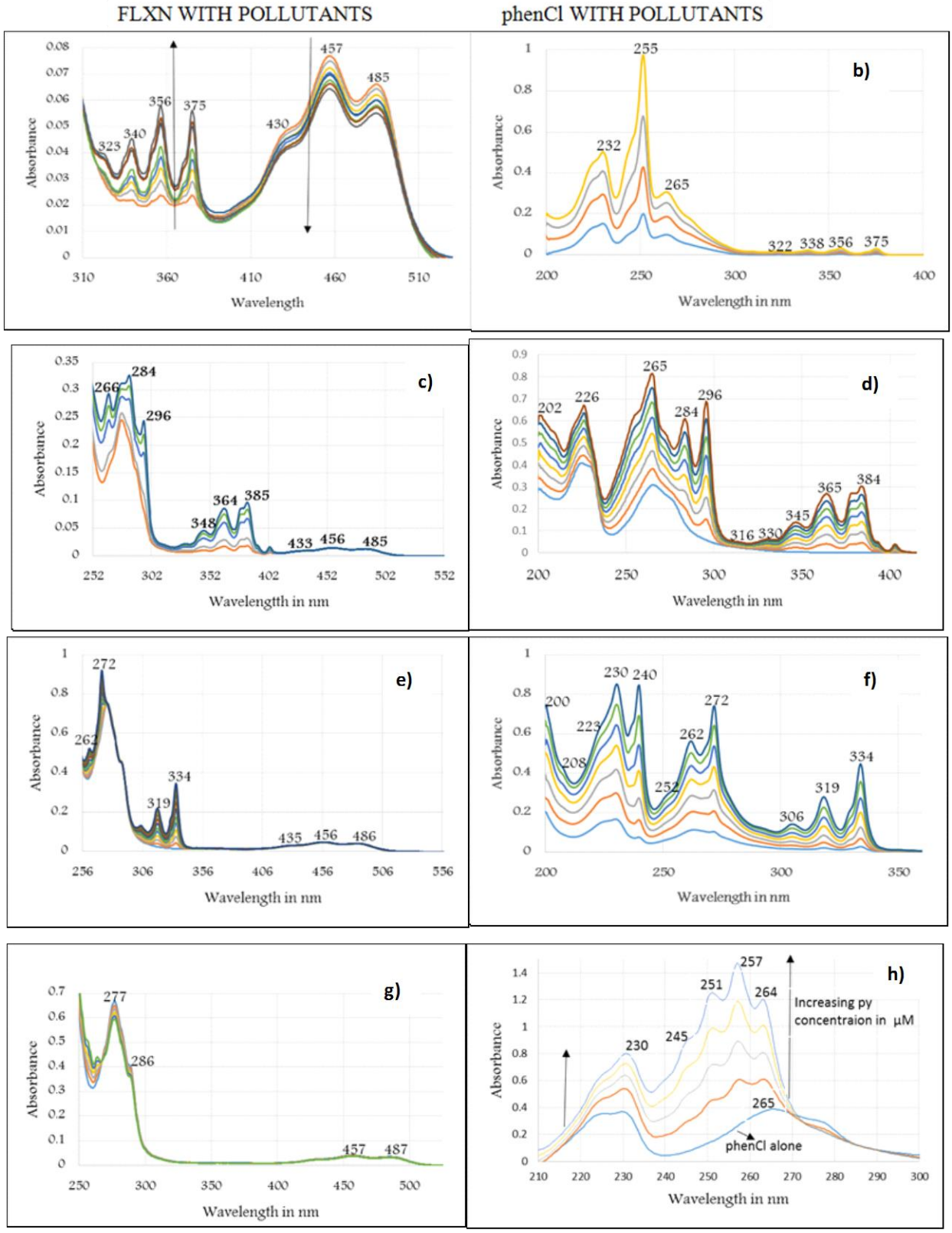

Figure 5. Absorption spectra for interaction of fixed FLXN and phenCl sensor reagents with increasing concentration of pollutants a) and b)- ANTH, c) and d) BaP, e) and f) - PRN and g) and h) for py respectively.

However, for PRN, such shift of the characteristic absorption band is not observed, but an isosbestic point can be clearly seen at 277 nm and the usual splitting of the absorption band of the sensor chemical, with shifting of its main absorption peak to 457 nm. As shown in Figure 5, pyridine has affected the absorbance of FLXN by also splitting the absorption band and shifting of the main absorption peak to 457 nm. It can be noted that, the absorption spectrum for py has changed too, giving a main peak at 278, and shoulder peaks at 288, 263 and 256 nm. There is also formation of an isosbestic point at 267 nm.

The absorption spectrum for phenCl has also changed after interaction with the pollutants. With ANTH, there is formation of a new prominent absorption peak at 252 nm. The peaks for phenCl at 232 nm and 265 nm were increasing in absorption intensity as the concentration for ANTH increases, this could point at formation of an adduct of phenCl with ANTH. The characteristic ANTH peaks can also be observed, although with slight shifts. After phenCl interaction with BaP, the absorption peak for this sensor chemical at 265 nm increased in absorption intensity with increasing concentration for BaP and this caused the broadening of the absorption band between 250 and 300 nm, with a shoulder peak at 254 nm. Also with BaP, the absorption peak at 232 nm shifted to 226 nm and was increasing in intensity as the concentration for BaP increased in solution. On interaction of phenCl with PRN, an absorption peak can be observed at 200 nm and formation of shoulder peaks at 208, 223.252 and 292 nm. It can also be observed that, the peak for the phenCl at 232 nm has shifted slightly to 230 nm has increased in absorption intensity. After interaction of phenCl with py, the peak for the sensor chemical at 232 nm shifted to 230 nm and increased in intensity with the increasing concentration for py. The peak at 265 nm for phenCl has slightly shifted to 264 nm and likewise increased in absorption intensity.

3.4. Fluorescence spectra for FLXN and phenCl with pollutants

The fluorescence spectra for the sensor molecules above with pollutants are as presented in Figure(s) 6. Scrutinising the emission spectra for interaction of FLXN with ANTH, the main emission peak for FLXN has slightly shifted towards the red end of the electromagnetic spectrum with a magnitude of 8 a.u, from 514 nm to 522 nm and has also an emission band between 420 and 470 nm with a shoulder peak at 447 nm. Interaction of FLXN with BaP shifts the main emission peak to 522 nm too and has emission band between 420 and 470 nm, with shoulder peaks at 454 and 427 nm. After interaction with PRN, the main emission peak for FLXN has also shifted from 514 nm to 522 nm and it has a shoulder peak at 474 nm which was formed as the concentration for PRN increased in solution. Inferred information from the spectra shows that, each PAH has shown characteristic change in the spectrum of the sensing molecule, with certain characteristic peaks and shoulder peaks. Pyridine too changes the emission spectrum for FLXN by shifting the main emission peak to 522 nm and also an emission peak at 335 nm which is quite intense as compared to that of FLXN.

These same pollutants, too changes the way phenCl interact with the electromagnetic spectrum. Interaction of phenCl with ANTH enhances the emission intensity for phenCl at 366 nm. The emission peak at 310 nm for phenCl has shifted to 307 nm with increasing concentration of ANTH and it has also been enhanced in emission intensity. When phenCl interact with BaP, the characteristic main emission peak for phenCl can be seen intact at 366 nm. However, the emission peak for phenCl at 310 nm has also shifted to 307 nm. The shoulder emission peak for phenCl can also be seen un-shifted. There appears to be two isosbestic points at 340 and 380 nm. The shoulder emission peak at 382 nm shifted to 393 nm forming what we can comfortably referred to as the 'foot' adjoining the prominent emission band between 398 and 500 nm formed as a result of interaction of phenCl with BaP. After interaction of PRN with phenCl, it can be observed from the spectra that, the main emission peak for phenCl at 366 nm has shifted towards the red-end of the electromagnetic spectrum to 373 nm. The emission band for phenCl has acquired three vibrational bands with the other two peaks at 382 and 392 nm. The emission shoulder peak at 353 nm has shifted towards the blue end of the electromagnetic spectrum to 351 nm and the emission peak for phenCl at 310 nm has also shifted towards the blue end of the electromagnetic spectrum to 302 nm.

Observing these changes after interaction of phenCl with PAHs, we can confidently infer that each PAH has a characteristic way of changing the emission spectrum for phenCl. Therefore if phenCl is chosen as the sensing molecule, it could be clearly deduced if it is ANTH or BaP or PRN present in solution of phenCl. When phenCl interacted with py, the emission peak at 310 nm shifted to 304 nm and increased in emission intensity with increasing pyridine concentration- a shift towards the blue end of the electromagnetic spectrum. The fluorescence spectra after interaction of the sensor chemicals with pollutants are as presented in Figure 6.

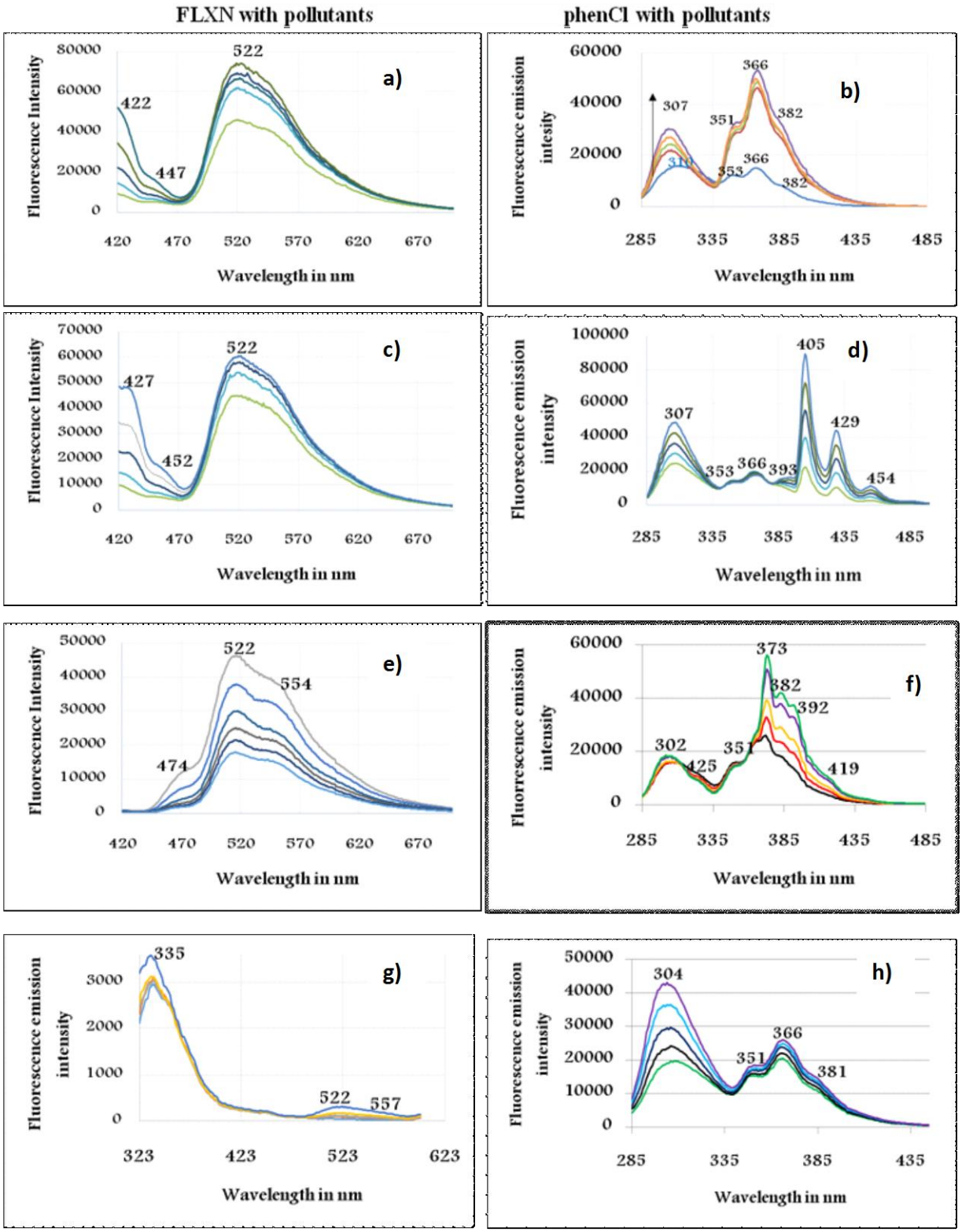

Figure 6. Fluorescence spectra for interaction of fixed FLXN and phenCl sensor reagents with increasing concentration of pollutants a) and b)- ANTH, c) and d) BaP, e) and f) - PRN and g) and h) for py respectively.

As mentioned earlier, in Figure 6 are presented fluorescence spectra after interaction of sensor chemicals with pollutants. The spectra on the left margin represent FLXN with pollutants and those on the right show phenCl with pollutants, which are captioned as 1, 2, 3 and 4, indicating, interaction with: ANTH, BaP, PRN and py respectively. As it is shown in Figure 6, the emission peak for phenCl at 353 nm has also shifted towards the blue end of the electromagnetic spectrum to 351 nm. The characteristic main emission peak for phenCl is not shifted and it still appears at 366 nm. After interaction of phenCl with py, the shoulder emission peak at 382 nm has slightly shifted to 381 nm.

3.5. Calibration plots for absorption study of the sensors with pollutants.

Presented in Figure(s) 7 are the absorption calibration plots for interaction of sensor molecules with the pollutant molecules. These calibration plots were obtained by selecting the maximum absorption peak after interaction of the sensors with the pollutants for a series of spectra of varying concentrations. As shown in Figure 7, the absorption intensity is on the vertical axis while the concentration is on the horizontal axis. The unknown concentration of the pollutants in cigarette smoke and vehicle exhaust pipe dust can be estimated from such calibration plots as mentioned earlier.

3.6. Calibration plots for Fluorescence study of the sensors and pollutants

After measuring the spectra of sensor chemicals with the neat pollutants, the maximum absorption peak for a series of spectra of different concentration were constructed using excel, the vertical axis showing the fluorescence intensity and the horizontal axis showing the increasing concentration of pollutants in the sensor matrix. These are the emission calibration plots as explained earlier. The calibration plots were used for estimation of the concentration of the pollutants of this study in the cigarette and vehicle exhaust pipe samples. Figure(s) 8 are the Fluorescence calibration plots for interaction of sensor molecules with the pollutant molecules. These calibration plots were used to estimate the unknown concentration of pollutants of the environmental samples of cigarette smoke and vehicle exhaust pipe dust sampled from CBD of Nairobi city. This can be achieved by getting the signal for the unknown concentration of the pollutant in same matrix where the known concentrations of the neat pollutants were measured in and with the same instrument and parameters as was done in this research. The signal obtained of the unknown concentration can then be extrapolated or interpolated to estimate the concentration of the unknown. The slope and intercept of the calibration plot can also be used to estimate the unknown concentration of the pollutants.

3.7. Environmental samples with sensor molecules

Sampling of cigarette smoke was carried out at a smoking zone in central business district (CBD) of Nairobi city. The sample was bubbled into a glass vial containing 2 ml of absolute ethanol through a plastic straw. The cigarette smoke was observed inside the Stoppard bottle, above the ethanol but with vigorous shaking, the smoke went into solution, forming a colourless solution of cigarette smoke in absolute ethanol. Exhaust pipe dust of Diesel engine Minibus was scraped from the vehicle's exhaust pipe system, using an aluminium metal spatula and the dust was then placed into a glass vial. These environmental samples were carried to the laboratory for spectroscopic analysis.

3.8. Absorption measurements for the environmental samples

The samples were measured on a Shimadzu1800 UV-VIS PC spectrophotometer in a quartz cuvette of 1 cm path length and a slit width of 1.5 nm. The unknown samples which are constituents of cigarette smoke and diesel engine vehicle exhaust pipe dust were dissolved in absolute ethanol. About 5 mg of vehicle exhaust pipe dust was mixed with ethanol and filtered using a plastic syringe, attached to an acrodisc syringe filter - 0.2 μm HT Tuffryn membrane. The resulting solution appeared orange-yellowish. The absorption spectra for the unknown samples alone were measured followed by the absorption spectra for the samples with the sensor molecules. Initially the spectrum for the sensor alone had also been acquired. The absorption spectra for the unknown samples alone and the unknown samples after interaction with the sensing molecules FLXN and phenCl are as presented in Figure(s) 9 and 10 respectively.

After interaction of FLXN with a solution of cigarette smoke, BaP, PRN and py peaks can be identified as shown in Figure 10 above. The peaks at 305,319 and 334 are for PRN; those peaks at 358,375 and 405 are for BaP; while those at 288 and 277 are typical peaks for py after interaction with FLXN. These peaks are characteristic for interaction of pure BaP, PRN and py with FLXN – spectra presented in Figure 5, minus the isosbestic point because there was no successive addition of aliquots of environmental samples during measurement. The peaks at 430, 457 and 485 are peaks for FLXN.

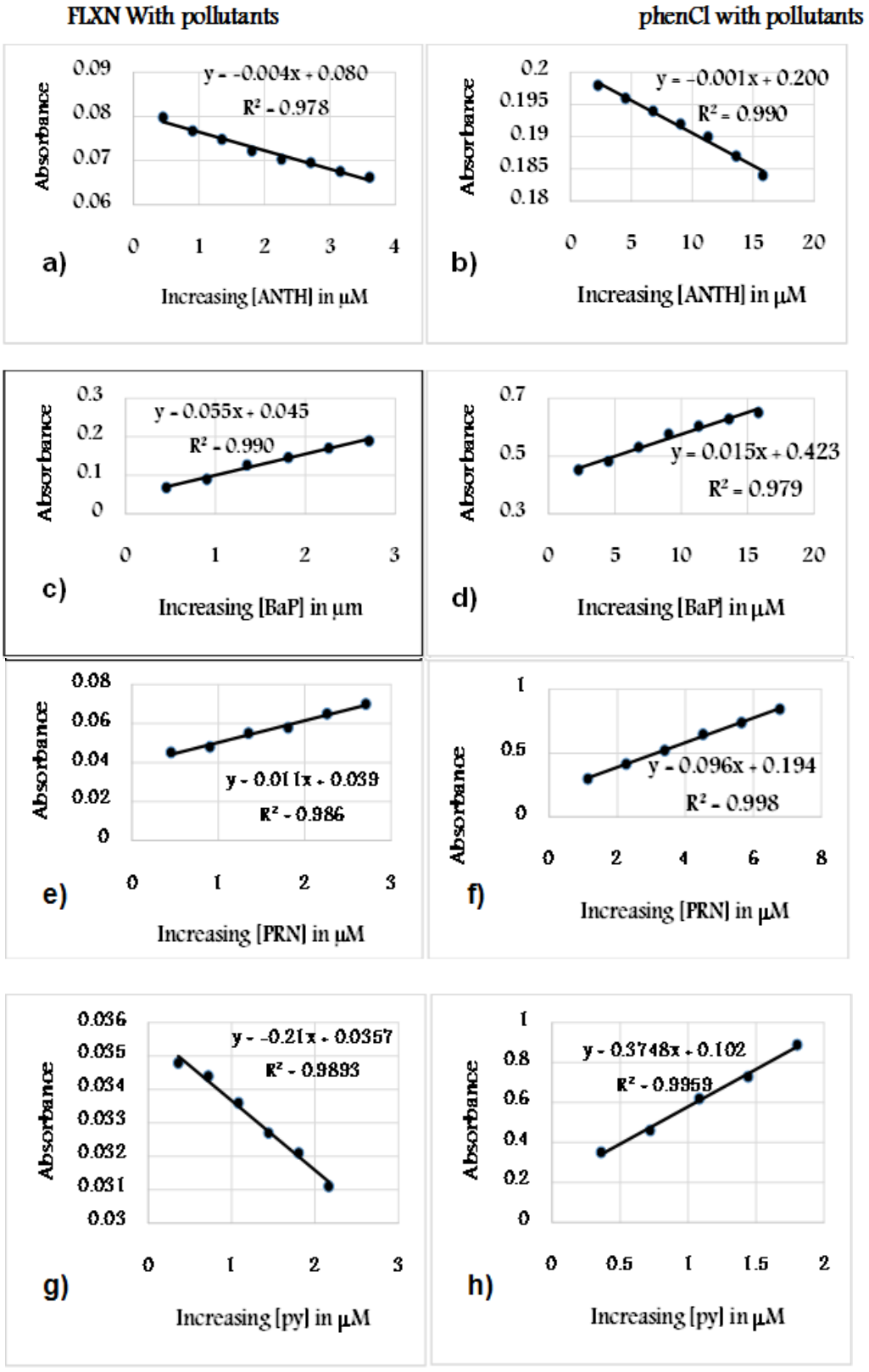

Figure 7. Absorbance calibration plots for interaction of fixed FLXN and phenCl sensor chemicals with increasing concentration of pollutants a) and b)- ANTH, c) and d) BaP, e) and f) - PRN and g) and h) for py respectively.

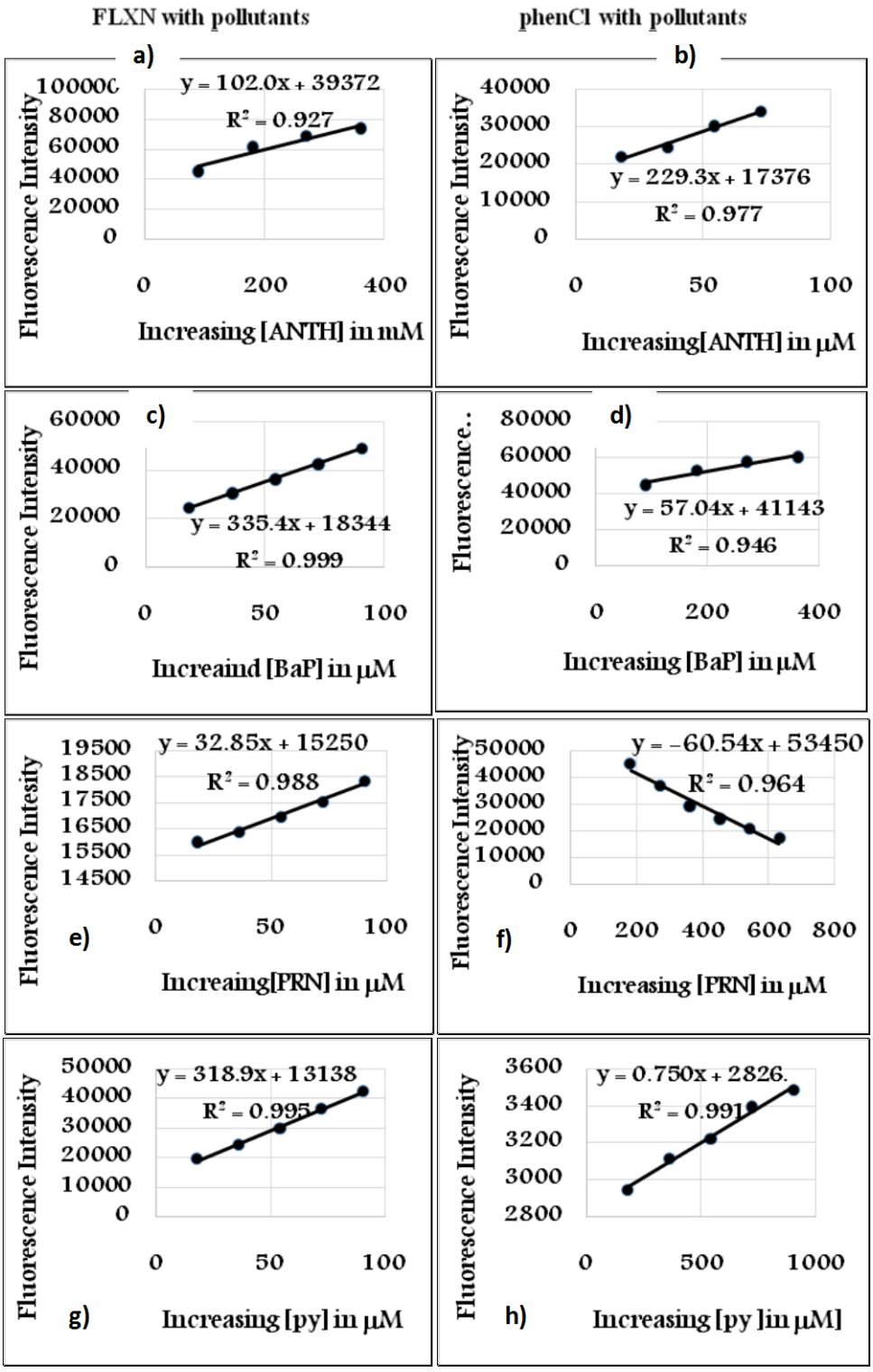

Figure 8. Fluorescence calibration plots for interaction of fixed FLXN and phenCl sensor chemicals with increasing concentration of pollutants a) and b)- ANTH, c) and d) BaP, e) and f) - PRN and g) and h) for py respectively.

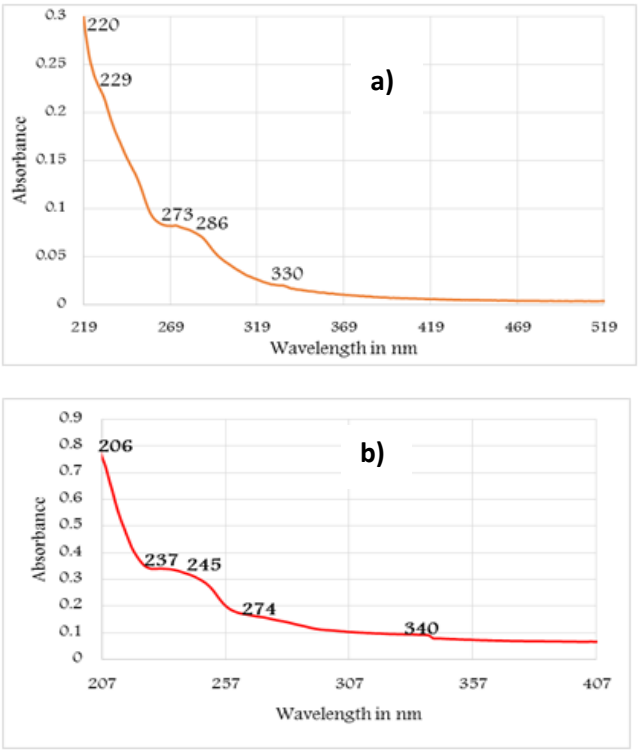

Figure 9. Absorption spectra for cigarette smoke sample (a) and vehicle exhaust pipe sample (b) in absolute ethanol.

After interaction of phenCl with cigarette smoke sample solution, the peaks: 208, 224,252, 272, 292, 319 and 334 are characteristic after interaction of PRN with phenCl. This may imply that phenCl could also have some selectivity towards PRN, noting that cigarette smoke has a mixture of PAHs including pyrene (PRN), benzo(a)pyrene(BaP), Benz(a)anthracene(BaA), phenanthrene(PHEN) to name but a few – it also contains other organic compounds including nicotine and nornicotine aside PAHs [Schmeltzet al 1964; Clayton et al 2013].

After interaction of phenCl with cigarette smoke sample solution, the peaks: 208, 224,252, 272, 292, 319 and 334 are characteristic after interaction of PRN with phenCl. This may imply that phenCl could also have some selectivity towards PRN, noting that cigarette smoke has a mixture of PAHs including pyrene (PRN), benzo(a)pyrene(BaP), Benz(a)anthracene(BaA), phenanthrene(PHEN) to name but a few – it also contains other organic compounds including nicotine and nornicotine aside PAHs [Schmeltzet al 1964; Clayton et al 2013]. Subsequently interaction with a solution of the sample from the vehicle exhaust pipe, with FLXN, characteristic peaks after interaction with BaP and PRN can be observed. When phenCl interacted with vehicle exhaust pipe sample also exhibited the characteristic peaks after interaction of phenCl with pure PRN. This also gives an indication that, phenCl selectively interacted with PRN out of all the mixture of other PAHs present in the exhaust pipe dust including: anthracene, benzo(a)pyrene, pyrene, phenanthrene, benzo(a)anthracene, floranthene Benzo(a)floranthene -these constituents of diesel engine dust as reported by [Malgorzata et al 2013]. Pyridine has not been reported to be among the constituents of vehicle exhaust pipe dust.

3.9. Fluorescence measurements for the environmental samples

Fluorescence measurements were accomplished using Infinite M 1000 Tecan Analyser. The samples as prepared for absorbance measurements were used for fluorescence measurements. The concentration for FLXN and phenCl was 90.3 μM, 100 μL aliquots of each sensing reagent placed in individual wells of Corning 96 Flat Bottom Black Polystyrol [COS96fb.pdfx] wells plate. Seven replicate measurements for each, thus of each sensor molecule with cigarette smoke solution and vehicle exhaust pipe extracted solution - 50 μL aliquots of the environmental samples were added to the sensors inside the wells and measurements performed. The excitation wavelength range for FLXN was 230 – 300 nm; emission start wavelength of 398 – 700 nm, with an emission maximum peak at 514 nm. The excitation and emission bandwidth(s) were 10 nm and 15 nm respectively. The z-position was manually set at 20000 μm and sample irradiated at 400 Hz flash frequency of 50 flashes with integration time of 20 μs. the temperature under which the measurements were performed was set at 25.4 ^{0}C. The excitation wavelength range for phenCl was 230 – 300 nm and the emission wavelength range was 285 – 500 nm with excitation and emission bandwidths at 5 nm. The temperature, z-position, flash frequency and the number of flashes was the same as for FLXN. The fluorescence spectra for FLXN and phenCl with the cigarette smoke and vehicle exhaust pipe samples are as presented in Figure 12.

As presented in Figure 12, it appears that, the sensing molecule FLXN specifically interact with BaP while phenCl specifically interact with PRN of all the PAHs present in exhaust pipe dust and of all the constituents in cigarette smoke, FLXN interact with BaP, PRN and py while phenCl specifically interacts with PRN as is shown by their characteristic spectra and peaks.

The absorption peak for pyridyl moiety in nicotine is reported to be at 240 nm, with λ_{max} for nicotine at 260 nm [Clayton et al 2013]. In the absorption spectrum for pyridine alone, in ethanol the 240 nm peak does not appear but there is a peak at 245 nm. Therefore as reported in literature, the pyridyl moiety absorbance at 240 nm in the spectrum for nicotine could be characteristic of this pyridyl alkaloid (Figure 13), which is lacking in the spectra obtained in this study – this shows that the sensing molecules of this study may not have reaction preference towards nicotine.

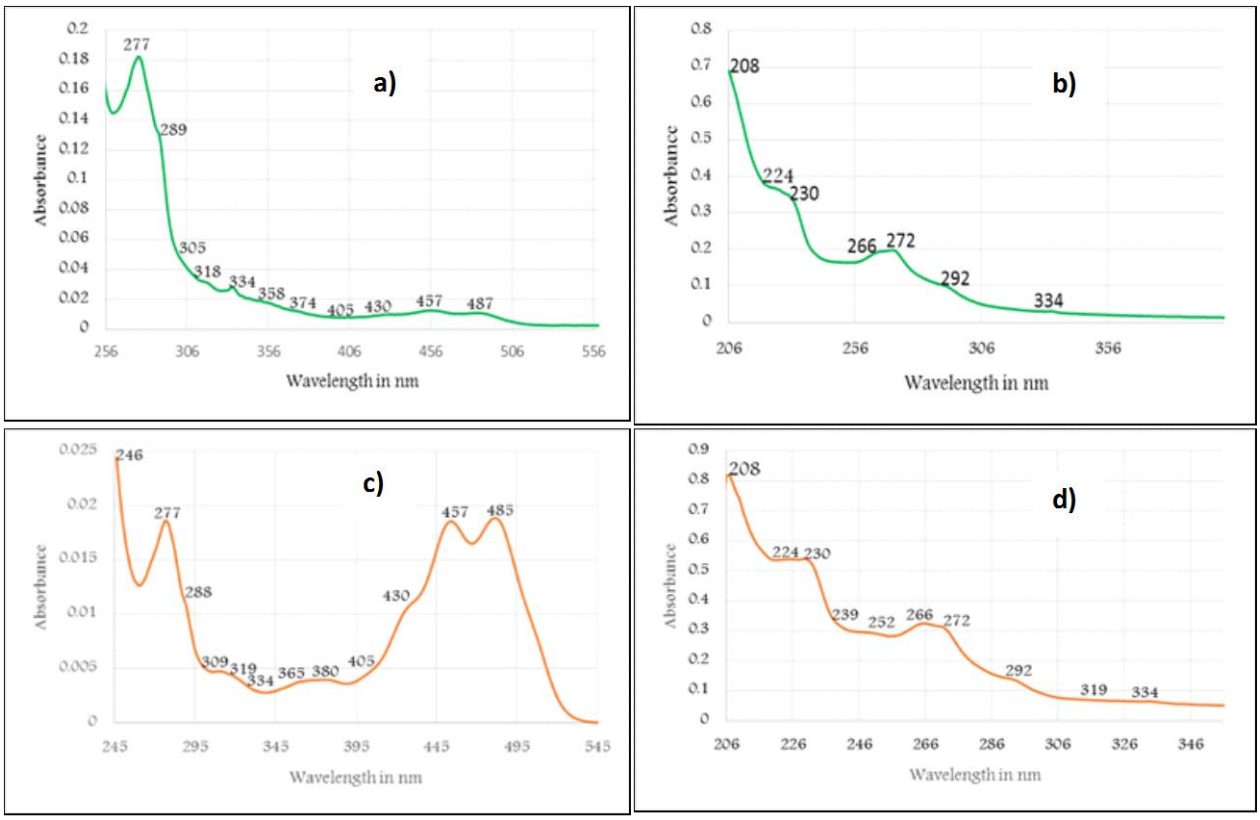

Figure 10. Absorption spectra for interaction of FLXN and phenCl sensor chemicals with cigarette smoke and exhaust pipe samples in ethanol: a) and b) cigarette smoke sample with FLXN and phenCl; c) and d) vehicle exhaust pipe sample with phenCl and FLXN.

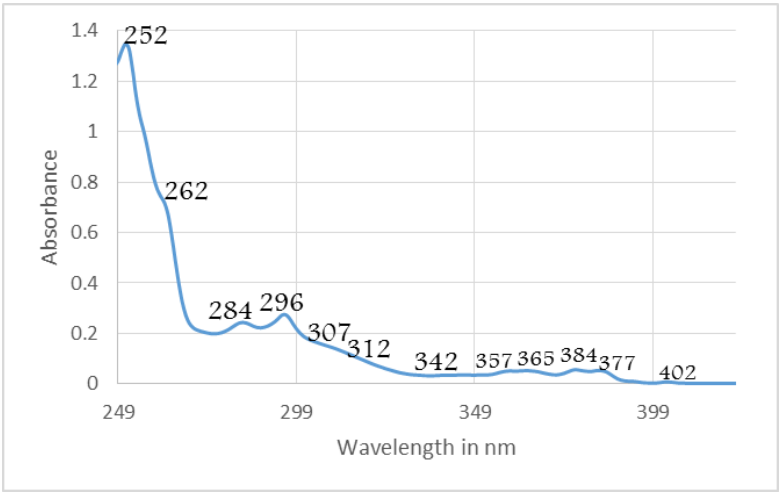

Figure 11. Mixture of 2.26 μM each in absolute ethanol for ANTH, BaP, PRN and py.

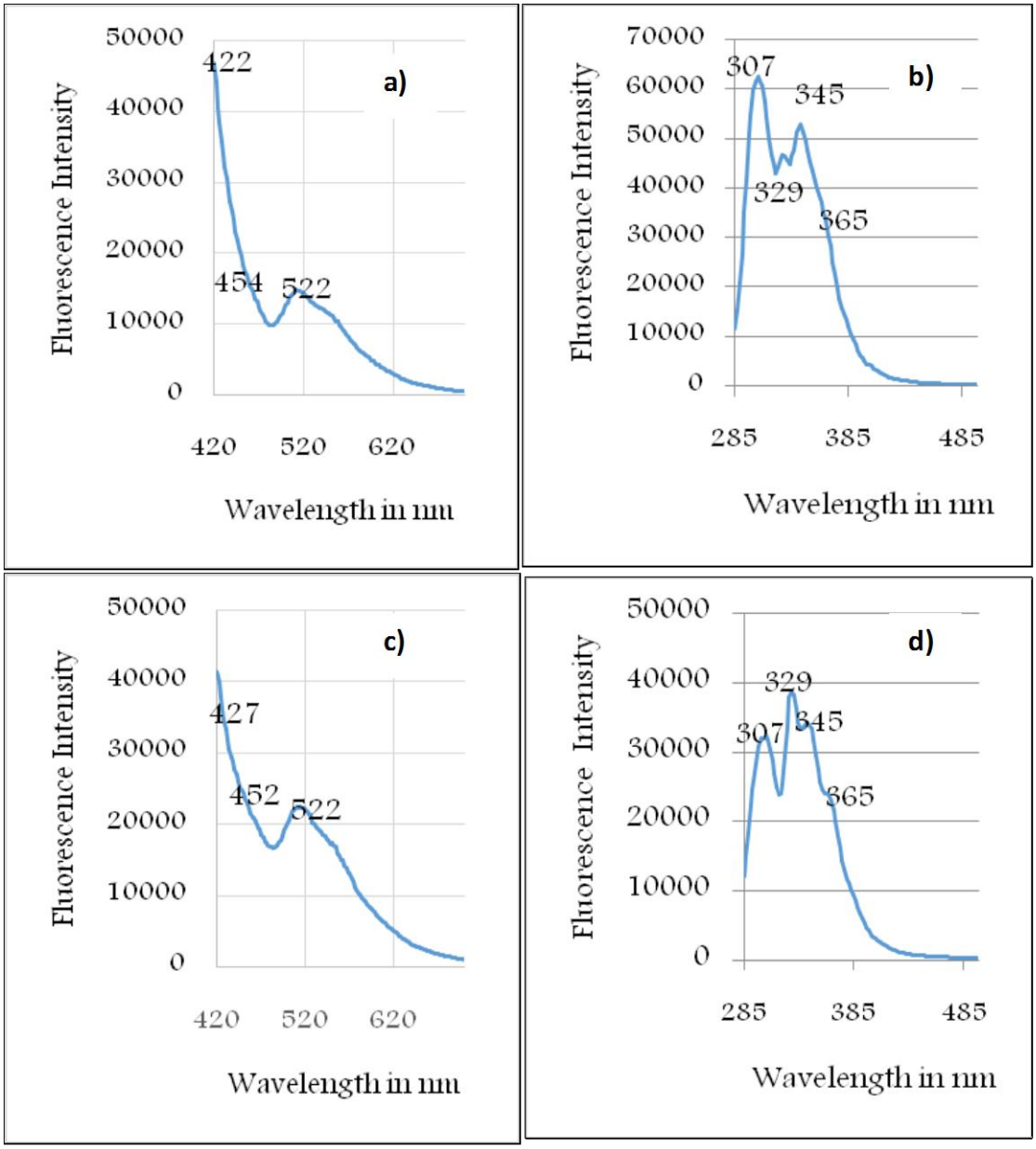

Figure 12. Fluorescence spectra for the sensing molecules FLXN and phenCl with:1) Cigarette smoke in absolute ethanol and 2) Vehicle exhaust pipe sample in absolute ethanol

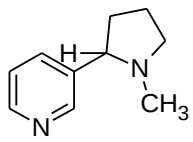

Figure 13. Structure of Nicotine

It is worth noting that nicotine is reported to be a major constituent of cigarette smoke [Clayton et al 2013].

3.10. Quantification of the environmental samples using calibration plots

Quantification of BaP, PRN and py in cigarette smoke and vehicle exhaust pipe environmental samples was pecked on the *Δ-signal.* Thus, the difference between the signals of the main absorption or emission peak of the sensor molecule alone with that of the sensor molecule with pollutants, on which the calibration plots were based. From the calibration plots of the sensor molecules with pollutants, the slope was used to evaluate the unknown concentration of BaP, PRN and py from the environmental samples (equation 4)- method adopted from literature. In Tables 1 and 2 are presented the calibration plots' slopes and estimated concentration of the environmental samples for absorbance and fluorescence respectively.

$$C_{unknown} = \frac{Signal\ of\ C_{unknown} - \text{int}\,ercept}{slope} \quad \ldots\ldots\ldots\ldots\ldots\ldots 3$$

Table 1. Absorbance calibration data for FLXN and phenCl for estimation of [BaP]**[1]**,[PRN]**[2]**& [py]**[3]** in A). Cigarette smoke environmental sample and B). Vehicle exhaust pipe respectively of samples from CBD – NAIROBI:

(A)

Sensor	Absorbance– intercept	Signal of envr. sample	Conc./μM
FLXN	-0.1567[1]	0.0172	0.54
	-0.0349[2]	0.1821	5.22
	-0.244[3]	0.13	0.53
phenCl	-0.0979[2]	0.296	3.02

(B)

Sensor	Abs - intercept	Signal of envr. sample	Conc./μM
FLXN	0.032[1]	0.0153	0.48
	-0.0349[2]	0.0186	0.53
phenCl	-0.0979[2]	0.308	3.14

Table 2. Fluorescence calibration data for FLXN and phenCl for estimation of [BaP][1],[PRN][2]& [py][3] in A). Cigarette smoke environmental sample and B). Vehicle exhaust pipe respectively of samples from CBD – NAIROBI:

(A)

Sensor	Absorbance - intercept	Signal of envr. sample	Conc./μM
FLXN	-43327.48[1]	21466	0.49
	-52844.51[2]	12,967	4.72
	-2819.1[3]	13304	0.25
phenCl	-12817.14[2]	50,234	3.92

(B)

Sensor	Abs - intercept	Signal of envr. sample	Conc/ μM
FLXN	-43327.48[1]	22,15522,	0.51
	-52844.51[2]	421	0.42
phenCl	-15217.14[2]	38,740	2.55

3.11. Detection Limit (LOD) and Quantification Limit (LOQ)

Limit of Detection (LOD) is defined generally as the lowest amount of a substance that can be distinguished from the blank (absence of that substance in the matrix) within a 99 % confidence level. Conversely, The International Union of Pure and Applied Chemistry (IUPAC) define LOD as the concentration or quantity derived from the smallest measure that can be detected with reasonable certainty for a given analytical procedure. Limit of detection can be affected by the accuracy of the model used to predict concentration from raw analytical signal. Limit of Quantification (LOQ) is defined as the lowest amount of analyte in a given matrix that can be quantitatively determined with suitable precision and accuracy.

Many researchers have used the blank signal to evaluate the LOD, which is then converted to concentration. Whereby, they take a replicate measurements (usually 7) of the blank (matrix minus analyte), then from this data, evaluation of the Relative Standard Deviation (RSD) or Standard Deviation (STDEV) is carried out. Then, 3 x (RSD or STDEV) of the blank signal give an initial value, which can then be estimated to LOD in terms of concentration. On the other hand, large environmental monitoring agencies like EPA have used spiked method [EPA MANUAL 1996]. Whereby, the blank matrix signal is obtained, subsequently spiked with a series of known concentrations of the analyte in question. Relative Standard

Deviation calculated and then the evaluation of LOD and LOQ carried out.

In this study, we adopted EPA and U.S Department of Natural Resources (DNR) methods, where 7 replicate absorbance measurements of fixed concentration of the sensing molecules with pollutants thus one spectrum at a time on different pollutants concentration was measured. This was achieved by adding aliquots in μL of known standard concentration of the pollutant under study. Standard Deviations were then evaluated of these data and from these standard deviations, the Limit of Detection (LOD) calculated using equation 4.

$$LOD = 3xSTDEV \quad \ldots\ldots\ldots\ldots\ldots\ldots\ldots\ldots\ldots\ldots\ldots\ldots\ldots\ldots 4$$

The LOD multiplied by 3, gives Limit of Quantification (LOQ). These results are as presented in Tables3 and 4 for absorbance and fluorescence respectively.

Presented in Table 5 is data for comparison of LOD and LOQ for this study and other organisations.

Presented in Table 6 is the data for Permissible Exposure Limits as recommended by the listed organisations for comparison with concentrations for the environmental pollutants' amounts obtained in this study.

4. Conclusion

It has been established from the experiments carried out in this study that, the sensing reagents FLXN and phenCl show specificity in interaction with pollutants identified for this study. Fluorescein (FLXN) specifically interacted with BaP, PRN, and py from cigarette smoke and 1, 10- phenanthroline chlororide monohydrate (phenCl) specifically interacted with PRN in cigarette smoke from a matrix containing other PAHs. From the vehicle exhaust pipe dust in ethanol, FLXN specifically interacted with BaP and PRN while phenCl specifically interacted with PRN.

The detection limits and quantification limits are relatively low, given that in this study, the LOD for BaP, PRN and py using phenCl as the sensor were 0.12, 0.061 and 0.17 μg/L respectively. These LODs were achieved by fluorescence method of analysis with PMT detector and they are lower than the PEL set at 0.2 μg/L by environmental pollution monitoring agencies. The low detection limits makes phenCl sensor for BaP, PRN and py. If we compare these results (Table 5), EPA analytical method reported LOD for py as 5.0 μg/L using GC-MS with fluorescence detector, whereas in this study we established LOD for py to be 0.17 μg/L using fluorescence method of analysis with PMT detector. In their study, OSHA established LOD for PRN to be 0.26 μg/L using HPLC analytical technique with UV-fluorescence detector while in this study, using phenCl sensor, we established LOD for PRN to be 0.061 μg/L using fluorescence method with PMT detector (Table 5). In this regard, phenCl as compared to FLXN could be a viable sensor for BaP, PRN and py to be developed since it has established LODs below PEL set by: ATSDR, EPA, NIOSH and OSHA as shown in Table 6. The sensor can therefore facilitate detection of micro-concentration of BaP, PRN and py.

When the calibration plots modelled in this study were used to evaluate the PAHs and py in cigarette smoke and vehicle exhaust pipe dust, it was established, as presented in Table(s) 1 and 2 that the amounts of pollutants are greater than permissible exposure limits as recommended by ATSDR, EPA, NIOSH, OSHA and WHO (Table 6). The pollution level for these carcinogenic chemicals released in the environment through cigarette smoking and vehicle emissions is hazardous to health and therefore calls for measures to reduce such levels to recommended Permissible Exposure Limits (PEL).

Acknowledgement

Prof. .Bulimo's research crew at KEMRI for their co-operation and support, that enabled us perform fluorescence study. Greatly so, to National Council for Science, Technology and Innovation (NACOSTI) – Kenya, for financial support – this enabled us reach our goals. Lastly to Jomo Kenyatta University of Agriculture and Technology for facilitating this research and Technical University of Kenya for allowing us use their UV-VIS Spectrophotometer.

References

[1] Analytical detection limit guidance and laboratory guide for determining Method Detection Limits(MDLs) manual – Department of natural resources, Wisconsin USA (April 1996).

[2] Brylee David B. Tiu, Reddithota J. Krupadam, and Rigoberto C. Advincula.Pyrene-imprinted polythiophene sensors for detection of polycyclic aromatic hydrocarbons. Sensors and Actuators B: Chemical Volume 228, (2016) 693–701

[3] Cañizares P and Luque de Castro M.D. Flow-through sensor based on derivative synchronous fluorescence spectrometry for the simultaneous determination of pyrene, benzo(e)pyrene and benzo(ghi)pyrene in water. Fresenius. J. Anal. Chem. 354 (1996) 291 – 295.

[4] Chen Y.C; Brazier J.J; Mingdi Y; Bargo P.R and Prahl S.A. Fluorescence-based optical sensor design for molecularly imprinted polymers. Sensors and Actuators B Vol. 102 (2004) 107 – 116.

Table 3. Calculated STDEV, LOD and LOQ for Absorbance of FLXN and phenCl with ANTH, BaP, PRN and Py solutions.

Pollutant	**STDEV of signal**		**$Signal_{unk}$- Intercept**		**STDEV(Conc./µM)**		**LOD µM**		**LOQ µM**	
	FLXN	phenCl	FLXN	phenCl	FLXN	phenCl	FLXN	phenCl	FLXN	phenCl
ANTH	**0.0047**	**0.005**	**-0.2077**	**-0.0598**	0.023	0.083	0.067	0.25	0.204	0.75
BaP	**0.0361**	**0.0749**	**-0.1293**	**-0.4085**	0.28	0.18	0.84	0.55	2.52	1.65
PRN	**0.0096**	**0.0134**	**-0.2551**	**-0.0979**	0.038	0.14	0.113	0.41	0.34	1.23
Py	**0.0014**	**0.047**	**-0.2551**	**0.2728**	0.006	0.17	0.017	0.52	0.050	1.55

Table 4. Calculated STDEV, LOD and LOQ for Fluorescence of FLXN and phenCl with ANTH, BaP, PRN and Py solutions.

Pollutant	**STDEV of signal**		**$Signal_{un-k}$ - Intercept**		**STDEV(Conc/µM)**		**LOD µM**		**LOQ µM**	
	FLXN	phenCl	FLXN	phenCl	FLXN	phenCl	FLXN	phenCl	FLXN	phenCl
ANTH	**5258**	**1693**	**-53118**	**-17147**	0.099	0.099	0.297	0.296	0.89	0.89
BaP	**3347**	**275**	**-43327**	**-18009**	0.077	0.015	0.23	0.046	0.70	0.14
PRN	**2206**	**153**	**-54055**	**-15217**	0.041	0.010	0.122	0.03	0. 37	0.09
Py	**42**	**942**	**-2819**	**-12819**	0.015	0.073	0.045	0.22	0.134	0.66

Table 5. Data for LOD and LOQ of this study and for some international agencies

ANALYST	**Pollutant**	**LOD; µg/L**		**LOQ µg/L**		**Analytical method**
		Absorbance	Emission	Absorbance	Emission	
This study	ANTH	0.5 (0.5)	0.53(0.53)	1.5(1.5)	1.59(1.59)	Absorbance
No brackets;	BaP	2.1(1.4)	0.58(0.12)	6.3(4.2)	1.74(0.36)	Fluorescence
FLXN	PRN	0.23(0.83)	0.25(0.061)	0.69(2.49)	0.75(0.183)	With PMT detector
Brackets; phenCl	Py	0.013(0.41)	0.36(0.17)	0.039(1.23	1.08(0.51)	

ANALYST	Pollutant	LOD; µg/L	LOQ µg/L	Analytical method
EPA	ANTH BaP PRN Py	0.02 5.0***		HPLC With UV-Florescence detector ***(GC-MS)
OSHA	ANTH BaP PRN Py	0.028 0.045 0.26	0.066 0.207 1.13	HPLC With UV-Florescence detector
NIOSH	ANTH BaP PRN Py	0.01 - 0.09 0.006 – 0.08 0.001 – 0.03	0.023 – 0.3 0.020 – 2.6 0.0036 – 0.99	HPLC With UV-Florescence detector

Table 6: PEL for ANTH, BaP, PRN and Py

AGENCY	PEL		Parts per billion (ppb)
	Air mg/m^3	Water mg/L	
ATSDR	**0.2**	***0.0002***	***0.2***
EPA	**0.2**	***0.0002***	***0.2***
NIOSH	**0.1**	***0.0001***	***0.1***
OSHA	**0.2**	***0.0002***	***0.2***

PEL for pyridine 5 ppm and 15 mg/m^3. Asterisks show same concentration converted from mg/L to ppb.

[5] Clayton P.M, Vas A.C, T. Bui, Drake F.A and McAdam K. Spectroscopic studies on nicotine and nornicotine in the UV-region. Journal of organic chemistry: chirality vol. 25 Issue 5 (2013) 265 -311.

[6] Dikert F.L, Besenbock H and Tortschanoff. M. Molecular imprinting through Van Der Waals interaction: Fluorescence Detection of PAHs in water. Advanced Materials 10 (1998) 149 – 151.

[7] Elosua C, Bariain C, MatiasI R., Rodriguez A, Colacio E, Salinas-Castillo A, Segura-Carretero A and Fernandez-Gutiérrez A. Pyridine Vapors Detection by an Optical Fibre Sensor. *Sensors 8*(2) (2008) 847-859.

[8] Fernandez-Sanchez J. F.; Carretero A. S.; Cruces-Blanco C. and Fernandez-Gutierrez A. Highly sensitive and selective fluorescence optosensor to detect and quantify benzo[a]pyrene in water samples. Anal. Chim. Acta (2004) 1-7.

[9] Ghini G, Trono C, Gianetti A, Puleo G.L, Luconi L, Amadou J, Giambastani G and Baldini F. Carbon nanotubes modified with fluorescein derivatives for pH sensing. Sensors and Actuators B. Chemical 179 (2013) 163 – 169.

[10] Gui R, An X and Huang W. An improved method for ratiometric fluorescence detection of pH and Cd^{2+}using fluorescein isothiocyanate – quantum dots conjugates. Analytica Chimica Acta 767 (2013) 134 - 140.

[11] Ishida M; Naruta Y. A Porphyrin – related macrocycle with an embedded 1, 10 – Phenanthroline moiety: Fluorescent Magnesium (II) ion sensor. Agewandte Chemie International edition 49(1) (2010) 91 – 94.

[12] Koganti A; Singh R; Ma B-L and Weyand E.H. Comparative analysis of PAH-DNA adducts formed in lung of mice exposed to neat coal tar and soils contaminated with coal tar. Environ. Sci. Technol. 35 (2001) 2704 – 2709.

[13] Körber R.W and Goschnick J. Rapid Screening of Organic Pollutants in Rubble with an Electronic Nose Based on a Metal Oxide Gas Sensor Microarray. Springer Science (2002) 157 – 162.

[14] Lai J, Niessner R, and Knopp D. Benzo[a]pyrene imprinted polymers: synthesis, characterization and SPE application in water and coffee samples. Analytica Chimica Acta, Volume 522, Issue 2 (2004) 137–144.

[15] Li T, Yang Z, Li Y, Liu Z, Qi T and Wang B. A novel fluorescein derivative as a calorimetric chemosensor for detecting copper (II) ion. Dyes and pigments 88(1) (2011) 103 – 108.

[16] Lin H- J, Chen C-Y. Thermo-responsive electrospun nanofibers doped with 1, 10- phenanthroline-based fluorescent sensor for metal ion detection. Journal of materials science volume 51, issue 3 (2016) 1620 – 1631.

[17] Malgorzata S, Malgorzata P, Dobrzynka E, Pyrzynska K and Baraniecka J. Polycyclic Aromatic Hydrocarbons Distribution in Fine and Ultrafine Particles Emitted from Diesel Engines. Pol. J. Environ. Stud. Vol. 22, No. 2 (2013), 553-560.

[18] NIOSH Manual for Analytical Methods (NMAM) July issue (1986).

[19] OSHA Manual (1996).

[20] Pierre J. A and Vo-Dinh T. Antibody-based Biosensor for Benzo(a)pyrene DNA-adduct. Polycyclic Aromatic Compounds, Vol.8 (1996) 45 – 52.

[21] Ripp. J. Analytical Detection Limit Gidance & Laboratory Guide for determining Method Detection Limit (MDL). Wisconsin Department of Natural Resources certification Program (1996) PUBL – TS – 056 – 96.

[22] Schmeltz I, Stedman R.L, Chamberlain W.J and Burdick D. Composition studies on tobacco bases of cigarette smoke. Journal of the Science of food and agriculture Vol. 15, Issue 11 (1964) 774 – 781

[23] Schmidt H; Ha B.N; PfannkucheJ; Amann H; Kronfeldt D and Kowalewska G. Detection of PAHs in sea water using Surface-Enhanced Raman Scattering (SERS). Marine pollution bulletin Vol. 49, 3 (2004) 229 – 234.

[24] Sironi L, Freddi S, D'Alfonso L, Collini M, Gorletta T, Soddu S and Chirico G. P53 detection by fluorescence lifetime on hybrid fluorescein isothiocyanate gold nanosensor. Journal of Biomedical nanotechnology 5(6) (2009) 683 – 691.

[25] Traviesa-Alvarez J.M., Sánchez-BarragánI, Costa-Fernández J. M, Pereiro R and Sanz-Medel A. Room temperature phosphorescence optosensing of benzo[a]pyrene in water using halogenated molecularly imprinted polymers. Analyst, 132, (2007) 218-223.

[26] Wang L, Huang Z, Gao, Q Liu Y, Kou Xand Xiao D. A Novel Pyrene Fluorescent Sensor Based on the π–π Interaction between Pyrene and Graphene of Graphene–Cadmium Telluride Quantum Dot Nanocomposites. Spectroscopy Letters,Volume 48, Issue 10 (2015) 748-756.

[27] Zhang J.; Dong J. H.; Luo M.; Xiao H.; Murad S. and Normann R. A. Zeolite-fiber integrated optical chemical sensors for detection of dissolved organics in water. Langmuir (2005) 8609-8612.

[28] Zhihui X, Fangjun H, Jing S, Yutao Y,Caixia Y, XuXiu Y and Shuo J. Sensitive Colorimetric and Fluorescent Detection of Mercury Using Fluorescein Derivatives. Open Journal of Biosensor, (2012) , 1, 44 – 52.

Available online at www.kenchemsoc.org

Journal of the Kenya Chemical Society 10-1 (2017), 58-69

JOURNAL OF THE KENYA CHEMICAL SOCIETY

Extraction and Characterization of Yellow Oleander (*Thevetia Peruviana*) Seed Oil, Meal and Analysis of Eggshells' Catalyst as Potential Feedstocks for Biodiesel Production in Kenya

Jeremiah O. Masime*[1], Eric Ogur [2], Betty Mbatia[3], Joseph Lalah[1], Austin O. Aluoch[1] and Geoffrey Otieno[1]

Department of Chemical Sciences and Technology[1],The Technical University of Kenya
Department of Mechanical and Mechatronic Engineering[2], The Technical University of Kenya
United States International University-Africa School of Pharmacy and Health Sciences [3]

*Correspondence author:*E-Mail: geoffrey.otieno@tukenya.ac.ke,geoffrey.otieno@gmail.com.*

Abstract

Biodiesels have a number of advantages such as reduced emission, improved combustion, however, their energy efficiency is still lower than that of petro diesel. Thevetia peruviana (Yellow Oleander) seed oil was extracted using n-hexane as a solvent in a Soxhlet extractor. The percentage yield was 61.78 ± 1.53 %, which makes yellow oleander seed a good source of the vegetable oil. Samples of yellow oleander oil extracted using the soxhlet method were then subjected to physico-chemical analysis. The composition of the incinerated waste eggshells catalyst was ascertained using XRF analysis and it was found that the ash obtained at 550 °C contained about Na_2O - 0.144, MgO - 1.159, P_2O_5 - 0.351, SO_3 - 1.195, CaO - 98.124 and SrO - 0.026as the major component for catalytic activation. The concentrations of the elements in yellow oleander meal and oil were determined using XRF and found to generally decrease except for the following which increased during extraction: SiO_2; from 0.000 to 3.858 mg/kgand Fe; from 1.1638 to 1.270 mg/kg. The rest decreased as follows,Al_2O_3; from 0.3929 to 0.198 mg/kg, S; from 18.90 to 7.05 mg/kg, and CaO; from 11.404 to 10.683 mg/kg and. These increase were attributed to concentration during extraction. The calorific values of the meal and oil were determined using a bomb calorimeter and the following values were obtained 29.8986 and 38.6470 Mj/kg respectively. The physico-chemical parameters for the oil tested included specific gravity, free fatty acid, saponification value, peroxide value, iodine value and yield. The values obtained were 0.87 ± 0.90, 1.41 ± 0.25 %, 197.33 ± 1.69 mg KOH/g oil, 1.88 ± 0.57 Meq0_2/kg, 80.77 gI_2/g and 62.76 ± 1.53 % respectively. Yellow oleander meal was found to contain 190540 mg/kg of total carbon, which is high, it can be used in the making of briquettes and charcoal instead of going to wastage. The only problem noticed were the high levels of CaO which form abrasive solids, these can result in injector and fuel pump wear, aswell as piston and ring wear, and may increase engine deposits. The presence of sulphur also implies the emission of SO_xgases and formation of sulphuric acid. The spectroscopic method used in analyzing the oil included GC/MS, FTIR and UV Visible spectroscopy. The eggshells also, registered the presence of relatively high levels of CaO, MgO and Al_2O_3 and other metals, this makes it a good heterogeneous catalyst. The studied physicochemical characteristics of the yellow oleander oil extract compared favorably with the conventional oil in the Kenyan market. The biodiesel standard ASTM D6751 and EN 14214 confirm that the yellow oleander oil can be processed and used as raw material in the production of a biodiesel.The yellow oleander meal and oil properties were analyzed as per ASTM and EN-standards.

Keywords: Extraction, Physico-chemical characterization, Yellow oleander oil, spectroscopy.

1. Introduction

The international oil consumption is projected to increase to about 36 % by 2030. Oil consumption in Africa may actually double by 2030 [1]. Internationally, crude oil reserves have continued to deplete, increased environmental threat and security concerns associated with the release of greenhouse gases have stimulated the search for alternative sources of petroleum based fuels [2]. Since 2007, biomass energy resources in Kenya, i.e. firewood, charcoal and agricultural wastes have contributed approximately 70 % of Kenya's total energy demand and provided for almost 90 % of rural household energy needs [1]. Although a recent discovery and

potential production of crude oil has been reported, the country still spends a large part of its foreign reserves on importation of white petroleum products for energy especially for the transport sector. This sends a red light on the need for a biofuel supplement in Kenya and biodiesel is often considered as good substitute for diesel powered vehicles [2]. The objective of the Kenyan vision 2030 is to help transform Kenya into a, "middle-income country providing a high quality life to all its citizens" [1]. One of the main constraints in achieving rapid and sustainable development in the country has been the high demand for energy. The government of Kenya has enacted a policy (Sessional Paper, No. 4 of 2004) and legislation (the Energy Act, No. 12 of 2006) that support the development of ethanol and biodiesel, and the department responsible for energy matters (the Ministry of Energy and Petroleum) has developed a biodiesel strategy through its National Biofuels Committee [2]. The National Development Plan also stipulates the need to ensure a balance between energy development and environmental protection and developments of alternative energy sources such as biodiesel not only provides good substitutes for conventional petroleum but also offer solutions for environmental conservation in form increased biomass cover and rainfall and carbon emissions reduction. The Kenya Biodiesel Association was formed with support from all sectors of the biofuels industry [1]. Compared with ethanol production, biodiesel production in Kenya is still unexploited.

Yellow Oleander *Thevetia peruviana*seeds have a waxy coating cover in order to reduce water loss which is typical of the oleanders family of plants. The stem and its fruit is deep red-black in color encasing a large seed [3]. The plant belongs to the family of Apocynaceae. In Nyanza, western part of Kenya where it flourishes very well, it is called 'Chamama', and it is commonly found around homes where it is used as fencing cover. The plant has a high biomass cover in form of green leaves which makes it useful as a crop that can be grown in large plantations to create expansive biomass cover for carbon sequestration. It is a perennial crop, drought tolerant and does not require a lot of care during field cultivation [4]. Mature yellow oleander fruit contains 2-4 seeds in a kernel. The plant has a high cover which makes it also a beneficial crop for carbon protection. All parts of the yellow oleander plant are toxic, due to the presence of glycosides and the seeds contain between 60 – 65 % oil [5]. Yellow oleander seed oil is free from sulphur and aromatic compounds [5]. Vegetable oils are a renewable, potentially inexhaustible source of energy and have an energetic content close to that of diesel fuel.The seed is not edible but it has nutritional values and can be used as an alternative source of protein for animal feeds formulation.

Ebiyemi *et al*., [6] found minor and unusual fatty acids composition of yellow oleander oil seeds from Enugu, Zaria, Edidi and Ilorin in Nigeria. They also found out that the number of kernels per fruit and the oil yield were significantly different among geographical locations [6]. Basumtary [7], alsofound the following compositionin yellow oleander seed oil; myristic acid, palmitic acid, stearic acid, oleicacid, linoleic acid, linolenic acid, arachidic acid and arachidonic acid.Jabar *et al*. [8] found; Myristic (14:0) - 0.18, Palmitic (C16:0) 19.10, Palmitoleic (C16:1) - 0.01, Stearic (C18:0) - 7.32, Oleic (C18:1) -53.41, Linoleic (C18:2) -19.04, Linolenic (C18:3) - 0.26, Arachidic (C20:0) - 0.11, Arachidonic (20:4) - 0.40, Behenic (C22/0) - 0.07 and Erucic (22/1) - 0.10. They also found 26.78 %saturated and 73.22 % saturated carboxylic acids.Oseni *et al*, found out that Yellow oleander oil containedpredominantly Stearic acid (6.23%), Palmitic acid(17.02%), Oleic acid (41.91%), Linoleic acid(11.89%), Linolenic acid (1.15%) and Arachidic acid(1.82) [9].The composition of oil determines the properties of thebiodiesel obtained. From these data one can see that oils from different sources have different fatty acid compositions, since they vary in their carbon chain length and in the number of unsaturated bonds they contain. The fatty acid profile of vegetable oils have a major role in biodiesel production processes as well as in quality of biodiesel [7].In this research it is our desire to find out if the yellow oleander from Kenya would be of different composition.

Eggshells are comprised of a network of protein fibers, associated with crystals of calcium carbonate ($CaCO_3$), magnesium carbonate ($MgCO_3$) and calcium phosphate ($Ca_3(PO_4)_2$), and other uncharacterized organic compounds and water. Among heterogeneous catalysts, CaO/MgO from waste eggshells is of interest because it has high activity and basicity, low solubility, is non toxicity, cheap and the fact that it can be reused severally[10]. This multi-metal ion status gives it a synergy effect that enhancesitscatalytic activity. This improves its trans-esterification activity and hinders the formation of soaps. In this study, X-ray Fluorescence Spectrophotometry was used to determine the mineral composition of eggshell in order to understand its catalytic properties for the trans-esterification of yellow oleander seed oil.

Buasri *et al.*, found the following data for chicken eggshells; Na_2O - 0.144 %, MgO – 1.159 %, P_2O_5 - 0.351 %, SO_3 – 1.195 %, CaO – 98.124 % and SrO 0.026 % respectively [11]. They found out that both duck and chicken waste eggshell catalysts had concentrations of CaO 98.93 and 98.12 wt.%, respectively [11]. This makes the waste eggshells potentially a good heterogeneous catalyst.In order to make the biodiesel production more sustainable, the utilization of waste

heterogeneous catalysts has been of recent interest Peng-Lim Boey*et al* [12].Waste oysters and chicken eggshellsidentifiedas effective catalysts in the trans esterification of soybean oil to methyl esters.The catalyst was found to be capable of being reused up to 13 times without losing its activity. The catalyst had both high surface area and Ca content which increased the yield to 90 % biodiesel in a 2 h [12].

The aim of this research study was to investigate the potential of yellow oleander oilfor a biodiesel raw material. The seeds were collected from Nyanza region in Kenya, the oil extracted and selected physco-chemical properties were analyzed. The catalytic properties of waste eggshells were also investigated for use as a green catalystto be used in the trans-esterification of the oil produced.

2. Materials and Methods

2.1. Collection of samples

Sampling of yellow oleander seeds took place in Gem Constituency, Siaya County, situated in Nyanza, Kenya. Its geographical coordinates are 0° 33' 36" North, 34° 17' 10" East. for Yellow Oleander seeds. Sampling was done for a period of four months (January to April 2015).Siaya County: 842,304 (Male - 47 % Female - 53 %); Poverty Rate (based on KIBHS %): 35.3, Gem Constituency: 160,675, Poverty Rate: 42.0 [7].

2.2. Chemicals and reagents

All solvents and chemicals used were of analytical grade, they were procured from commercial suppliers including Travotech Agencies Limitedand Kobian Kenya Limited in Nairobi. The chemicals were used without further treatment.

2.3. Yellow oleander seeds Kernel Sample Preparation

Freshly matured yellow oleander seeds were handpicked in Gem Constituency, Siaya County, Kenya and transported in a plastic bag to the laboratory in TU-K in Nairobi. The seeds were weighed using an electronic balance JT601N and the average wet weight was recorded. The fleshy cover of the kernel containing the seeds were also removed, discarded and the seeds sundried for at least 2 weeks. This was to allow them to undergo biodegradation. The dried seeds were later weighed and grounded to powder using a manual grinding machine [13].

2.4. Gravimetric analysis: Oil extraction and analysis

Extraction was done using n-hexane as a solvent in the solvent extraction methods using a 250-mL Soxhlet apparatus under a hood in the laboratory for 2 hours. This method was also discussed by Basumatary *et al.* [14] and Oseni *et al.* [15].Gravimetric determination of total oil content of the seed was done according to the equation:

$$Yellow\ oleander\ seed\ oil\ (\%) = \frac{Weight\ in\ gms\ of\ seed\ oil\ extracted}{weight\ in\ gms\ of\ powdered\ dry\ seeds} x\ 100$$

2.5. Moisture content

Water content affectsthe calorific value of a biofuel.Itdecreases the density of the pellets considerably, causes formation of soap, interferes with its catalytic effectiveness and results in lowyields of the biodiesel [16].The method used by Yarkasuwa *et al.*can be employed in finding the moisture content [17]. % Moisture content= $\frac{W_2 - W_3}{W_{2-} W_1}$ x 100, Where, W_1 = weight of crucible, gm, W_2 = weight of crucible + sample, gm, W_3= weight of crucible + sample after heating, gm. Moisture content = $\frac{122.0474-108.3932}{122.0474-65.6102} = \frac{13.6542}{56.4372}\ x\ 100 = 24.19\ \%$

Mishra *et al.,* [18], found 4.97 % for yellow oleander seed, and Musa *et al.,* [38]. also found a moisture content of 30 % in the fruit of the same plant.

2.6. Volatile matter

The quantity of volatile matter in a fuel influencesits combustion behavior. Fuel having low volatile matter and high fixed carbon content will take long time to burn unless they are powdered.

Sample were treated according to the method described by Mishra *et al.*,[18]. $\%\ volatile\ matter = \frac{W_5-W_6}{W_5-W_4}\ x\ 100$, Where, W_4 = weight of empty crucible, gm, W_5= weight of empty crucible + sample, gm, W_6=weight of empty crucible + sample after heating, gm, $\%\ volatile\ matter = \frac{80.936-47.8475}{80.936-44.7386} = \frac{33.0885}{36.1974}\ x\ 100 = 96.76\ \%$

Mishra *et al.,* [18], found 91.05 % particulate matter for yellow oleander seed.

2.7. Measurement of calorific value

The calorific value of biomass sample can be measured by using bomb calorimeter. Following formula can be used to calculate the calorific value. $Calorific\ value\ \left(\frac{Kcal}{Kg}\right) = \frac{(W+w)x\ 4.12x\ (T1-T2)}{X}$, Where, W = weight of water in calorimeter, Kg,w = water equivalent of apparatus, T_1 = initial temperature of water, °C, T_2= final temperature of water, °C and X = weight of fuel sample taken, Kg.

2.8. Physico-chemical properties

The physico-chemical properties of the extracted oil were determined and compared with the standard values of vegetable oil. The parameters considered included; free fatty acid, iodine value and the saponification value as explained by Ibiyemi *et al.* [6]. The ASTM standards used included the following; ASTM D5555, ASTM D1959 and ASTM D464 respectively [17], and the peroxide value was determined according to AOCS Official Method Cd 8-53 (2003) [17].

2.8.1. Estimated molecular mass, acid value, specific gravity, peroxide saponification values and iodine value

The saponification value was determined according to titrimetric method discussed by Dimberu *et al.* [18]. The value was calculated according to the equation [18]. $Saponification\ vale = \frac{V_0 - V_1\ x\ C\ x\ 56.1}{m}$

Where 56.1 is equivalent weight of KOH, V_0 is the volume in ml of standard HCl solution used for the blank test, V_1 is the volume in ml of the standard HCl solution used for sample, C is the exact concentration of the standard HCl (0.5 N) solution and m is the mass in gram of the test portion (2 g).

For the determination of the acid value, the method described by Dimberu *et al* [18 was used. The acid value was calculated according to Okpuzor *et al.*, 2009 [19]. $Acid\ value = \frac{56.1\ x\ V\ x\ M}{x}$. Where 56.1 is equivalent weight of KOH, V is the volume in ml of standard volumetric KOH solution used, M is the exact concentration in KOH solution used (0.1 N); x is the mass in grams of the test portion (1 g) [18]. NB:- Acid Value (AV) = 1.99 xFree Fatty Acid (FFA).

The estimated molecular mass of the yellow oleander oil was calculated using the formula used by Wu*et al.* [45]; Estimated R.M.M of yellow oleander oil= $\frac{56.1\ x\ 1000\ x\ 3}{SV - AV}$, Estimated R.M.M of yellow oleander oil= $\frac{56.1\ x\ 1000\ x\ 3}{197.33 - 2.268} = \frac{168300}{195.062} = 862.80$

Where SV is the saponification value, 56.1 is equivalent weight of KOH and AV is the acid value of the yellow oleander oil.

The specific gravity is the ratio between the density of the yellow oleander oil, and water as a reference substance.The specific gravity is expressed without units. Specific density= $\frac{Density\ of\ oil}{Density\ of\ water} = \frac{\rho_{oil}}{\rho_{water}} = \frac{mass\ of\ oil}{mass\ of\ water}$. Vegetable oils will typically have a specific gravity ranging from 0.903 to about 0.921 depending on the fatty acid composition of the oil and its temperature [20]. Rick Da Tech [20] found out that for three different temperatures for measuring density, 15.5 ºC, 20 ºC and 25 ºC,as the temperature increased the density of the oil decreased. Specific gravity of oil can be removed by reacting the of polar compounds from the oil by alkali during trans esterification [17].

The peroxide value was evaluated according to AOCS Official Method Cd 8-53 (2003) [21]. This was done according to the method discussed by Dimberu *et al.* [18]. Peroxide value was calculated according to the equation:$Peroxide\ value = \frac{10\ x\ (V_1 - V_2)}{x}$. Where: V_1 volume of 0.01 N $Na_2S_2O_3$ for determination of test sample in ml, V_2 volume of 0.01 N $Na_2S_2O_3$ for determination of blank solution in ml and x is mass of test portion in g (5 g) [18].

The iodine value (IV) gives a measure of the average degree of unsaturation of a lipid: the higher the iodine value, the greater the number of C=C double bonds. By definition the iodine value is expressed as the grams of iodine absorbed per 100g of lipid. This was done using the Lubrizol test procedure [46]: Iodine valuewas calculated using the following law: $Iodone\ value = \frac{(A-S)x\ N\ of\ Na_2S_2O_3\ x\ 0.127\frac{g}{meq}\ x\ 100}{Weight\ of\ sample\ (g)}$

A: V ml of $Na_2S_2O_3$ volume for blank S: V ml of $Na_2S_2O_3$ volume for sample.

2.9. Spectroscopic analysis

2.9.1. Fourier Transform Infra-Red Spectrometry (FTIR) analysis

The FTIR analysis was carried out using FTIR-600 Spectrophotometer with a NaCl cell. This machine was equipped with attenuated total reflectance (ATR) accessory which was used to obtain the infra-red spectra of the yellow oleander oil samples [22]. This spectrophotomeder uses a DLATGS (Lanalin-doped deuterated triglycerine sulphate) sensitive pyroelectric detector that provides a good signal-to-noise ratio and allows reduction of analysis time was used to collect FTIR spectra. For FTIR spectra recording a small quantity of the oil sample in a thin film was used [22].

2.9.2. Gas Chromatography-Mass Spectrometry (GC-MS) analysis

A GC-MS QP2010 PLUS (Shimadzu, Japan) was used for the analysis of the extracted oil. A RTX-5 ms column (5% diphenyl, 95% dimethylpolysiloxane stationary phase), 30 m × 0.25 mm i.d × 0.25 μm film thickness (Restek, USA) was used [23]. The columntemperature was programed at 70 ºC was raised at 10 ºC/min to 240 ºC, the holding time was 4 min, with an injection temperature of 250 ºC. The carrier gas used was helium with a flow rate of 40.8 mL/min. The detector that was used is a quadrupole mass spectrometer (MS) with electron ionization (EI) at 70 ev in full scan mode [23].

2.9.3. UV-VIS Spectra analysis of the oil

UV-vis spectroscopy was performed using a UV – 1800 SHIMADZU spectrophotometer model ENG 240 V, this was explained by Viswanathan*et al.*[24]. Most absorption spectroscopy of organic compounds is based on or electrons to the excited state. The absorption spectra for these transitions fall in the region of wavelength 200–700 nm. These transitions need an unsaturated group in the molecule to provide the electrons [24]. The UV spectrum of vegetable oils involves the electronic absorption of fatty acids; in particular, the 230-270 nm band shows high absorption when conjugated dienes and trienes of unsaturated fatty acids are present [25].

3. Results and Discussion

3.1. Physicochemical properties

The physicochemical propertiesof yellow oleander oil are summarized in table 2 below. The yield of 62.60 ± 3.57 % obtained in this study corresponded to the theoretical range of 60 – 68 % oil content expected, and it also confirmed the yellow oleander is rich in oil that can produce viable quantities for biodiesel processing.

Table 2: Physicochemical properties

Analytical Parameter (n=4)			ASTM/ KEBS
	This study Mean ± s.e	Jabar *et al.*(2014)	
Weight of kernel/fruit %	31.49 ± 0.26		-
Oil yield %	61.67 ± 0.66	63.5	-
Saponification Value (mgKOH/g)	197.33 ±1.69	162.3	190 - 209
Acid Value (mg KOH/g)	2.268 ± 0.57	7.50	4
Free Fatty Acid value (%)	1.44 ± 0.25	3.75	2
Specific gravity	0.87 ± 0.11	0.922	0.86 – 0.90
Peroxide value (mEg O_2/kg sample)	1.88 ± 0.57	3.52	10
Iodine value gI_2/100g	80.77	106.00	120
Relative Molecular Mass	862.80		

The calculated molecular mass of yellow oleander oil was 862.0,this is high, and causes the oil to be viscous. This, together with the presence of oxygen in yellow oleander seed oil, makes it a good lubricant. Trans-esterification reaction is used to reduce the viscosity of the yellow oleander oil triglyceride thereby making the characteristics of the biodiesel close to diesel fuels, this process increases the volatility margin of the oil and improves engine performance. If yellow oleander is adopted as as a raw material for the preparation of biodiesel it would be best to trans-esterify the oil.Ibeto *et al.*, [26] reported the following results for the following non edible oil seeds; squashes (14.08 %), sponge (92.50 %), guard (12.30 %) and melon (44.85 %) respectively [26]. Hence yellow oleander seed registered a relatively higher value. The percentage of kernel was 36.45 % (after drying), and this is an indication of lower wastage during the extraction of the oil. The 38 % (by weight) residue that was left after extraction can also go towards the preparation of animal feeds but this needs to be investigated to determine toxicity.

The quality of the yellow oleander seeds oil extracted was evaluated by determining its physicochemical properties and the results are presented and compared with other data in Table 2 above. These values are also in line with values reported in other studies as reported by Ibiyemi *et al.*[6]. The acid value (AV) of a vegetable oil is an important variable in considering the quality of oil because the lower the AV the better the quality of the oil. Free fatty acids (FFA) and AV measure the presence of both corrosive free acids and oxidation products. Acid value increases with days of storage under uncontrolled conditions. This results into the formation of significant amount of soap during the trans-esterification reaction. Soap formed during the reaction interferes with the separation of the biodiesel from glycerine [27]. From the results obtained, the free fatty acid values (FFA) for yellow oleander seed oil was 1.44 which is lower than 3.75 obtained by Jabar *et al.* [28]. The free fatty acids are generally degradation products of the vegetable oil esters, with the free fatty acids breaking away from the triglycerides. A higher free acid value decreases the oil quality. The values obtained for yellow oleander seed oil analyzed in this study were low. The value recorded was below the ASTM standards of 2 % for FFA and AV of 4 mgKOH/g. Similar results were obtained by Deka *et al.*, Yarkasuwa *et al.*, Adebowal *et al.*, Oseni *et al.*, Ogunneye *et al.* and Usman *et al.*, obtained 0.284, 2.4, 3.4, 1.96, 0.665 and 0.62 % respectively [7]. Therefore, the extracted oil can be taken through a trans-esterification reaction directly.

The saponification value (SV) is used for checking adulteration and can be used to indicate the presence of free fatty acids which lead to soap formation. To avoid soap formation a heterogeneous catalyst have been used in order to inhibit soap formation, they are more selective to biodiesel (purer product), and simplify the glycerol purification (99 %purity glycerol can be produced against 75% in the homogeneous process) [22]. In this study, the yellow oleander oil had a saponification value of 197.3, which was higher than 162.43 mgKOH/g observed by Jabar *et al.* [28] but within the American Society for Testing and Materials (ASTM) and Kenya Bureau of Standards (KEBS) standard of 190 - 209 mgKOH/g. The peroxide value (PV) of the oil increases with the storage time, temperature and contact with air. Vegetable oils exposed to both atmospheric oxygen and light show a much larger increase in peroxide value during storage. This indicates that if the vegetable oils are to be used for the purpose of biodiesel production, then they have to be utilized as soon as they are produced or extracted [29]. Peroxide value of 1.88 was registered in this study and this corresponded closely to 3.1 – 3.9 mEq O_2/kg obtained by Ibiyemi *et al.* [6] and was below the ASTM/KEBS standard of 10 mEq O_2/kg. High peroxide value suggests that this yellow oleander oil has a high content of unsaturated fatty acids, which are responsible for oxidative rancidity. Research has shown that oils having high percentages of peroxide are unstable and tend to grow rancid easily [29]. The yellow oleander oil that was produced in this research was safe and could be used immediately.

Iodine values of 80.77 gI_2/g was observed in both yellow oleander oil. Adebowal *et al.,* and Usman *et al.*,obtained the following levels for yellow oleander oil, 71.20, 84.50 and 79.40 gI_2/g [7], $Iodine\ value = \frac{(34.63-18.73)x\ 0.1\ x\ 0.127\ x\ 100}{0.25} = 80.77\ gI_2/gm$Iodine value of 120 in EN 14214 serves to restrict certain vegetable oils as biodiesel feedstock. Iodine value obtained for yellow oleander oil was lower, this shows that the oil contains a lower number of unsaturated bonds and is a non-drying oil. With an IV of 80.77 gI_2/g, this fell within the range of 50 – 100 gI_2/g for semi-siccative mono-unsaturated oils. For these class of oil the iodine value can increases with time. Yellow oleander oil is therefore susceptibility to oxidative rancidity. Hence, it is advisable to keep them in cool, air tight, and dark places [29].

The specific gravity is an important parameter to use in testing diesel fuel injection systems, these it had to be maintained within tolerable limits to allow optimal air to fuel ratios for complete combustion [26]. A specific gravity of 0.87 was observed for yellow oleander seed oil and this was slightly lower than 0.922 observed by Jabar *et al.* [30], but within the 0.87–0.90 ASTM/KEBS range for biodiesel. Similar results were obtained by Deka *et al.*, Yarkasuwa *et al.*, Adebowal *et al.*, Osenu *et al.*, Duraisam *et al.*, Ogunneye *et al.* and Usman *et al.*, obtained 0.899, 0.921, 0.905, 0.92, 0.843 and 0.929 respectively [7]. According to ASTM D287, Standard Test Method for API Gravity of Crude Petroleum and Petroleum Products (the Hydrometer Method), a biodiesel will have specific gravity in the range of about 0.86 to 0.90, since values below 0.90 would confirm that the liquid is a biodiesel. This yellow oleander seed oil meets all the properties prescribed in the biodiesel standards ASTM D6751 and EN 14214 for biofuel feedstock. This makes the plant a potential raw material for the production of biodiesel in Kenya.

Lund developed an equation that can be used to predict the density of a vegetable oil [31]. It is known as the Lund relationship:$sg\ (15\ ^{\circ}C) = 0.8475\ +\ 0.00030\ SV\ +\ 0.00014\ IV$, $Specific\ gravity\ (15\ ^{\circ}C = 0.8475 + 0.00030\ x\ 197.33 + 0.00014\ x\ 80.77$, $Specific\ gravity = 0.8475 + 0.059199 + 0.0113078 = 0.9180068$, *where sg is the specific gravity of vegetable oil at* 15 ℃, SV is the saponification value, and IV is the iodine value of the oil.The result obtained in this equation is slightly less than the observed value of 0.921.

3.2. Cetane Index

CN is the parameter that is used to determine the quality of diesel fuel and is always proportionate to the fuel ignition delay timein CI engines. A fuel's CN rating can be applied to determine ignition characteristics of biodiesel fuels. The cetane number can be calculated using the equation adopted by Gerpen [32];$Cetane\ index\ =\ 46.3 + \frac{5458}{SV} - 0.225\ x\ IV$, $Cetane\ index\ =\ 46.3 + \frac{5458}{197.33} - 0.225\ x\ 80.44, Cetane\ index\ =\ 46.3 + 27.66 - 18.099 = 55.789\ \%$

Diesel engines will operate better on fuels whose CN value is above 50 [32]. In this study the CN for yellow oleander oil was 56.Nwakaire*et al.,* [33].Found a cetane number of63.55 for yellow oleander oil this was higher than the ASTM value of 47 (min).This means that yellow oleander oil can run a diesel engine.

3.3. GC/MS Acid profile

A GC/MS spectrum is the fingerprint of any particular batch of vegetable oil. It shows us the unique identity and properties of the vegetable oil. Essential oil GC/MS reporting shows all the chemical components that make up the vegetable oil (figure 1).

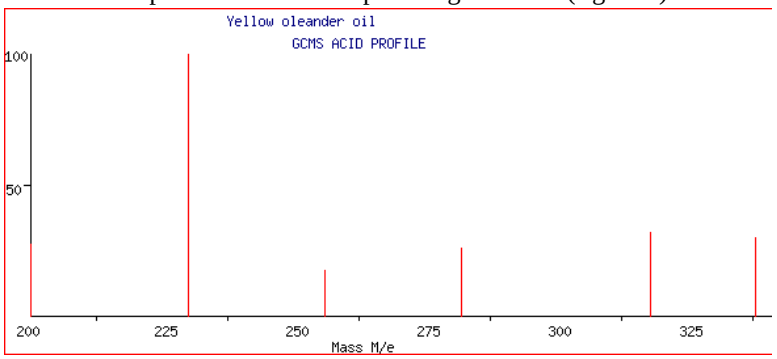

Figure 1: GC/MS Acid profile for yellow oleander oil

The acid profile in yellow oleander oil according the GC-MS spectral data shown in figure 1 and table 3 are as follows; Arachidonic acid **[**$CH_3(CH_2)_{12}COOH$**],** 13.76 % . This varied from the results obtained by Ogara (0.48 %, Kenya) [34] and Lumwanya *et al.*, [7] (0.4 %, Nigeria). Erucic acid **[**$CH_3(CH_2)_7CH{=}CH(CH_2)_{11}COOH$**]** contentwas 12.76 %, and oleic acid [$CH_3(CH_2)_7CH$ = CH $(CH_2)_7$ COOH**],** 11.08 %. Ogara (Kenya) [34], Oluwaniya *et al.* [7] (Nigeria) and Usman *et al.* (Nigeria) [27] obtained 57.75, 64.3 and 42.69 % respectively. The percentage of palmitoleic acid **[**$CH_3(CH_2)_5CH{=}CH(CH_2)_7COOH$**]** was 7.37 %, Usman *et al.* obtained 0.25 %. The composition of Myristic acid **[**$CH_3(CH_2)_{12}COOH$**]** was 43.24 %, Usman *et al.* obtained 0.32 % [19] and 11.79 % for lauric acid **[**$CH_3(CH_2)_{10}COOH$**]** [27]. In this research there were no conjugated double bonds in the oil.

3.4. FTIR Spectrum of yellow oleander oil

Fourier transform infrared (FTIR) spectroscopy is used like a fingerprint to identify functional groups in a molecule. This is because different molecules cannot produce the same pattern or wavelength. When molecules are exposed to infrared radiation, they absorb radiation at very specific wavelengths.

Table 3:Acid profile for yellow oleander oil

Fatty Acid Profile	**This Study**	Oluwaniya *et al.*	Usman *et al.*	Ogara
Arachidonic acid [C20:4]	13.76	0.4	-	0.48 ± 0.06
Arachidic acid [C20:0]	-	-	-	16.65 ± 2.75
Erucic acid [C22:1]	12.76			
Linolenic acid [C18:3]	-	-	-	-
Linoleic acid [C18:2]	-	6.3	0.54 ± 0.13	21.33 ± 0.16
Oleic acid [C18:1]	11.08	64.3	42.69 ± 2.22	51.75 ± 1.49
Stearic acid [C18:0]	-	11.8	6.82 ± 0.54	16.65 ± 2.20
Palmitoleic acid [C16:1]	7.37	-	0.25 ± 0.01	-
Palimitic acid [C16:0]	-	17.1	19.50 ± 0.84	8.34 ± 0.75
Myristic acid [C14:0]	43.24	-	0.32 ± 0.06	-
Lauric acid [C12:0]	11.79			

The values are means ± se, n = 4

This technique can also be used in identifying the material composition of a sample. Figure 2 above gives the FTIR spectrum of yellow oleander oil. This test method is relatively quick to perform and is capable of simultaneously detecting multiple functional groups. Secondly, the size of the peaks is a direct indication of the amount of the specific material found in the sample.

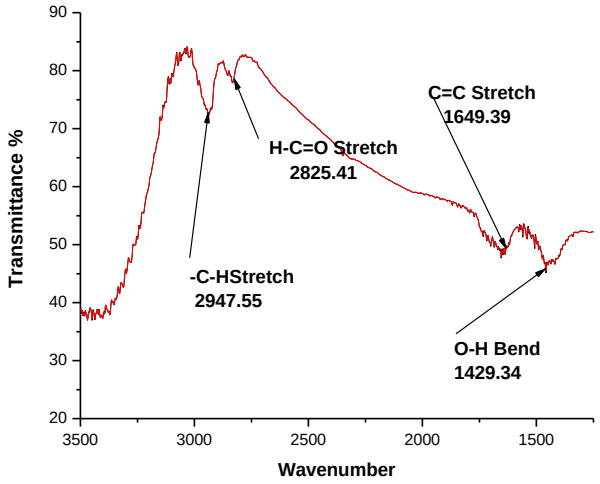

Figure 2: FTIR Spectrum of yellow oleander oil

In this study, from figure 2, the following band lengths were identified from the FTIR spectrum:2938.27 cm^{-1} respectively, C-H stretch for alkanes; 2826.75 cm^{-1};for H-C=O for carboxylic acids and 1453 cm^{-1} (Broad), -O-H bending for alkanes respectively.

Ofoegbu*et al*., [35] obtained the following results on yellow oleander seed oil FTIR spectrum: very strong and broad hydroxyl peaks at wavelengths of 3471.02 and 3793.14 cm^{-1} respectively. A variable alkene C=C bond at wavelength of 1452.45 cm^{-1}, a medium strength cyanide bond at wavelengths of 2035.93 and 2343.59 cm^{-1} which confers a degree of toxicity to the oil confirming the effect of the compositional presence of thevitin (toxic component of the oil). Also at wavelengths of 2677.9 and 2859.56 cm^{-1} the oil showed medium and strong bond strengths respectively of Aldehyde functionality [35].

3.5. UV Visible Spectrum of yellow oleander oil

As indicated in figure 2 absorption peaks for yellow oleander oil were at 200.05, 221.09 and 243.08 nm respectively. Conjugated molecules absorb energy easily than the isolated double bonds because the energy gap since the electronic transfer is very small [24].These molecules absorb energy even lower wavelengths of UV-Vis spectrum visible from 400-800 nm [24].Only conjugated alkenes molecules cause shift in (maximum wavelength); as the conjugation increases, the shift also increases. So, the presence of large number of molecules of conjugated unsaturated alkenes in yellow oleander oil is responsible for the absorption of large UV radiations by it.Marín *et al*., [36], analyzed sunflower and castor oil biodiesel and observed signals at 260, 254 and 248 nm which corresponded to transitions and π - π^* between 250-260 nm of the double bonds and n-transitions of the presence π^* of the carboxylic acids. They found out that the most significant variation between castor and sunflower biodiesel were noted at 228 and 224 nm which they explained using the transitions π - π^* of carboxylic acids λ and unsaturated β[36].

Figure 3 above gives the UV Visible spectrum of yellow oleander oil. It confirms that the yellow oleander oil had no conjugated double bonds in its structure. The UV-VIS analysis was obtained using SHIMADZU UV-2500PC series, at a wavelength range of 200.00 to 900.00 nm, sampling interval of 0.5. Auto scan mode, measuring mode (absorbance), slit width of 2.0 and light source change wavelength of 360.0 nm [35].UV Visible spectroscopy is a sensitive and reliable method that can be used for monitoring degradation of oils.Karmakar *et al*.[23], analyzed the transformer oil using UV visible, they observed that, absorption peaks of aged oils are located in the 200-380 nm region, where as no absorption peaks were found in the same region in the case of fresh oil [23]. The in-service aged oil had a higher absorbance than the laboratory aged oil. So they concluded that the UV

spectroscopy has the ability to analyze the condition of an oil. In case of fresh oil the absorbance was found to be very low which indicates it was still fresh [23]. For yellow oleander oil the absorption spectrum was between 195-350 nm, this means that it was still fresh, and could be used in the production of biodiesel[23].

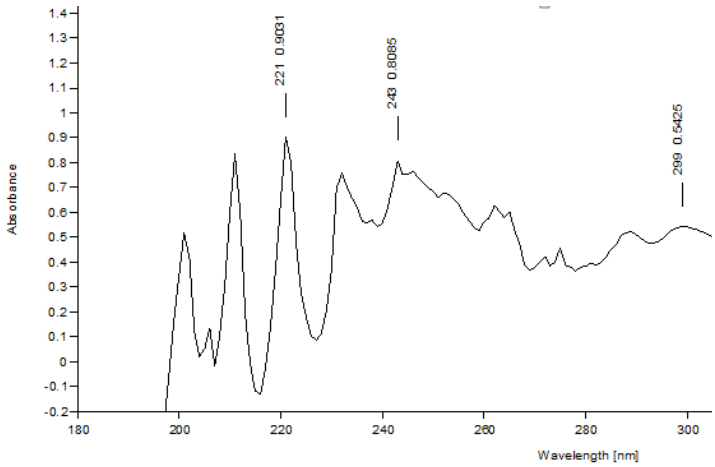

Figure 3: UV Visible Spectrum of yellow oleander oil

3.6. Characterization of the waste eggshell

From figure 4 below, CaO and MgO had the highest concentrations of 90.46 and 4.38 % , respectively, in eggshells. Buasri *etal*. [10], also found the concentrations of 98.124 % CaO and 1.159 MgO % respectively. Kawashima *etal*. [37], suggested that the Ca series catalysts have higher catalytic activity for the trans-esterification reaction. The advantage of coexistence of two different basic-oxide components in the catalyst for trans-esterification has also been emphasized. The base sites over heterogeneous catalysts active centers for trans-esterification [37]. This makes incinerated eggshells a better heterogeneous catalyst.

3.7. Concentrations of elements in yellow oleander seeds powder using XRF

The data for XRF analysis of yellow oleander seed meal and oil are represented in table 4. The results have shown that Al_2O_3, P_2O_5, S, Cl, K_2O, CaO, Ti, Cr, Mn, Fe, Cu, Zn, Rb and Sr were major components of the yellow oleander seeds meal (Table 4). These levels were found to be generally high.Özcan [38] found similar results for different oil seeds. The levels of K content in the mealwas found to be high (14.552 mg/kg), which was higher than the ASTM recommended level of $5\,mg/kg$. This was followed closely by CaO at 11.404, and$10.683\,mg/kg$for the meal and oil respectively.Chlorine level in the meal was $2.078\,mg/kg$ which was higher than the ASTM value of $2\,mg/kg$. Apparently, no chlorine was detected in the oil. The concentrations of the rest of the elements in yellow oleander meal and oil generally decreased during extraction., Al_2O_3; 0.3929 to 0.198mg/kg, P_2O_5; 1.823 mg/kg to ND, S; 18.90 to 7.054 mg/kg, Cl; 2.078 mg/kg to ND, K_2O; 14.552 mg/kg to ND, CaO; 11.404 to 10.683 mg/kg, Ti;1.112 to 0.854 mg/kg, Cr; 0.1102 mg/kg to ND, Mn; 0.1198 mg/kg to ND, Cu; 0.0343 to 0.00698 mg/kg, Zn; 0.1432 to 0.0183 mg/kg, Rb; 0.0205 mg/kg to ND to and Sr; 0.075 mg/kg to ND. It was only SiO_2that increased from 0.000 to $3.858\,mg/kg$. This increase may be attributed to concentration during extraction. All values in the oil except for CaO were below the ASTM maximum contamination levels.CaO is one of the most used heterogeneous catalyst in trans-esterification reactions, since it has many advantages such as low price, long catalyst life, highactivity and requires only moderate reaction conditions. The presence of Al_2O_3, CaO and SiO_2may assist in synergy during the trans esterification process. Potassium and calcium presence in the yellow oleander raw mealcauses them to react with water if present and oil to form soaps. CaO forms abrasive solids, which can cause injector, and fuel pump wear, piston and ring wear, and may also increase engine deposits [16]. It also causes soap formation and this leads to filter blockages and adhesion of injection pumps.

Due to the high-temperature produced a combustion engine, chlorine and sulphur present in the meal react with corresponding elements found within the engine to produce acids. Chlorine present in a biofuel may have harmful effects on the environment. Chlorine reacts with hydrogen to produce hydrochloric acid, sulphur also reacts with excess oxygen from air to form a mixture of sulphur dioxide (SO_2) and sulphuric trioxide (SO_3). Suplhur concentration of $7.054\,mg/kg$ registered in the yellow oleander seed oil will cause problems regarding emissions of SOx [39]. Water vapor from the engine would normally condense, and, reacts with sulphur trioxide to form sulphuric acid(H_2SO_4) and corroding films.Thompson*et al* [40] also did a research on the sulfur content in selected oils and fats and their corresponding methyl esters. They found out that, generally biodiesel contains less sulfur than fossil diesel. They also noticed that the elemental composition of a vegetable oil may varyaccording to the soil conditions where the oilseed crops grow, which may in turn affect the sulfur content in the seeds and/or in the oils [40], and that rapeseed and mustard recorded $9{,}000\,mg/kg$ of sulphur. In each case, the seed mealshad even higher sulfur content than the parent seeds after oil extraction [40].

Chlorine reacts with hydrogen to form hydrogen chloride gas (HCl) which dissolves in condensed water vapor to form hydrochloric acid.Chlorine can also form salts of some of the minerals chlorides found in the yellow oleander seed plant, and can lead to the production of a number of harmful halogenated compounds [39].The concentration of chlorine decreased from $2.078 \pm 0.002\,mg/kg$ mg to ND levels during extraction. On the other hand the concentration of S; dropped from

18.90±0.037mg/kg in the meal to$7.054 \pm 0.033\ mg/kg$ in the oil. This value was found to be lower than the ASTM standard of $500\ mg/kg$ and it implies that yellow oleander oil is safe, but must be treated first before use in order to remove the traces of sulphur present.

Table 4: Concentrations of elements in yellow oleander seeds powder and oil using XRF

Element	Concentration in mg/kg		ASTM D6751
	Meal	**Oil**	
Al_2O_3	0.3929 ±0.177	0.198 ±0.159	2.7 mg/kg
SiO_2	0.000±0.106	3.858±0.100	
P_2O_5	1.823±0.070	0.000±0.057	10 mg/kg
S	18.90±0.037	7.054 ±0.033	500 mg/kg
Cl	2.078 ±0.002	0.000±0.001	2 mg/kg
K_2O	14.552±0.027	0.000±0.012	5 mg/kg
CaO	11.404±0.021	10.683±0.018	5 mg/kg
Ti	1.112 ±0.008	0.854±0.011	
Cr	0.1102±0.004	0.000±0.006	≤ 10 mg/kg
Mn	0.1198±0.005	0.000±0.004	
Fe	1.1638±0.006	1.271±0.004	5 mg/kg
Cu	0.0343±0.000	0.00698±0.000	0.1 mg/kg
Zn	0.1432±0.001	0.0183±0.000	≤ 200 mg/kg dry
Rb	0.0205±0.001	0.000±0.000	
Sr	0.075±0.001	0.000±0.177	

Phosphorus concentration in the meal was, $1.823\ mg/kg$, which was found to be lower than the ASTM standard of $10\ mg/kg$. The presence of phosphorus could have been attributed to the phospholipids available in the yellow oleander seed. High levels of phosphorus have been shown to damage catalytic converters used in emission control systems [16]. The concentration of phosphorus (P_2O_5) dropped from $1.823 \pm 0.070\ mg/kg$in the meal to $ND\ levels$ in the oil. This means that the biodiesel produced will be free from phosphorus contamination.

From the table 5, CaO had the highest concentration of 90.457 % (Ca-72.5, 240.18 mg/kg), followed by MgO; 4.382 % (Mg - 23, 320.80 mg/kg), Al_2O_3; 1.663 % (Al - 2, 942.55 mg/kg), and P_2O_5 2.99 % (P - 8, 025.80 mg/kg), the rest of the elements had the following concentrations; S -144, 900.00 , Cl - 2, 106.70, Sr - 11, 718.80, Cu -54.34 , Zn - 107.60, Cr - 21, 422.58 , Ti - 2, 109.60 and Fe - 100.16 mg/kg respectively. The presence of relatively high levels of CaO, MgO and Al_2O_3makes the eggshells a base and a strong heterogeneous catalyst, because it contains more than one metal ions. Rohim*et al* found the following concentration in calcined waste eggshells; MgO - 0.690 %, CaO - 98.560 %, Al_2O_3- 0.100 %, CuO - 0.027 % and SrO - 0.051% respectively [44]. They also confirmed that CaO in a major compound in the eggshell. FTIR analysis of the functional group of eggshell showed that Ca - O bond had existed at 670 cm^{-1}, which proved that CaO had completely decomposed from $CaCO_3$[44].

Table 5: Elements present in eggshells

Element	Egg Shells XRF (%)	Element	Percentage of each cation in XRF	Mass of each element in mg/kg
CaO	90.45	Ca	72.524	725, 240.18
MgO	4.382	Mg	2.332	23, 320.80
Al_2O_3	1.663	Al	0.294	2, 942.55
P_2O_5	2.990	P	0.802	8, 025.80
S	0.022	S	14.49	144, 900.00
Cl	0.022	Cl	0.210	2, 106.70
Sr	0.081	Sr	1.171	11, 718.80
Cu	0.006	Cu	0.005	54.34
Zn	0.001	Zn	0.010	107.60
Cr	0.001	Cr	2.142	21, 422.58
Ti	0.022	Ti	0.210	2, 109.60
Fe	0.035	Fe	0.010	100.16

3.8. Total carbon

This was analyzed using the carbon analyzer, Multi EA 4000, the peak graph is represented in the figure 4 below. The operating principle of the device is based on the high-temperature combustion (1000 – 1500 °C) of samples in oxygen flow. It has a furnace which provide high temperature necessary for sample decomposition.

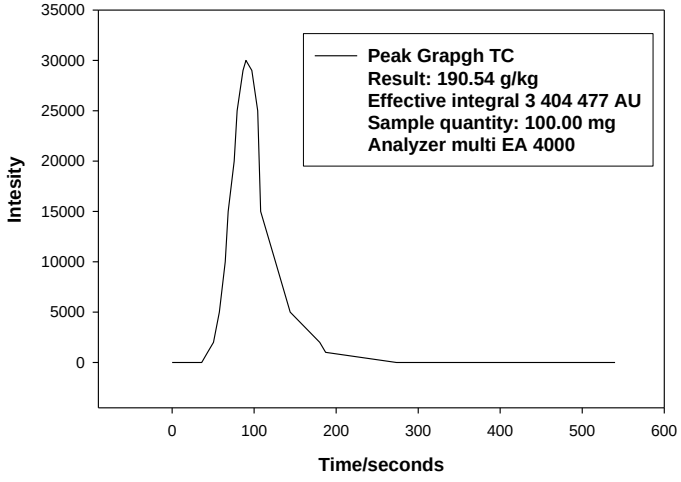

Figure 3: Carbon analyzer peak graph for total carbon in yellow oleander seed meal

The peak area of the peak graph is proportional to the total carbon (TC) concentration in the sample such that the TC content can readily be determined from a calibration curve [40].

Results indicated the level of $190540\ mg/kg$ (19.054%). Since yellow oleander meal contained $190\ 540\ mg/kg$ of total carbon, it can be used in the making of briquettes and charcoal instead of going to wastage. High total carbon content in the meal makes it to form a high grade biomass for fuel [41].

3.9. Calorific values

The calorific value of a fuel is the quantity of heat produced by the combustion of that fuel at constant pressure and under standard temperature and pressure. It is an important parameter for comparing the consumption of yellow oleander seed meal with the oil produced by the seed. The carorific value was obtained using a bomb calorimeter and the results are represented in table 6 below. From table 6 the calorific value of yellow oleander oil is higher than that of the seed meal.

Table 6: Table Calorific values of the yellow oleander meal and oil

Bomb ID 1	Meal	Oil
Weight	1.000	1.000
Gross Heat	29.8986 MJ/kg	38.6470 MJ/kg

Higher heating value (calorific value) of a vegetable oil can be also be calculated depending on its chemical composition using the equation adopted by Demirbas [32]; $HVV(MJ/Kg) = 43.43 - 0.041SV + 0.015IV$. For yellow oleander oil;

$HVV(MJ/Kg) = 49.93 - (0.041 \times 197.33) + (0.015 \times 80.77) = 53.051$

Another equation for HHV for vegetable oils based on proximate analysis adopted by Demirbas [32] is: $HVV(MJ/Kg) = 79.014 - 43.12d$. For yellow oleander oil; $HVV(MJ/Kg) = 79.014 - (43.126 \times 0.87) = 41.49$. The estimated calorific values of 41.49 and 53.015 MJ/kg are higher than the experimental value of 38.6470 MJ/kg, which can be attributed to heat loss to the surrounding during the experiment. Duraisamy*et al.,* [42], found a calorific value of 40.148 MJ/Kg for yellow oleander oil, this was found to be in line with the results in this research. Gravalos *et al.,* [42]alsofound out that the net calorific values of fats and oils that ranged from 36.247 to 37.294 J/g , the expected value should be in the range of $39.000 - 48.000\ Mj/Kg$ [43]. In this research we found a gross value of 38.6470 $MJ/kg$for yellow oleander oil, which was actually higher than the recommended standards. The recommended calorific value of solid biomass is$14.400 - 17.400\ Mj/Kg$[43], and since the calorific this makes both the yellow oleander seed meal and the oil good fuels.

4. Conclusion

Results showed that most of the yellow oleander oil seed meal and oil samples investigated in this study contained low levels of Al_2O_3, SiO_2, S, CaO, Ti, Cr, Fe, Cu and Zn than the ASTM recommended levels. Only CaO registered higher values, this can interfere with the properties of the biodiesel produced. The difference in content may also be attributed to difference in climatic conditions and that the source of the raw materials used were different. The elemental contents of the raw yellow oleander oil needs to be identified, and the negative elements removed before use. Carbon content of the meal was relatively high, this means that it can be used in the preparation of briquettes and charcoal as fuel. Furthermore the calorific value of the meal and the oil were found to be high implying that both can make used as fuel. The eggshells also, registered the presence of relatively high levels of CaO, MgO and Al_2O_3 and other metals, this makes it potentially a good heterogeneous catalyst.

References

[1]. Endelevu Energy (2008). A Roadmap for Biofuels in Kenya. Opportunities and Obstacles. Gesellschaft Für Technische Zusammenarbeit (German Technical Cooperation - GTZ) Kenya & Ministry of Agriculture, Government of Kenya, 17 May 2008, pp 1-15

[2]. Anjanabha Bhattacharya and Pawan Kumar (2009). Water Hyacinth as a Potential Biofuel Crop. GA 31794, USA, ISSN: 1579-4377

[3]. Robert Quigley (2007). Biodiesel: The good, the bad and additives. Lubrizol Limited, Biofuels International, pp 1 – 3

[4]. Rock and Maurice Korpelshoek (2007). Bioethers Impact on the Gasoline Pool. Biofuels 2007, www.digitalrefining.com/article/1000210, pp 1 -9

[5]. Sheriff O. Ajala and E. Betiku (2014); Yellow Oleander Seed Oil Extraction Modeling and Process Parameters Optimization: Performance Evaluation of Artificial Neural Network and Response Surface Methodology. Article first published online: DOI: 10.1111/jfpp.12366

[6]. Ibiyemi, A., Fadipe O., Akinremi O. and Bako S. (2002). Variation in Oil Composition of *Thevetia Peruviana Juss* "Yellow Oleander" Fruit Seeds. Journal of Applied Sciences and Management, Journal of Applied Sciences and Environmental Management, Vol. 6, No. 2, 61-65

[7]. Sanjay Basumatary (2015). Yellow Oleander (Thevetia peruviana) Seed Oil Biodiesel as an Alternative and Renewable Fuel for Diesel Engines: A Review, International Journal of ChemTech Research, Vol.6, pp 2823-2840

[8] J. M. Jabar, L. Lajide, I. O. Bakare and M. T. Oloye (2016). Extraction and Characterization of Vegetable Oil from Thevetia Peruviana and Jatropha Curcas Seeds. FUTA Journal of Research in Sciences, ISSN: 2315 – 8239

[9]. Oseni, M. I, Obetta, S. E. and Orukotan, F. V.(2012). Evaluation of Fatty Acids Profile of Ethyl Esters of Yellow Oleander and Groundnut Oils as Biodiesel Feedstock. American Journal of Scientific and Industrial Research, ISSN: 2153-649

[10]. Achanai Buasri, Nattawut Chaiyut, Vorrada Loryuenyong, Chaiwat Wongweang, Saranpong Khamsrisuk (2013). Application of Eggshell Wastes as a Heterogeneous Catalyst for Biodiesel Production. Sustainable Energy, 2013, Vol. 1, No. 2, 7-13

[11]. Achanai Buasri, Nattawut Chaiyut, Vorrada Loryuenyong, Chaiwat Wongweang, Saranpong Khamsrisuk$_1$(2013). Application of Eggshell Wastes as a Heterogeneous Catalyst for Biodiesel Production, Sustainable Energy, 2013 1 (2), DOI: 10.12691/rse-1-2-1, pp 7-13.

[12]. Peng-Lim Boey, Gaanty Pragas Maniama∗, Shafida Abd Hamid(2011). Performance of calcium oxide as a heterogeneous catalyst in biodiesel production: A review, Chemical Engineering Journal 168 (2011) 15–22

[13]. Nwakaire, J. N., Durugu S. (2013): Determination of Physio-Chemical Properties of Oleander Seed Oil, Nigerian Journal of Technology (NIJOTECH) Vol. 32. No. 3: ISSN: 1115-8443

[14]. Basumatary S. and Deka D. (2014). Transesterification of Yellow Oleander (Thevetia peruviana) Seed Oil to Fatty Acid Methyl Esters (Biodiesel) using a Heterogenous Catalyst Derived from Rhizome of Musa Balbisiana Colla. International Journal of ChemTech Research, Vol 6, No. 4: 2377 – 2384

[15]. M. I. Oseni, B. E. Agbi and I. O. Ogamenyi (2012). Extraction and Analysis of Chemo-physical Properties of Yellow Oleander Oil as Lubricant. British Journal of Applied Science & Technology, ISSN: 2231-0843,Vol.: 4, Issue 6: (21-28)

[16]. Tina Rita Celli Zezza, Michelle de Souza Castilho, Nelson Ramos Stradiotto (2012). Determination of phosphorus in biodiesel using 1:12 phosphomolybdic modified electrode by cyclic voltammetry. Fuel 95 (2012): 15–18

[17] Yarkasuwa C., Wilson D. and Michael E. (2013). Production of Biodiesel from Yellow Oleander (*Thevetia Peruvian*) Oil and its Biodegradability. Journal of the Korean Chemical Society, Vol. 57, No. 3:377-381

[18]. Dimberu G. Atinafu, and Belete Bedemo (2011). Estimation of total free fatty acid and cholesterol content in some commercial edible oils in Ethiopia. Bahir DAR, Academic Journals, Journal of Cereals and Oil seeds Vol. 2(6), pp.71-76

[19]. Okpuzor J, VI Okochi, HA Ogbunugafor, S Ogbonnia, T Fagbayi, C Obidiegwu, (2009). Estimation of cholesterol level in different brands of vegetable oils, Pak. J. Nutr. 8: 57-62.

[20]. Rick Da Tech (2016). Specific Gravity and Biodiesel, Make Biodiesel, Retrieved from, http://www.make-biodiesel.org/Biodiesel-Chemsitry/specific-gravity-and-biodiesel.html

[21]. AOCS (2003). Official Method Cd 8-53. American Oil Chemists Society, Champaign, IL. Accessed on www.bioriginal.com.

[22]. Arumugam Sivasamy, Kien Yoo Cheah, Paolo Fornasiero, Francis Kemausuor, Sergey Zinoviev, and Stanislav Miertus,(2009).Catalytic Applications in the Production of Biodiesel from Vegetable Oils, InterScience, 2009 Wiley-VCH Verlag GmbH & Co. KGaA, Weinheim, ChemSusChem 2009, 2, 278 – 300

[23]. Hussain K and Subrata Karmakar(2014). Condition Assessment of Transformer Oil using UV-Visible Spectroscopy. Iinstitute of Electrical and Electronic Engineering, 978-1-4799-5141-3/14

[24]. K. Anil Kumar and K. Viswanathan (2012). Study of UV Transmission through a Few Edible Oils and Chicken Oil, Journal of Spectroscopy.Volume 2013, Article ID 540417, pp 1-5

[25]. Anna Grazia Mignani, Leonardo Ciaccheri, Andrea Azelio Mencaglia1 and Antonio Cimato$_2$, (2012). Optical Absorption Spectroscopy for Quality Assessment of Extra Virgin Olive Oil. InTech Europe. www.intechopen.com, ISBN 978-953-307-921-9, pp 47 – 63

[26].Cynthia Nkolika Ibeto, Chukwuma Obiajulu Benedict Okoye, and Akuzuo Uwaoma Ofoefule (2012), Comparative Study of the Physicochemical Characterization of Some Oils as Potential Feedstock for Biodiesel Production. ISRN Renewable Energy, Volume 2012, Article ID 621518, pp 1-5

[27] Usman, L.A., Oluwaniyi, O.O., Ibiyemi, S.A., Muhammad, N.O. And Ameen, O.M. (2009). The potential of Oleander (Thevetia peruviana) in African agricultural and industrial development: a case study of Nigeria. Journal of Applied Biosciences 24: 1477 – 1487, ISSN 1997–5902

[28]. J. M. Jabar, L. Lajide, A. O. Adetuyi, B. J. Owolabi, I. O. Bakare, T. G. Abayomi and A. L. Ogunneye, Yield, Quality, kinetics and thermodynamics studies on extraction of Thevetia peruviana oil from its oil bearing seeds.Journal of Cereals andOilseeds. Vol. 6(5), pp. 24-30, June 2015, ISSN 2141-6591

[29]. Pandurangan M. K., Murugesan S. and Gajivaradhan P. (2014). Physico-chemical properties of groundnut oil and their blends with other vegetable oils. Journal of Chemical and Pharmaceutical Research, 6(8):60-66, ISSN : 0975-7384

[30] Birnin-Yauri U.A. and Garba S. (2011): Comparative Studies on Some Physicochemical Properties of Baobab, Vegetable, Peanut and Palm Oils. Nigerian Journal of Basic and Applied Science, 19(1): 64- 67

[31]. A. A. Refaat (2006). Correlation between the chemical structure of biodiesel and its physical properties, Int. J. Environ. Sci. Tech., 6 (4), 677-694, ISSN: 1735-1472

[32]. Demirbas A. (2003). Relationships between lignin contents and fixed carbons of biomass Samples", Energy Convers Mgmt, 44, pp. 1481-1486.

[33]. J. N. Nwakaire J. N. Nwakaire, S. Durugu (2013). Determination of Physio- Determination of Physio-Chemical Properties of Oleander Chemical Properties of Oleander Seed Oil for Biodiesel Production. Nigerian Journal of Technology (NIJOTECH), Vol. 32. No. 3, pp. 440 – 442

[34]. Ogara Rose S. (2013). Evaluation of Nuitritional Properties of Yellow Oleander (Thevetia Peruviana) Seeds in Kenya. Food Science and Quality Management,Vol.22, ISSN 2224-6088 (Paper) ISSN 2225-0557 (Online), www.iiste.org

[35]. Ofoegbu, O. and Kelle, I. H.(2013). Determination of the Edibility of Thevita Peruviana Seed Oil Using GC-MS, FTIR and UV-VIS Analysis. Journal of Basic and Applied Scientific Research, Vol.3 (12)385-391, ISSN 2090-4304

[36]. María Juana García Marín, Francisco Prieto García, (2012). Obtaining and Characterization of Biodiesel from Castor Oil (*Ricinus communis*) and Sunflower (*Helianthus annuus*) Grown in Tabasco, Mexico. International Journal of Applied Science and Technology, Vol. 2 No. 9, pp 1-12

[37]. Refaat, A. A., (2011). Biodiesel production using solid metal oxide catalysts. Int. J. Environ. Sci. Tech., 8 (1), 203-221, ISSN: 1735-1472

[38]. M. Musa Oscan (2006). Determination of the mineral compositions of some selected oil-bearing seeds and kernels using Inductively Coupled Plasma Atomic Emission Spectrometry (ICP-AES).Grasas Y Aceites, 57 (2), 211-218, ISSN: 0017-3495

[39]. Biomass Energy Center (2016), Emissions, retrieved from http://www.biomassenergycentre.org.uk/portal/page?_pageid=77,103200&_dad=portal&_schema=PORTAL

[40]. Shimadzu (2016). TOC Application Handbook, Shimadzu, Excellence in Science, Retrieved from, https://www.shimadzu.be/sites/default/files/TOC_application_handbook_12K.pdf

[41]. Ismaila A., Zakari I. Y., Nasiru R., Tijjani B. I., Abdullahi I. and Garba N. N. (2013). Investigation on biomass briquettes as energy source in relation to theircalorific values and measurement of their total carbon and elemental contentsfor efficient biofuel utilization, Pelagia Research Library, Advances in Applied Science Research, 2013, 4(4):303-309

[42]. Gravalos I., Gialamas T., Koutsofitis Z., Kateris D., Tsiropoulos Z., Xyradakis P., Georgiades A. (2008). Energetic Study on Animal Fats and Vegetable Oils Using Combustion Bomb Calorimeter. Journal of Agricultural Machinery Science, 4 (1): 69 - 74

[43]. The Engineering ToolBox (2016). Fuels - Higher Calorific Values, Retrieved from; http://www.engineeringtoolbox.com/fuels-higher-calorific-values-d_169.html

[44]. Rohazriny Rohim, Razi Ahmad, Naimah Ibrahim, Nasrul Hamidin, Che Zulzikrami Azner Abidin (2014). Characterization of Calcium Oxide Catalyst from Eggshell Waste, Advances in Environmental Biology, Vol. 8 (22), Pages: 35-38

[45]. Han Xu, Xiaoling Miao, Quingyu Wu (2006). High Quality Biodiesel from Microalgae Chrorella Protothecoides by heterotrophic growth fermenters, ScienceDirect, Journal of Biotechnology, 126(2006), 499 – 507

[46]. Lubrizol Test Procedure (2006). Iodine Value, Lubrizol, TP-AATM-112-01

Available online at www.kenchemsoc.org

JOURNAL OF THE KENYA CHEMICAL SOCIETY

Journal of the Kenya Chemical Society 10-1 (2017), 70-75

Enrichment of Hg, Sn, As, Al, Mn and Fe in Surface Sediments and Surface Water of Winam Gulf, Lake Victoria

David M.K. Ongeri,[1] Solomon Omwoma*,[2] Joseph O. Lalah,[3] Karl-Werner Schramm,[4] and Bernard Michalke[4]

[1]Department of Chemistry, Maseno University, P.O. Box 333-40105, Maseno, Kenya.
[2]Department of Physical Sciences, Jaramogi Oginga Odinga University of Science and Technology, P.O. Box 210-40601, Bondo, Kenya.
[3]Department of Chemical Science and Technology, Technical University of Kenya, P.O. Box 52428-00200, Nairobi, Kenya.
[4]HelmholtzZentrum Muenchen, German Research Centre for Environmental Health, Ingolstaedter Landstrasse 1, D-85764 Neuherberg, Munich, Germany.
Corresponding Author: Email:solomwoma@yahoo.com*

Abstract

Evaluation of pollutant levels in an aquatic ecosystem is an essential system management tool. The levels of Al, As, Fe, Hg, Mn, and Sn in Winam Gulf of Lake Victoria are hereby reported. The sampling sites, Carwash and Dunga beach, are areas on the shore of the lake where drinking water, fishing and tourism take place. The Analyzed surface sediments and water samples show anthropogenic addition of Al, As, Fe, Hg, Mn, and Sn into the lake with corresponding water mean concentrations (in µg/L) of 710, 0.74, 1,200, 0.071, 397 and 0.021 in Kisumu city Carwash area and 524, 0.070, 1,550, 0.070, 299 and 0.020, in Dunga beach area, respectively. The surface sediment concentrations (mg/Kg wet wt) are 26,200, 1.52, 69,200, 0.033, 4,730 and 0.904, at the Carwash area and 21,700, 0.375, 31,400, 0.024, 1600 and 0.805, at Dunga beach area, respectively. Although the mean concentration levels of Al, As, Hg, Mn and Sn in surface sediment and water were within the UK freshwater limits, the concentration of Fe was more elevated above the recommended freshwater quality criteria which could cause concern due its potential negative impact on aquatic organisms. All the metals were enriched and the enrichment factors (based on Al crustal concentration) ranged from 0.79 (As) at Dunga beach to 15.64 (Mn) at Kisumu Carwash area, showing that enrichment of the metals was, in general, higher at the relatively more polluted sites at Kisumu Carwash area.

1.0. Introduction

Recent studies of trace elements in surface water and sediment within Winam Gulf, Lake Victoria focus on common toxic elements that include iron (Fe), lead (Pb), cadmium (Cd), zinc (Zn), copper (Cu) and chromium (Cr) [1-8]. Monitoring of other elements such as Hg, As and Sn, has not been done despite their known toxic effects in aquatic environments. Majorly, the gap is created by limitations in analytical instruments with atomic absorption spectrophotometry (AAS) dominating the reported results. AAS present analytical inadequacies in their measurement due to analyte losses during sample preparation, low detection limits and lack of suitable lamps for their detection. Analysis of trace metals such as As, Hg and Sn in water and sediment is complex due to their chemical reactivity and speciation in the aquatic environment. During sample digestion, losses of Hg, As and Sn, can occur and this makes their determination quite inaccurate.

Mercury (Hg) presents a major health risk both to humans and aquatic life [9-13]. In the aquatic environment, it exists in inorganic and organic forms and, methyl mercury, which is the most toxic form of the element, is considered a global pollutant of major public health concern when its concentrations are above natural background levels [9, 12-14]. The primary source of Hg exposure is through consumption of contaminated fish [9, 12-14]. The need to monitor mercury contamination in Winam Gulf is supported further by the current sporadic use of mercury in artisanal gold mining activities along the shores of the lake, in places such as

Macalder and Migori, where Hg has been detected in samples from the lake, rivers and streams at levels that can cause human poisoning and toxicity to aquatic organism [9, 11, 15-19].

Tin (Sn) is equally ubiquitous in the environment as it is used widely in many products including containers, electrical components, construction materials, transportation equipment and various industrial products such as stabilizers, biocides, catalysts, glass coatings and agrochemicals. The major forms of tin in environment are inorganic or organotin compounds from natural and anthropogenic activities and through leaching from disposal waste in landfills [15, 20, 21]. However, Sn does not evoke alarming concern because its ambient environmental levels are generally quite low, except in the vicinity of pollution sources. However, like Hg, Alkyl compounds of tin, like those of Hg, are highly toxic and bio-accumulative even in non-polluted ecosystems. In particular, the three butylated (tributyl, dibutyl, butyltin) tin species, which are used in many industrial products, are quite stable and bio-accumulative in aquatic organisms, birds and human organs through food chain transfer [21, 22].

Arsenic (As) has not been a major concern in Kenya, despite its known toxicity and frequent prevalence in drinking water in forms of arsenate and arsenite in other countries [23, 24]. Although arsenic is rapidly excreted, primarily through the urine [23, 24] inorganic arsenic is carcinogenic to humans where it can induce carcinomas of the skin, urinary bladder, lung, and possibly other tissues [23, 25]. Exposure to As is through drinking water, occupational (mining) inhalation, diet, and biocides and pharmaceuticals [26]. Inorganic arsenic in the aquatic environment is bio-transformed into organo-arsenic compounds by biota and more than 20 organo-arsenic compounds such as dimethylarsinic acid, methylarsonic acid, arsenocholine, tetramethylarsonium ion, arsenite and arsenobetaine have been identified [20]. Although hot spots of As prevalence in Kenya are not yet known, high levels of total As with mean concentrations above 50 mg/kg, the WHO recommended limit in sediment, were recently reported in samples taken from rivers and streams in the artisanal gold mining areas in Macalder and Migori located on the shores of Winam Gulf [15, 18, 19].

Surface waters contain high Al, Fe and Mn concentrations since they are major elements in the earth's crust. The amount of Al, Fe and Mn in solution from normal weathering is only a small proportion of their total in the environment, but perturbations of normal weathering and changes in water properties such as pH, dissolve organic matter (DOM) and anionic electrolytes concentrations can substantially increase their solubility and mobility in the aquatic environment (especially at low pH) [27]. At high concentrations above the recommended levels Al, Fe and Mn are toxic to fish; phytoplanktons such as Cylotella Menehiniana; algae and common freshwater bacteria such as Cyanobactreia species, diatoms, alga, protozoa; invertebrates such as shrimps and fish [27-29]. The major sources of these metals in the aquatic environment include natural weathering processes, aerial/rainfall deposition and anthropogenic activities such as municipal wastewater and sewage sludge discharge, mining and mineral processing and emissions from various industrial activities and products such as paints and biocides [30]. Consequently the global community has established limit guidelines for these metals with respect to drinking water quality, aquatic life, irrigation water and water for recreation [31]. These three metals, unlike Hg, As and Sn, have previously been analyzed in samples taken from various locations along Winam Gulf. The continuous monitoring of all these metals is necessary in order to establish their anthropogenic sources and distribution in the lake. This research aimed at determining the total concentrations of As, Hg, Sn, Mn, Al and Fe in two polluted sites along the Winam Gulf. The samples were analyzed by Inductively Coupled Plasma - Mass Spectrophotometry (ICP-MS) and evaluated in terms of their enrichment factors [32]. The enrichment factors of these six metals are, in addition, compared with enrichment factors of Pb, Cd, Cu, Zn, Co, Cr, Ni and Mo, which have been calculated for two sites, based on recent data obtained in a recent report [6]. In this study, the sampling sites were on locations on Winam Gulf where drinking water, fishing and tourism, are some of the major activities and therefore regular monitoring of these contaminants is needed.

2.0. Materials and methods

2.1. Sampling of water and surface sediment

The study area comprised of two sampling sites along Winam Gulf of Lake Victoria, namely Kisumu Carwash bay (KC) and Dunga Beach (DB). Both sites are located in Kisumu city, which lies between 0º0.4'S to 0º0.6'S and 34º13'E to 34º52'E, and an altitude of 1134 m above sea level see Fig. 1. Samples were collected in July 2014 during the dry season. Surface sediment (0-5 cm layer) samples were taken from five sampling points at each site located 2 m distance inside the lake from the shore, in five replicates, using a stainless steel Ekman grab. The samples were placed in polyethylene (PE) sampling bottles and stored in a refrigerator overnight before transportation to Helmholtz Zentrum Muenchen, Germany, for analysis. Water samples were collected by immersing PE 1-litre sampling bottles underneath the water surface, leaving the bottles to fill up and then closing them tightly using plastic cocks. They were also stored in the refrigerator overnight before being taken to Germany for analysis. The sampling bottles were pre-cleaned with detergent, rinsed thoroughly with de-ionized water, followed by 6% HNO_3, and then with de-ionized water before use.

2.2. Analysis by ICP-MS

Aqua-regia acid digestion method was used. Five (5) g wet sediment sample was placed in a Pyrex digestion flask, treated with 28 mL of aqua-regia (30% HCl:70% HNO_3 (3:1) mixture) and pre-digested on a hot plate for 2 hours in a vacuum hood. The Predigested samples were left to cool under the vacuum hood for 4 hours to about 24 ^oC, and filtered through ash-less Whatman 41 filter into 100-mL glass volumetric flask.

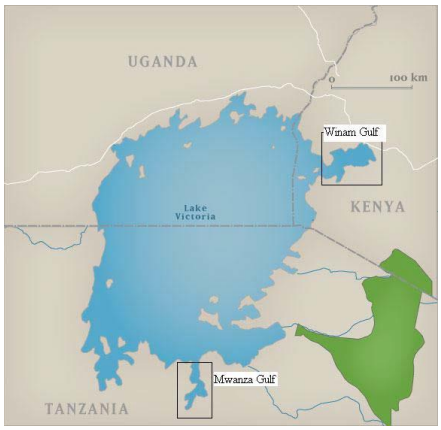

Fig. 1. Map of Lake Victoria showing the study sites [8]

The filtrate was made up to 100 mL using 0.5 M HNO_3 (aq) before analysis by ICP-MS (X-series 2 ICP-MS model) using an automated inbuilt calibration technique developed in the trace metal analysis laboratory in HelmholtzZentrum Muenchen, which involved automatic quantification of the trace metals based on regularly calibrated six point calibration curves generated in situ for each analyte, with data storage in a computer connected to the instrument. Analysis was based on calibration curves prepared from multi-element standard solutions (Calibration Standards Method 200.7) from Sigma and Aldrich. The % recoveries were obtained for each analyte by spiking known reference sediment standards before taking them through aqua regia digestion and analysis, respectively. Water samples were filtered through ash-less Whatman No. 41 filters and aliquots analysed by ICP-MS.

The enrichment factors (EF), were calculated by the formula: $EF = (X/Al)_{sample} / (X/Al)_{crust}$, where X = concentration of metal and Al = concentration of Al [32]. Apart from the EF of the six elements analysed in this study, the EF for Pb, Cd, Cu, Zn, Co, Cr, Ni and Mo were calculated for comparison, using the same formula but basing on recent data reported in literature for the two the sites [6].

3. Results and discussion

The data collected in this study are presented in Tables 1 and 2. It was found that the concentrations of the heavy metals in Kisumu carwash (KC) water were significantly higher than the corresponding metal concentrations in samples from Dunga (DB) water except for Fe, where Dunga registered significantly higher concentrations. The significant high concentrations (see Tables 1 and 2) in Carwash were attributed to numerous anthropogenic activities in the area such as cleaning of vehicles and entry of industrial effluent through River Kisat, unlike in Dunga area where there was less influence of anthropogenic activities.

Kisumu Carwash bay area of Winam Gulf has been known to be the most polluted part of the lake with other metals such as Cu, Zn, Pb, Cr and Cd, from previous monitoring, and their main sources reportedly including car washing activities, oil spills, runoff during rainfall, influent rivers and streams collecting contaminants from agricultural inputs, industrial effluents, municipal waste and wastewater treatment plants [4-6]. Minor anthropogenic influences at Dunga beach include effluents from Nyamasaria River and runoff from human settlements, hence lower levels of metal contamination measured at this site. Kisumu City land surface slopes towards Carwash area which enhances drainage of contaminants from the city that include metallic residues from welding activities, motor vehicle garages and construction sites, making Carwash area to be more polluted compared to other parts of Winam Gulf.

In surface sediment, Fe registered the highest concentration while Hg recorded the lowest in both sampling sites (Table 1). The mean levels of Fe and Mn in surface sediment surpassed the probable effect concentrations (PEC) [33, 34] for freshwater ecosystems and therefore indicated that sediments were polluted at the two sites with Fe and Mn. The concentrations of dissolved metals in the water samples from both sites decreased as follows: Fe>Al>Mn>As>Hg>Sn. The concentrations of all the heavy metals analyzed, except Fe, were below water quality criteria guidelines for UK and therefore no potential negative effects on aquatic organisms such as diatoms (desired freshwater concentration criteria: 1.5-50 mg/L), alga (1.9-5 mg/L), protozoa (16-51.8 mg/L) indicated [29]. The mean levels of Hg and Sn for both Carwash and Dunga were above background levels although As mean level was below background level at the two sites.

The concentrations of the analyzed heavy metals in Kisumu carwash surface sediment were significantly higher than corresponding metal concentrations in Dunga surface sediments (Table 2). The concentrations in sediment ranked, from highest to the lowest, from Fe>Al>Mn>As>Sn>Hg for Carwash and Fe>Al>Mn>Sn>As>Hg for Dunga area. The small difference in this order due to Sn and As concentration, could be attributed to the difference in characteristics of the sediment of the two areas.

The levels of the metals in the two sites were also compared by their accumulation factors. The accumulation of the metal from water to sediment was calculated by dividing the metal concentration in sediment by metal concentration in water and the data is presented in Table 3. All the metals recorded higher accumulation in Carwash sediment compared to Dunga sediment (Table 3) except for Al. Higher metal accumulation in Carwash bay area was attributed to more intense human

activities in this area that has led to high organic matter content which in turn aids in higher metal binding and accumulation. The metal accumulation factors decreased as follows: Sn>Al>Fe>Mn>As>Hg. The metal Hg registered very low accumulation factor (404) in range of hundreds while metals such as Fe, Sn and Al, all recorded accumulation factors of over 38,000. Based on these data, it would imply that toxic heavy metals like As and Hg can have extreme toxicological effects when water gets contaminated with them. Therefore, As and Hg levels in Winam Gulf is of concern to aquatic environment and needs to be monitored.

Table 1: Al, As, Fe, Hg, Mn, Sn concentrations in water (µg/L), means and least square differences.

	Al		As		Fe		Hg		Mn		Sn	
Water	KCW	DBW	KCW	DBW	KCW	DBW	KCW	DBW	KCW	DBW	KCW	DBW
1	501	531	0.702	0.684	906	1590	0.0795	0.0693	331	419	0.0194	0.0235
2	913	534	0.722	0.801	1390	1480	0.0702	0.0760	296	266	0.0295	0.0251
3	660	500	0.815	0.728	1290	1690	0.0586	0.0821	359	254	0.0107	<0.0012
4	823	478	0.780	0.690	1340	1760	0.0703	0.0677	293	409	0.0210	0.0121
5	653	529	0.665	0.633	1060	1250	0.0762	0.0559	706	149	0.0265	<0.0012
Mean	710	514	0.739	0.707	1200	1550	0.0710	0.0702	397	299	0.0214	0.0202
	612		0.722		1380		0.0706		348		0.0208	
LSD	126	20.3	0.049	0.046	171	151	0.0055	0.0071	123	91.7	5.26	5.42
	97.8		0.0148		178		0.000380		48.8		0.000593	

Note: All data corrected to 3 significant figures; KCW: Car Wash site water; DBW: Dunga Beach site water; 1,2,3,4,5 represent sampling points.

Table 2: Al, As, Fe, Hg, Mn, Sn concentrations in sediment (mg/Kg wet weight), means and least square differences.

	Al		As		Fe		Hg		Mn		Sn	
Sed	KCS	DBS	KCS	DBS	KCS	DBS	KCS	DBS	KCS	DBS	KCS	DBS
1	23200	28600	1.57	0.592	62600	41100	0.028	0.0322	3970	2630	0.823	0.612
2	23800	24000	1.71	0.334	67700	32600	0.027	0.0278	4550	1370	0.725	2.050
3	32100	34000	1.34	0.458	78400	35800	0.037	0.0306	4950	1100	1.240	0.854
4	20300	12400	1.52	0.237	72000	25100	0.026	0.0169	5160	1460	0.521	0.293
5	31700	9700	1.48	0.252	65100	22400	0.047	0.0140	5000	1420	1.210	0.217
Mean	26200	21700	1.52	0.375	69200	31400	0.033	0.0243	4730	1600	0.904	0.805
	24000		0.95		50300		0.029		3160		0.855	
LSD	4500	8600	0.09	0.120	4830	6120	0.007	0.0071	373	414	0.257	0.517
	2240		0.575		18900		0.0042		1570		0.049	

Note: All data corrected to 3 significant figures; KCS: Car Wash site sediment; DBS: Dunga Beach site sediment; 1,2,3,4,5 represent sampling points.

Table 3: The estimated accumulation factors of metals in surface sediment based on mean total concentrations

Metal	Site	Concentration in sediment (ppb)	Concentration in water (ppb)	Accumulation factor	Mean accumulation factor
Fe	Carwash	69,160,000	1,197.000	57,777	38,991
	Dunga	31,400, 000	1,554.000	20,205	
Al	Carwash	26,220,000	710.000	36,929	39,596
	Dunga	21,740,000	514.000	42,262	
Mn	Carwash	4,726,000	397.000	11,904	8,617
	Dunga	1,596,000	299.000	5,330	
As	Carwash	1,524	0.737	2,067	12,989
	Dunga	375	0.707	530	
Sn	Carwash	904	0.021	43,047	41,649
	Dunga	805	0.020	40,250	
Hg	Carwash	32.7	0.071	460	404
	Dunga	24.3	0.070	347	

Note: Estimated accumulation factor = metal concentration in sediment (ppb)/metal concentration in water (ppb)

The scope of this study was however restricted since only two sites were considered and the water column particulate bound metals were not analyzed. The estimated accumulation factor is only useful in demonstrating the difference between the concentrations of heavy metals in water and sediment for the same ecosystem but cannot be used for showing the enrichment factors due to anthropogenic sources in both locations. Sediment concentrations of metals were higher than water concentrations. In this case, the accumulative factors confirmed that Dunga beach is less contaminated by heavy metals. The enrichment factors (EF) in sediment are often taken as the standard indicators for showing anthropogenic additions [32, 35-37]. The enrichment factors are given in Table 4 showing enrichment of Hg, Sn, Mn and Fe at both sites in Winam Gulf. As was enriched at Kisumu Carwash area.

The EF values for Mn and Fe where higher than As, Hg and Sn suggesting anthropogenic influences (Table 4). Furthermore, the enrichment factors for Dunga Beach were lower than Carwash area, confirming more anthropogenic influences at the later site. For comparison, significant enrichment of Pb, Cd, and Zn in Kisumu Carwash, in particular, as well as Cu, Co, Cr and Mo in Kisumu Carwash and Usoma beach (which is far from the industrial city) was found (Table 4). The results therefore indicate that factors influencing heavy metal mobility and enrichment are from diverse sources and, not just industrial/municipal effluents only.

Table 4. Enrichment factors of heavy metals in surface sediment in Winam Gulf

Metal	*Crustal conc (ppm)*	*EF (KC)*	*EF (DB)*	*EF (UB)*
Al	82,300	-	-	-
Hg	0.08	1.28	1.15	nd
Sn	2	1.42	1.53	nd
As	1.8	2.66	0.79	nd
Mn	950	15.64	6.39	8.52
Fe	56,300	3.86	2.12	3.95
**Pb*	12.5	21.51	nd	6.30
**Cd*	0.2	36.99	nd	44.97
**Cu*	55	2.47	nd	2.48
**Zn*	70	6.95	nd	12.21
**Co*	25	2.88	nd	2.73
**Cr*	100	1.80	nd	2.00
**Ni*	75	0.74	nd	1.19
**Mo*	1.5	4.25	nd	36.88

Note: EF: Enrichment factor; conc: concentration; KC: Kisumu Carwash; DB: Dunga Beach; UB: Usoma Beach; *: based on literature [6, 32]; nd: not determined due to lack of data.

4. Conclusion

Analysis of surface sediment and water samples taken from two sites in Winam Gulf, i.e. Kisumu Carwash and Dunga beach revealed anthropogenic additions of As, Hg, Sn, Mn, Fe and Al into the lake. Although the mean concentrations in surface sediment and water were within freshwater limits in accordance to United Kingdom standards, the concentration of Fe was above the recommended quality criteria, which may pose a concern due to its potential negative impact on aquatic organisms. The results indicate enrichment of the measured pollutants indicating a possibility of continued lake pollution hence the need to manage anthropogenic factors. Although this study provided new baseline data on the six elements and their enrichment in Winam gulf, future studies should consider effects of seasonal variations because their concentration levels and enrichment factors are expected to vary during the rainy season.

Acknowledgement: This project was funded by the Alexander von Humboldt Foundation of Germany (Group Linkage Project, Ref. No. 3.4-Fokop-DEU/1064266).

References

[1] J.O. Lalah, E.Z. Ochieng, S.O. Wandiga, Sources of heavy metal input into Winan Gulf, Kenya, Bull. Environ. Contam. Toxicol. 81 (2008) 277-284.

[2] J. Mwamburi, Comparative spatial metal concentrations and partitioning in bottom sediments of two tropical freshwater lake basins, Kenya, Lakes and Reserv. Res. Manage. 18 (2013) 329-355.

[3] E.Z. Ochieng, J.O. Lalah, S.O. Wandiga, Analysis of heavy metals in water and surface sediment in five rift valley lakes in Kenya for assessment of recent increase in anthropogenic activities Bull. Environ. Contam. Toxicol. 79 (2007) 570-576.

[4] D.M.K. Ongeri, J.O. Lalah, S.O. Wandiga, K.W. Schramm, B. Michalke, Levels of Toxic Metals in Multisectoral Samples from Winam Gulf of Lake Victoria, Bull. Environ. Contam. Toxicol. 82 (2009) 64-69.

[5] M.K.D. Ongeri, J.O. Lalah, S.O. Wandiga, Speciation of Cd, Cu, Zn, Fe and Pb in sediments from Lake Victoria basin, Kenya, Environmentalist 30 (2010) 254-259.

[6] D.M.K. Ongeri, J.O. Lalah, B. Michalke, K.-W. Schramm, Speciation study of trace elements in surface sediment of Winam Gulf, Lake Victoria, by sequential extraction, aqua-regia acid digestion, and ICP-OES, Toxicol. Environm. Chem. 96 (2014) 1489-1500.

[7] E. Oyoo-Okoth, A. Wim, O. Osano, Use of the fish endoparasite Ligula intestinalis (L., 1758) in an intermediate cyprinid host (*Rastreneobola argentea*) for biomonitoring heavy metal contamination in Lake Victoria, Kenya Lakes Reserv. Res. Manag. 15 (2010) 63-73.

[8] D.O. Ogoyi, C.J. Mwita, E.K. Nguu, P.M. Shiundu, Determination of Heavy Metal Content in Water, Sediment and

Microalgae from Lake Victoria, East Africa, Open Environm. Eng. J. 4 (2011) 156-161.
[9] S. Omwoma, C.S. Lagat, J.O. Lalah, P.O. Owuor, K.-W. Schramm, Recent Advances on Mercury Speciation in Aquatic Ecosystems, Health Effects and Analytical Techniques, Brit. J. Appl. Sci. Technol. 19 (2017) 1-37.
[10] M.L. Campbell, Mercury in Lake Victoria (East Africa): Another Emerging Issue for a Beleaguered Lake? , Ph.D. Thesis University of Waterloo, Ontario, Canada. (2001).
[11] L.M. Campbell, O. Osano, R.E. Hecky, D.G. Dixon, Mercury in fish from three rift valley lakes (Turkana, Naivasha and Baringo), Kenya, East Africa Environ. Pollut. 125 (2003) 281-286.
[12] O. Escobar-Sa´nchez, F. Galva´n-Magan˜a, R. Rosı´les-Martı´nez, Mercury and Selenium Bioaccumulation in the Smooth Hammerhead Shark, Sphyrna zygaena Linnaeus, from the Mexican Pacific Ocean Bull. Environ. Contam. Toxicol. 84 (2010) 488-449.
[13] O. Escobar-Sánchez, J. Ruelas-Inzunza, X.G. Moreno-Sánchez, A.K. Romo-Piñera, M.G. Frías-Espericueta, Mercury Concentrations in Pacific Angel Sharks (Squatina californica) and Prey Fishes from Southern Gulf of California, Mexico.
, Bull. Environ. Contam. Toxicol. (2007) DOI: 10.1007/s00128-00015-01708-00120.
[14] USEPA, Fish tissue criterion for methylmercury to protect human health document, EPA-823-R-01-001, Office of Water,Washington, DC. http://www.epa.gov/waterscience/criteria/methylmercury/document.html., (2001).
[15] J.S. Ogola, W.V. Mitullah, M.A. Omulo, Impact of gold mining on the environmental and human health: A case study in the Migori gold belt, Kenya. , J. Environ. Geochem. Health 24 (2002) 141-157.
[16] L.M. Campbell, R.E. Hecky, J. Nyaundi, R. Muggide, D.G. Dixon, Distribution and food-web transtransfer of mercury in Napoleon and Winam gulfs, Lake Victoria, East Africa., J. Great Lakes Res. 29 (2003) 267-282.
[17] P.S. Ramlal, F.W.B. Bugenyi, G.W. Kling, J.O. Nriagu, J.W.M. Rudd, L.M. Campbell, Mercury Concentrations in Water, Sediment, and Biota from Lake Victoria, East Africa. , J. Great Lakes Res. 29 (2003) 283-291.
[18] B.O. Odum, A.O. Mustapha, J.P. Patel, H.K. Angeyo, Energy dispersive x-ray fluorescence analysis of mine waters from the Migori gold mining belt in southern Nyanza Kenya, Bull. Environ. Contam. Toxicol. 87 (2011) 260-263.
[19] B.O. Odum, A.O. Mustapha, J.P. Patel, H.K. Angeyo, Multielement analysis of Migori (southern Kenya) artisanal goldmine ores and sediments by energy EDX-ray fluorescence technique: Implications of occupational exposure and environmental impact Bull. Environ. Contam. Toxicol. 86 (2011) 484-489.
[20] K.A. Francesconi, J.S. Edmonds, Arsenic and marine organisms, Adv. in Inorg. Chem. 44 (1997) 147-189.
[21] K. Inagaki, A. Takatsu, T. Watanabe, Y. Aoyagi, T. Yarita, K. Okamoto, K. Chiba, Certification of butyltins and phenyltins in marine sediment certified reference material by species-specific isotope-dilution mass spectrometric analysis using synthesized 118Sn-enriched organotin compounds, Anal. Bioanal. Chem. 387 (2007) 2325-2334.
[22] Y. Cheo, I. Yoo, Y. Kim, K.S. Jeong, C.S. Sim, N. Choy, J. Kim, J.B. Eum, Y. Nakajima, Y. Endo, Y.J. Kim, A case study of acute organotin poisoning, J. Occup. Health 49 (2007) 305-310.
[23] NRC, National Research Council : Subcommittee on Arsenic in Drinking Water, 1999. Arsenic in Drinking Water, National Academy Press, Washington, DC. (1999).
[24] IARC, International Agency for Research on Cancer IARC Monographs on the Evaluation of Carcinogenic Risks to Humans Volume 84: Some Drinking-Water (2004).
[25] K.P. Cantor, J.H. Lubin, Arsenic, internal cancers, and issues in inference from studies of low level exposures in human populations Toxicol & Appl. Pharmacol. 222 (2007) 252-257.
[26] GESAMP, Review of potentially harmful substances – arsenic, mercury and selenium. , Rep. Stud. GESAMP 28 (1988) 1-172.
[27] R.W. Gensemer, The bioavailability and toxicity of Aluminiun in aquatic environments Crit. Rev. Environ. Sci. and Technol. 29 (1999) 315-450.
[28] B. Phippen, C. Horvath, R. Nordin, N. Nagpal, Ambient aquatic life guidelines for iron. Overview report. Water Stewardship Division. , Ministry of Environment, British Columbia (2008).
[29] W. Xing, G. Liu, Iron biogeochemistry and its environmental impacts in freshwater lakes. , Fresenius Environ. Bull. 20 (2009) 1339-1342.
[30] P.D. Howe, H.M. Malcoholm, S. Dobson, Manganese and its compounds: Environmental impacts, Concise International Chemical Assessment Document 03. UNEP Report, Geneva (2004).
[31] G.A. Butcher, Water Quality Criteria for Alumnium, Ministry of Environment and Parks, British, Columbia (1988).
[32] J.H. Rule, Assessment of trace element geochemistry of Hampton Roads Harbour and lower Chesapeake Bay area sediments, Environ. Geol. Water Science 4 (1996) 209-219.
[33] D.D. MacDonald, C.G. Ingersoll, B. T.A., "Development and Evaluation of Concensus-based Sediment Quality Guidelines for Freshwater Ecosystems." Archiv. Environ. Contamin. Toxicol. 39 (2000) 20-31.
[34] D.R. Persaud, R. Jaagumagi, A. Hayton, Limitlines for Protection and Management of Aquatic Sediments in Ontario. Ontario: , Standards Development Branch, Ministry of Environment (1993).
[35] K.M. Huang, S. Lin, Consequences and implication of heavy metal spatial variations in sediments of the Keelung River drainage basin, Taiwan, Chemosphere 53 (2003) 1113-1121.
[36] C.K. Jain, Metal fractionation study on bed sediments of River Yamuna, India, Water Res. 38 (2004) 569-578.
[37] E.Z. Ochieng, J.O. Lalah, S.O. Wandiga, Athropogenic Sources of heavy metal input into the Indian Ocean Coast of Kenya, Bull. Environ. Contam. Toxicol. 83 (2009) 600-607.

Available online at www.kenchemsoc.org

Journal of the Kenya Chemical Society 10-1 (2017), 76-83

JOURNAL OF THE KENYA CHEMICAL SOCIETY

Development of a Method for estimating the Concentration of Endocrine Phenolic compounds in surface water using HPLC technique

Hussein Kehinde Okoro[1,2]*, Oladipo Adeniyi Victor,[1] Kazeem Adebayo Basheer[3], Benjamin Olawale Orimolade,[1] Catherine Jane Ngila[2]

[1]Material and Environmental-Analytical Research Group, Department of Industrial Chemistry University of Ilorin, P.M.B. 1515. Ilorin, Nigeria.

[2] Analytical-Environmental and Membrane Nanotechnology Research Group, Department of Applied chemistry, University of Johannesburg, P.O. Box 17011, Doornfontein 2028, Johannesburg, Republic of South Africa

3. Central Research Laboratory, University of Lagos, Akoka Campus, Lagos, Nigeria

Corresponding Author: Email*hkoadeola@gmail.com, okoro.hk@unilorin.edu.ng

Abstract

Research on phenolic compounds is of current interest since they have important biological and pharmacological properties. HPLC is one of the advanced techniques for routine analysis of phenolic compounds. In this research, the determination of phenolic compounds in four different locations along the Oyun River, in North-central Nigeria was carried out using HPLC. Samples were collected from the upper, middle and lower stream from each of the sampling stations. The collected samples were extracted, pre-concentrated and analysed by HPLC technique. Among the phenolic compound studied, chlorophenol has the highest concentration of 13.01 ppm at location 4 (Unilorin Dam) while 2,4dinitrophenol has the lowest concentration of 2.036 ppm at location 1 (Oyun). Phenol was not detected in all the samples collected. The experimental results demonstrated that HPLC method offers excellent recoveries and could be employed for environmental sample analysis. In view of the rapidity, simplicity, environment-friendly nature, the optimised method was an excellent alternative detection technology for phenol analysis and can be widely employed in environmental and other related fields.

Keywords: Phenols, HPLC, Oyun River, endocrine, recovery, optimization

1.0. Introduction

Phenolic compounds such as halogenated and nitrated phenols are present in the aquatic environment due to their widespread use in many industrial processes such as the manufacture of plastics, dyes, drugs, antioxidants, pharmaceuticals, paints, pulp, paper and wood preservatives and pesticides.[1-4]Disposal of these chemicals or pollutants without proper treatment may lead to serious health risks to humans, animals and aquatic systems.[1]Phenols possesses hazardous health effects; these can be chronic and acute. Irregular breathing and weakness may result from long-term exposure to phenolic compounds. Chronic systemic effects due to phenol exposure are: anorexia, weight loss, diahorea and dark colouration of urine.[5, 6, 7]Repeated or prolonged skin contact with phenol may result in dermatitis or even second and third degree burns due to phenol caustic and defeating properties.[8] It may also cause harmful effects on the central nervous system and heart.[8] Phenolic compounds have also been accused of carcinogenicity. Identification and monitoring of these compounds at trace level in surface waters are imperative because they are persistent in the environment.[9, 10]

One of the problems of developing countries like Nigeria is improper management of the enormous amount of wastes generated by various anthropogenic activities. More problematic is the indiscriminate disposal of such wastes into water bodies' especially freshwater reservoirs. This has often rendered these natural resources unsuitable for both primary and secondary usage. Industrial effluent contamination of natural water bodies has emerged as a major challenge in developing and densely populated countries like Nigeria.

River systems are the primary means for disposal of waste, especially the effluents from industries that are near them. These effluents have a great influence on the pollution of the water body in which they can alter the physical, chemical and

biological nature of the receiving water body. **Increased industrial activities, agricultural activities and domestic uses have led to pollution stress on surface water**. Despite the environmental consequences of surface water pollution by industrial effluents, many river systems in developing countries especially Nigeria are still being contaminated by industrial influents.[11, 12]

Endocrine disrupting chemicals (EDCs) has been reported over decades. They are class of chemicals **emanating** from xenobiotic and exogenious origins. Several phenolic compounds such as bisphenol A, nitrophenols and chlorophenols have been identified as EDCs. EDCs, act by mimicking or inhibiting the natural actions of the endocrine system in animals and humans such as synthesis, secretion, transport and binding. The presence of EDCs in the aquatic systems is a serious environmental problem.[13-17]

Toxic organic contaminants such as Phenolic EDCs should be removed **from effluents** before discharge into natural water bodies due to serious environmental risks it possesses. At concentrations below 1 µg/L, phenols can affect the taste and odour of water. Phenolic concentration above 2 mg/l is considered to be toxic to fish and concentration ranges between 10 to 100 mg/l would result in death of aquatic life within period of 4 days.[8] Biodegradability of phenols is only 90% in surface water after a one-week, and the aquatic toxicity of phenol (LC_{50}) is 12mg/l. In EU countries, the allowed maximum concentration of phenol in drinking water is 0.5 mg/l.[18]

In recent years, many researchers used adsorption method for phenolic removals such as activated carbon, zeolites, biosorbents etc. Many modifications have been used to improve the adsorption efficiency of activated carbon. Potassium permanganate as an oxidant has been used widely and more on the impact of modification on adsorption capacity has been studied.[19]Many works have been conducted on distribution and occurrence of phenolic EDCs in drinking water. [20, 21, 22]

In view of the impact of phenolic compounds in surface water, there is therefore need to establish a method for the determination and quantification of phenols in surface water. Several analytical techniques have been developed for the determination and quantification of phenols in recent years. Among these analytical techniques, High performance liquid chromatography (HPLC) is presently the most popular and reliable analytical technique for the analysis of phenolic compounds. HPLC have been used with detectors such as UV, electrochemical detector and colorimetric detector for phenols analysis.[23, 24]

The major aim of this research work is to develop, optimize sensitive and selective method for the determination of some phenolic compounds in environmental matrixes. Water samples collected from Oyun River was used to validate the developed method using High Performance Liquid Chromatography (HPLC) technique.

2. Materials and Methods

2.1 Description of sampling site

The study area is located in Ilorin, North Central Nigeria with the region font code of Africa/Middle East. It is located at an elevation of 269 meters above sea level with population of 736,113. It lies between latitude 8˚24'N and 8˚36N and between longitude 4˚10'E and 4˚36'E.[25] The city has a humid tropical climate, which is characterized by wet and dry season. Rainy season in the city begins towards the end of March and ends in October with 2 peak periods in June and September. Temperature is uniformly high throughout the year and open air isolation can be very uncomfortable during the dry season.[26]Ilorin is underlain by igneous metamorphic rock basement complex, which are neither porous nor permeable except in places where they are deeply weathered or have zones of weakness.[26] The coordinates and the map of the sampling sites are presented in Table 1 and Figure 1 respectively.

Table 1 Coordinates of Sampling Sites

Sample	Sampling Location	Latitude	Longitude
1	Oyun	8° 31.528' N	4° 36.08' E
2	Police Headquarter Barack	8° 31.745' N	4° 36.055' E
3	Ago Ayekele	8° 27.444' N	4° 37.418' E
4	Unilorin Dam	8° 28.050' N	4° 39.799' E

2.2 Reagents and chemicals

High analytical grade chemicals were used. The chemicals include 2,4-dinitrophenol, phenol, nitrophenol and chlorophenol which were used to prepared working standards. Other chemicals used for analysis include 0.02 N sulphuric acid (H_2SO_4), nitric acid (HNO_3), silver nitrate ($AgNO_3$), potassium chromate (K_2CrO_4), buffer solution (indicate the specifics), eriochrome Black T, 0.01M EDTA, Dichloromethane and anhydrous sodium sulphate (Na_2SO_4).

2.3 Preparation of standard solution

Stock solutions (1000 mg/L) of standard 2,4-dinitrophenol, phenol, nitrophenol and chlorophenol were prepared. Serial dilutions of these standards were done to obtain series of concentrations (50 ppm, 25 ppm, 12.5 ppm, 6.25 ppm, 3.13 ppm) which were used to establish retention time Rt and calibrations plots

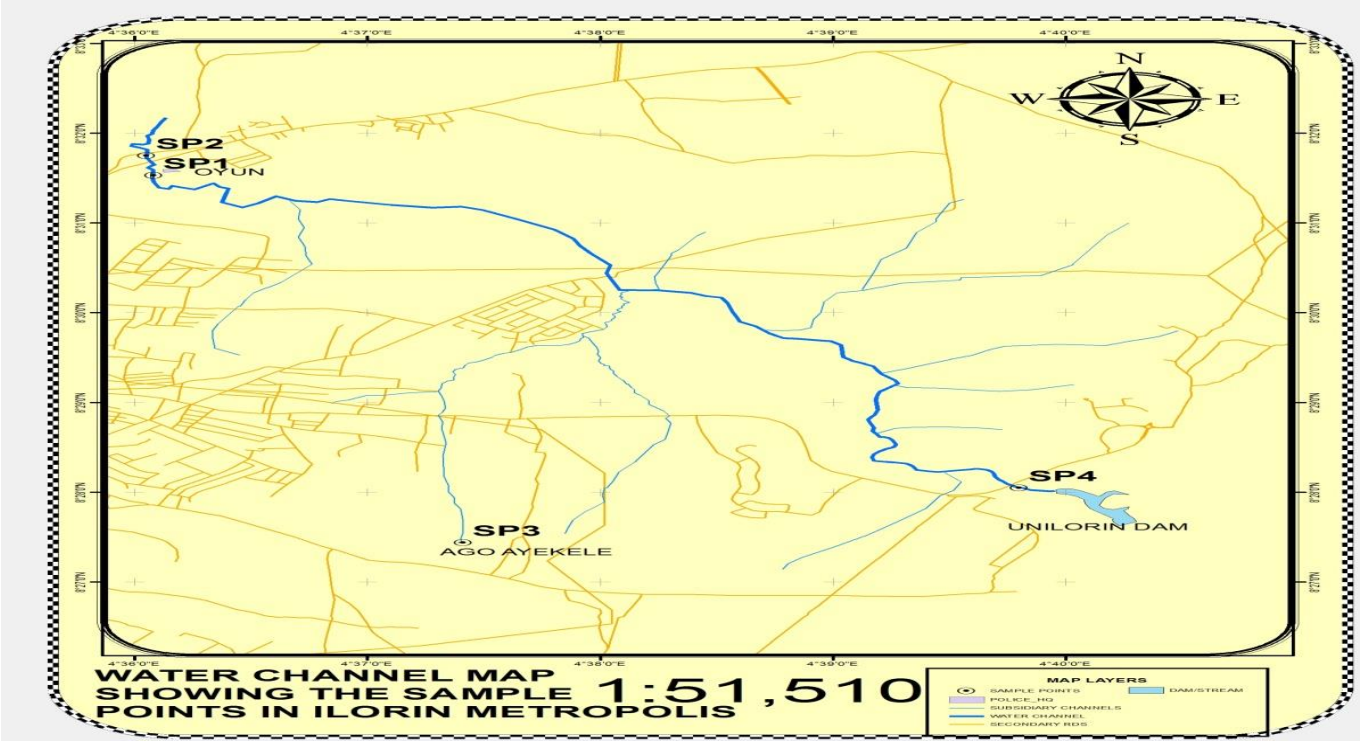

Key: Sp 1- Oyun; Sp 2- Police headquarters barrack; Sp 3- Ago Ayekale;Sp 4- Unilorin dam

Figure. 1 Map of Ilorin showing the study area on Oyun River

2.4. Sample collection and preservation

A thorough survey of the study area was conducted prior to sampling. The rivers were mapped out for sampling and water samples were collected upstream and downstream of the four study areas. Each water sample were collected in a clean amber bottle which was soaked in 3 ml of concentrated nitric acid for 24 hours, washed thoroughly with soap and then rinsed with deionized water. The sampling bottles were dipped inside the river and locked so as to avoid any form of air trapping into it. The water samples which were collected at upper, middle and lower stream of the river was denoted with 'a', 'b' and 'c' respectively. The collected water samples were taken into the laboratory where the pH was measured and acidified with 4 ml of conc. H_2SO_4 (0.2% v/v) and was kept at 4^{o}C until analysis. The physico-chemical parameters were also determined.

2.5 Analysis of physiochemical parameters of the water samples

The temperature, pH, turbidity and conductivity of the water samples were determine using thermometer, pH meter, turbidity meter and conductivity meter respectively. Total Suspended Solids (TSS), Total Dissolved Solids, hardness and chloride were determined following the standard methods.[30]

2.6 Instrumentation

In determination of phenol at low concentration, HPLC method with liquid-liquid extraction was employed. Analyses were performed on an Agilent technologies 11100 series HPLC instrument with a Ultra-Violet (UV) detector. HPLC chromatographic conditions are shown in table 2.

Table 2 HPLC Operating Conditions

Instrumentation	Operating conditions
Column	Zorbax Eclipse XDB –C18
Column temperature	Room temperature
Column dimension	4.6x 250 mm
Flow rate	1ml/min
Detector	UV Detector
Particle size	5 micron
Wave length	262nm
Injection Volume	10µl
Mobile Phase	Acetonitrile & HPLC Grade water (50:50) v/v

2.7 Extraction of phenols

A sequential liquid–liquid extraction procedure was applied to the river water samples using dichloromethane after acidification to pH 2 with conc. H_2SO_4 (0.2% v/v). 100 ml of the water sample was measured into 250 ml separating funnel and extracted twice with 25 ml of dichloromethane in 30

minute by shaking with hand. The stopper was removed and allowed to settle for 20 minutes. After the extraction, the organic layer was concentrated by rotary evaporation at room temperature under reduced pressure to approximately 1 mL and dried by filtration over 1g of anhydrous granulated sodium sulphate (Na_2SO_4).[14]

2.8 Determination of resolution, linearity and solubility of the phenolic compound

The phenol standards were firstly examined to check their solubilities in organic solvent; they were found to be soluble in the mixture of methanol and demineralised water. These compounds were fully scanned using UV spectrophotometer and found out that they absorb between 260 and 270nm but when the compounds were ran individually across the wavelength using HPLC Agilent 1100 series it was found out that the wavelength of maximum absorbance was around 262 nm. Then the individually phenol compounds was ran to ascertain their retention time. The later was mixed together to see how they would resolved and it was found out that there were separations among the phenol compounds. This was adopted and series of concentrations were prepared to run linearity of the method.

2.9 Quality assurance

Quality assurance is defined as a set of activities or procedures which are adopted to ensure that all quality requirements are being met.[27] Quality assurance was employed to the sample and chemicals used to prevent lower errors and verify the accuracy of the calibration standards while the control standards were used to monitor the accuracy of the instrument used. Water samples collected from Oyun River were used to validate the results. The experiment was carried out in triplicate at each location to obtain reliable results.[28] For recovery study, an ultra-pure water (purified water) was spiked with a mixture of phenol compounds containing about 12.5 ppm. the mixture was extracted using 10 ml of a mixture of methanol and N- hexane (50:50 v/v). The extraction was repeated twice using the same solvents. The organic phases collected were pooled together and clean up using a column packed with silica gel and the eluate was concentrated using nitrogen concentrator. The concentrate was later reconstituted to about 1ml with mobile phase before injection.

3. Results and Discussion

3.1. Physicochemical parameters

The results of the physic-chemical parameters which include pH, temperature, turbidity, conductivity, TSS, TDS, chloride and hardness of the water samples are presented in Table 3.

The observed pH values of the samples varied between 5.2 and 7.1 with the lowest values recorded in Location 3 while the highest values were recorded in Location 1.All the values complied with both WHO and USEPA standards.[31, 32] The water temperature of Oyun River ranged between 26.81 ºC to 28.81 ºC. The lowest value (26.81 ºC) was found in location 1 and the highest temperature value (28.81 ºC) was found in location 4. However, all the values complied with WHO and USEPA standards permissible limits for surface water.[31, 32]These values also correspond to the values obtained by Adewoye on his work on Asa River.[33] The mean values obtained for conductivity ranged between 40.30 µS/cm and 60.05 µS/cm. Electrical conductivity is mostly influenced by dissolved salts such as sodium chloride and potassium chloride. The mean values were found to comply only with USEPA standard limit as other regulatory bodies are silent on permissible limits for conductivity in surface water.[34] These values also correspond to the values obtained by Mobin*et al* on his work on Turag River but are lower than 68.60µS/cm reported by Umunnakwe and Ogamba.[35, 36.]

TSS and TDS values ranged from 187.16 to 298.49 mg/L and 278.14 to 392.47 mg/L, respectively. These values were higher than the WHO maximum permissible limit, TSS (20 mg/L) and TDS (200 mg/L).[31] TSS relatively measures the physical or visual observable dirtiness of a water resource. Therefore location 4 had more dirt and dissolved substances in the water samples. TDS are indication of the degree of dissolved substances such as metal ions in the water.[36] Lowest chloride value (28.29 mg/L) was recorded in location 2 while the highest chloride value (45.55 mg/L) was observed in location 4due to the basis of soil porosity and permeability. The high content of chloride in the aquatic systems is responsible for a large amount of organic matter which in turn causes eutrophication.[37] The value of hardness ranged between 219.32 mg/L – 532.68 mg/L. The lowest value (219.32 mg/L) was recorded in location 4 and the highest value (532.68 mg/L) was recorded in location 1. Calcium ions make major contribution to the hardness of river water. These values also correspond to the values obtained by Dubey, on his work on Kshipriver water at Ujjain, India.[38]

3.2. HPLC results

The results from the HPLC analysis of the prepared standards, concentrations of phenolic compounds in the samples and results of the spiked river water sample are presented in Tables 4, 5 and 6, respectively.

In this study, four phenolic compounds (2,4 –Dinitrophenol, Phenol, Nitrophenol, Chlorophenol) were examined in all the twelve water samples taken at four different sampling locations along Oyun River. The calculation of concentration of the compounds are based on the area of peaks (mAU*min). The mean concentration for the four phenolic compounds for water samples shows that the highest concentration for toxic 2,4-dinitrophenol was found at 2.258 ppm in location 3 and the lowest value was recorded as 2.014 ppm in location 2.

Nitrophenol was found at 0.891 ppm in location 1. The highest concentration of Chlorophenol was 13.010 ppm at location 4 and the lowest value was recorded as 7.185 ppm at location 1. Phenol was not detected probably due to the presence of very low concentrations in water samples because it is diluted or may not be present in water samples at the selected locations. The LOD/LOQ was established using statistical graph with the concentration shown in table 7. Recovery studies were carried out and quantitative recoveries of 87.2%, were recorded for 2,4- dinitro -phenol; Phenol (83.90%); Nitro phenol (74.80) and Chloro phenol (96.07%) in that order (Table 6) The absence or lower concentration of other derivatives of phenols is probably due to their volatility, dissolution, biological degradation and photo oxidation.[39] It can also be seen that the concentration of the phenolic compounds in location 4 is higher than the other three sampling locations due to chlorination of mono and polyaromatic compounds present in the soil and water of the location.

Table 3 Physico-chemical parameters of river water samples

S/N	pH	Temp	Turbidity	Conductivity	TSS(mg/L)	TDS(mg/L)	Chloride (mg/L	T.H(mg/L)
1	7.1±0.26	26.81± 0.38	51.36 ± 0.77	47.72 ± 0.78	187.16± 22.04	278.12± 38.25	34.32 ± 3.72	532.68±132.44
2	6.4± 0.20	27.73± 1.05	50.77 ± 6.72	40.77 ± 1.82	207.06± 30.42	298.38± 37.91	28.29 ± 0.40	253.03± 40.00
3	5.2± 0.15	26.89± 0.10	42.04 ± 0.79	40.30 ± 3.20	249.34± 2.39	339.29± 3.59	30.62 ± 0.82	248.00± 23.06
4	6.0± 0.21	28.81± 0.24	56.48 ± 2.97	60.05 ± 1.70	298.49± 34.75	392.47± 25.09	45.55 ± 1.42	219.32± 19.00

Table 4 Results of the four phenolic compounds obtained from standard solution of 12.5 ppm

Peak	Name	Ret Time (min)	Type	Width (min)	Area (mAU*s)	Area (%)
1	Dinitrophenol	2.203	VV R	0.146	1660.585	33.282
2	Phenol	3.949	VV R	0.070	3036.210	60.852
3	Nitro phenol	4.289	VV R	0.080	241.991	4.85
4	Chlorophenol	5.673	VB R	0.097	50.726	1.017
Totals					4989.512	

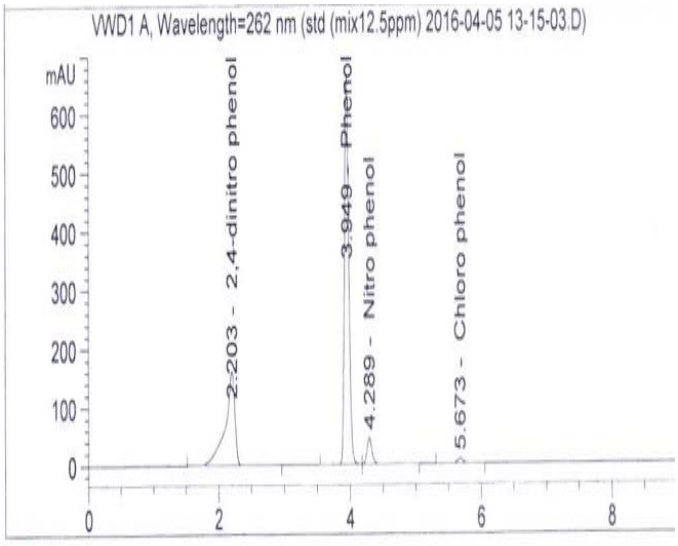

Figure. 2 Typical chromatogram obtained from a standard solution of 12.5 ppm

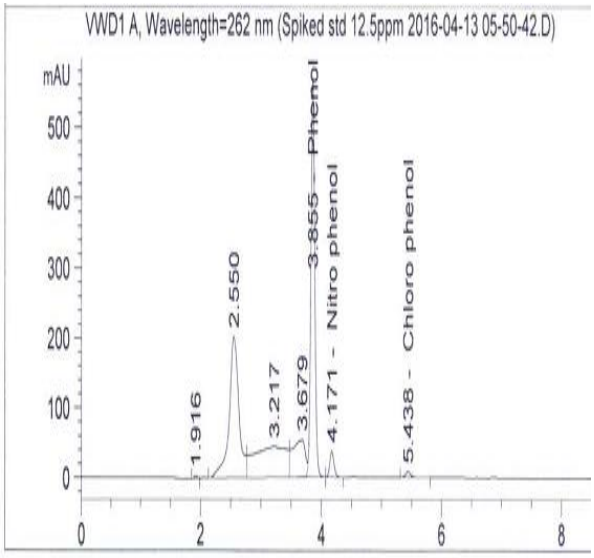

Figure 3 Typical chromatogram of spiked water sample

Table 5 Concentrations of the four phenolic compounds at different locations.

ANALYTE	Sample1	Sample2	Sample 3	Sample 4 (ppm)
2,4dinitrophenol	2.036	2.014	2.258	2.158
Phenol	N.D	N. D	N.D	N. D
Nitrophenol	0.891	N.D	N.D	N.D
Chlorophenol	7.185	N. D	N.D	13.01

ND=Not Detectable

4. Conclusions

Studies of the detection and quantification of phenolic compounds in water is of great interest in order to make water safer for utilization. HPLC, with various detection possibilities, or their combinations, has been a preferred technique for routine analysis of phenolics compounds. The concentrations of each phenol in water samples at location 1 (Oyun), 2 (Police Headquarters), 3 (Ago Ayekale) and 4 (Unilorin dam) of Oyun River were determined. Samples were collected from the upper, middle and lower stream from each of the sampling stations. The collected samples were extracted, pre-concentrated and analysed by HPLC technique. The highest and lowest concentrations were obtained in the river water samples at location 4 (Unilorin Dam). Almost similar results were obtained from location 1 (Oyun). The experimental results demonstrated that this HPLC method offers excellent recoveries and could be employed for environmental sample analysis. Therefore, the developed method can be used as an alternative detection method for analysis of phenols in environmental and other related field.

Table 6 Results obtained from spiked water sample

Peak	Ret Time (min)	Type	Width(min)	Area (mAU*s)	Area %	% Recovery	Name
1	1.916	BV	0.058	13.463	0.179		Nil
2	2.162	-	0.000	0.000	0.000	87.20	2,4-dinitrophenol
3	2.55	BV	0.169	2279.513	30.232	-	-
4	3.217	VV E	0.470	1678.485	22.261	-	-
5	3.679	VV E	0.216	791.138	10.493	-	-
6	3.855	VB R	0.068	2547.379	33.785	83.90	Phenol
7	4.171	BB	0.073	180.939	2.400	74.80	Nitrophenol
8	5.438	BB	0.091	49.132	0.652	96.07	Chlorophenol
Totals				7540.048			

Table 7 LOD and LOQ concentrations for the four analytes.

Analyte	LOD (ppm)	LOQ (ppm)
2,4dinitrophenol	1.406992	4.643074
Phenol	3.951142	11.97316
NitroPhenol	1.68463	5.104938
Chlorophenol	1.57589	4.77525

Acknowledgment

The authors acknowledge the Department of Industrial Chemistry, University of Ilorin, Ilorin, Nigeria for making laboratory equipment available. Acknowledgements also go to Mr. Jameel Asani of the Department of Religion Studies, Faculty of Humanities, University of Johannesburg, South Africa for the editorial assistance. The main author Dr HK Okoro, also wish to thank the University of Johannesburg for providing library database during the preparation of this manuscript.

References

1. Sun, X. Wang, C. Li, Y. Wang, W &We, J (2015). Treatment of phenolic wastewater by combined UF and NF/RO processes. Desalination, 355, 68–74.
2. Kazemi, P. Peydayesh, M.Bandegi, A. Mohammadi, T&Bakhtiari, O (2014) Stability and extraction study of phenolic wastewater treatment by supported liquid membrane using tributyl phosphate and sesame oil as liquid membrane. ChemEng Res Des, 2014, **92,**375–83.
3. Mohammadi, S. Kargari, A. Sanaeepur, H. Abbassian, K. Najafi, A &Mofarrah, E (2015) Phenol removal from industrial wastewaters: a short review. Desalination and Water Treatment 2015, 53, 2215–34.
4. Moore, JW &Ramamoorthy, S (1984) Organic chemical in natural waters, applied monitoring and impact assessment, *Springer-Verlag*, **2**, 234.
5. Kulkarni, SJ & Kaware,JP (2013) Review on research for removal of phenol from wastewater. International Journal of Science Research Publication. 3, 1–4.
6. EPA (2008) Toxic Release Inventory National Analysis, accessed December 2015. Available from: http://www.epa.gov/.
7. Mukherjee, S.Basak, B.Bhunia, B. Dey, A & Mondal, B (2013) Potential use of polyphenoloxidases (PPO) in the bioremediation of phenolic contaminants containing industrial wastewater. Review Environmental Science Biotechnology 12, 61–73.
8. Srinivasulu, K.Balasubramani, K &ManishaVidyavathy, S (2016) Effect of process parameters on the phenol removal rate from petrochemical effluents using electrochemical method. 2016
9. Shamar, JM (2013) Determination of Some Phenols in Tigris River by HPLC. Ibn Al-Haitham Journal for Pure & Applied Science, 26(1), 251-253.
10. Smith, CJ. Perfetti, TA., Morton, MJ. Rodgman, A. Garg, R. Selassie, CD. AndHansch, C (2002) The Relative Toxicity of Substituted Phenols Reported in Cigarette Mainstream Smoke. *Toxicological Sciences*, 69, 265 – 278.
11. Etim, EU &Onianwa, PC (2013). Impact of Effluent of an Industrial Estate on Oruku River in Southwestern Nigeria. World Applied Sciences Journal,21, 1075-1083.
12. Richardson, SD &Ternes,TA. (2011) Water Analysis: Emerging Contaminants and Current Issues. Analytical Chemistry, 83, 4614–4648.
13. Ahel, M. Giger, W & Koch, M (1994) Behavior of alkylphenolpolyethoxylate surfactants in the aquatic environment—I. Occurrence and transformation in sewage treatment. Water Research, 1994, 28, 1131–1142.
14. Staples, CA. Dorn, PB. Klecka, GM. O'Block, ST &Harris, LR (1998) A review of the environmental fate, effects, and exposures of bisphenol A. Chemosphere, 36, 2149–2173.
15. Ying, GG. R.S. Kookana, RS &Ru,YJ (2002) Occurrence and fate of hormone steroids in the environment. Environmental International28, 545–551.
16. Ying, GG. Williams, B &Kookana, R (2002) Environmental fate of alkylphenols and alkylphenolethoxylates—a review. Environmental International28, 215–226.
17. Pothitou, P &Voutsa, D (2008) Endocrine disrupting compounds in municipal and industrial wastewater treatment plants in Northern Greece. Chemosphere, 73, 1716–1723.
18. Zhang, J. Chen, J &. Li, X (2009) Remove of Phenolic Compounds in Water by Low-Temperature Plasma: A Review of Current Research.
19. Zhang, J (2013) Phenol Removal from Water with Potassium Permanganate Modified Granular Activated Carbon.
20. Wang,L et al. (2012) Monitoring of selected estrogenic compounds and estrogenic activity in surface water and sediment of the Yellow River in China using combined chemical and biological tools. Environmental Pollution, 165, 241–249.
21. Wang, Let al. (2011) Assessing estrogenic activity in surface water and sediment of the Liao River system in northeast China using combined chemical and biological tools. Environmental Pollution, 159, 148–156.
22. Jiang, Wet al. (2012) Assessment of source water contamination by estrogenic disrupting compounds in China. Journal Environment Science, 24, 320–328.
23. Hossain, MA&Salehuddin, SM (2009) Quantification of phenol in surface water by gas chromatography and mass spectroscopy Asian Journal of Energy & Environment 10(2), 91-98.
24. Neng, NR &Nogueira,JMF (2014) Determination of Phenol Compounds in Surface Water Matrices by Bar Adsorptive Micro extraction-High Performance Liquid Chromatography-Diode Array Detection.*Molecules*,19, 9369-9379; doi:10.3390/molecules19079369

25. Kolawole, OM, Olayemi, AB. &Ajayi, KT (2011) Managing flood in Nigerian cities: Risk analysis and adaptation options, Ilorin city as a case study. Archives of Applied Science Research, 3(1), 17-24.
26. Oriola, E &Bolaji, S (2012) Urban Flood Risk Information on a River Catchment in a Part of Ilorin Metropolis, Kwara State. Nigeria. Information and Knowledge Management, 2(8).
27. Rauf, MA &Hanan, A (2015) Quality Assurance Considerations in Chemical Analysis. Quality Assurance Journal, 12, 16–21.
28. Briggs,R (1996) Water Quality Monitoring - A Practical Guide to the Design and Implementation of Freshwater. ISBN 0419223207.
29. Eaton, AD. Clesceri, LS. Rice, EW &Greenberg, AE (2005) Standard Methods for the Examination of Water and Wastewater, 21st ed. American Public Health Association, Washington, DC, USA, 2005.
30. P.N. Patil, D.V. Sawant and R.N. Deshmukh, Physico-chemical parameters for testing of water- A review. *International Journal of Environmental Sciences*, 2012, 3, 1194-1207.
31. WHO Geneva, Guidelines for drinking-water quality (electronic resource), 3rd edition incorporating 1st and 2nd addenda, 2008, 1.
32. USEPA, National Recommended Water Quality Criteria. Office of Science and Technology (4304T), 1-21, 2009.
33. Adewoye, SO (2013) Seasonal Assessment of Impact of Industrial Effluent Discharges on the Water Quality of Asa River, Ilorin Nigeria. International Journal of Research in Environmental Science and Technology. ISSN 2249–9695.
34. Mobin, MN. Islam, MS. Mia, MY. and. Bakali, B (2014) Analysis of Physicochemical Properties of the Turag River Water, Tongi, Gazipur in Bangladesh. *J. Environ. Sci. & Natural Resources*, 2014, **7**(1), 27 – 33.
35. Umunnakwe, JE. andA.S. Ogamba, AS (2012) Preliminary Assessment of Industrial and Human Activities on Some Physicochemical and Bacteriological Parameters of Bundu–Ama Creeks, Port Harcourt Rivers State Nigeria. International Journal of Science and Advanced Technology, 2012, **2**(11), 132.
36. Efe, SI.Ogban, FE. Horsfall, M &Akporhornor, EE (2005) Variation of physicochemical characteristics in water resources quality in western Niger delta region. Nigeria. J. Appl. Science Environment Management, 9, 191-193.
37. Jayalakshmi, V. Lakshmi, N &SingaraCharya,MA (2011) Assessment of Physico-Chemical Parameters of Water and Waste Waters in and Around Vijayawada. International Journal of Research in Pharmaceutical and Biomedical Sciences, 2(3), 1041-1046.
38. S. Dubey(2013) Analysis of Physico-Chemical Parameters of Kshipriver Water at Ujjain, India. International Research Journal of Environment Sciences, 2(7), 1-4.
39. Tolosa,I. Bayona, JM. Albaiges, J (1991) Identification and occurrence of brominated and nitrated phenols in estuarine sediments. Marine Pollution Bulletin, 1991, **22**(12), 603-607.